Politecnico di Torino

Engineering Department

Master's Degree in
Biomedical Engineering

Master's Degree Thesis

Stress mitigation through adapted binaural beats

Candidates:

Domè Antonella

Guidubaldi Aurora

Supervisor:

Prof. Mesin Luca

Co-supervisor:

Ing. Raggi Matteo

Academic Year 2023/2024

Abstract

The use of binaural beats (BB) for neurostimulation is an innovative technique useful for regulating brain activity and relieving stress. The aim of this thesis is to develop a closed-loop neurostimulation protocol to investigate whether the use of BB adapted to the subject's stress in real-time can improve cognitive performance and modulate stress in healthy individuals. This study evaluate whether the adapted stimulation with BB in the alpha band is more effective compared to stimulation with constant BB and to the control condition without stimulation.

The research included the validation of artificial intelligence models to identify stress levels in real time using physiological signals such as electroencephalogram (EEG) and the electrocardiogram (ECG).

The experimental protocol required each participant to complete four acquisition sessions, each including three minutes of relaxation and five minutes of mathematical operations with two levels of difficulty. The four experimental settings included a calibration phase to train the regressor for stress recognition, a session with constant BB stimulation, a session with adaptive BB stimulation and a control condition without stimulation. Calibration was always conducted first, while the other sessions were randomized. During the experiment, the subjects listened to relaxing music to isolate them from external noise, with brown noise added in neurostimulation phases to mask BB stimuli, making them inaudible. In the adaptive stimulation phase, the modulation was performed by assessing the subject's stress state in real time every ten seconds and changing the beat frequency of the stimulation accordingly, while the other phases were conducted in offline mode.

EEG and ECG data were recorded using the Enobio 8-channel device and the NIC2 software. The data collected were used to train three different machine learning models. The Random Forest (RF) showed adequate timing for real-time acquisition and good performance in recognizing stress levels. EEG and ECG data from twenty healthy subjects were analyzed to identify significant features discriminating between the stressful and relaxed state, while cognitive abilities were assessed through reaction time (RT), accuracy of responses and the inverse efficiency score (IES).

Results indicate that both stimulation conditions improve cognitive performance and reduce stress levels compared to the control condition. Statistical tests showed that the use of adap-

tive BB had a more pronounced effect, with a significant decrease in RT and an improvement in IES scores compared to both constant BB ($p < 0.001$) and the control group ($p < 0.001$). The Fisher Ratio identified standard deviation, range, and maximum value as the most useful metrics for discriminating between relaxation and stress states, with the right frontal and left parietal as the most relevant hemispheres.

This study confirms the hypothesis that adaptive stimulation with BB is effective in improving cognitive functions and mitigating stress, highlighting the potential of this technique as a non-invasive resource for mental well-being. The results highlight the variability of individual reactions to BB and the importance of further studies to improve the neurostimulation model, which could include integrating new ECG and EEG metrics, testing different algorithms for stimulation, and using additional physiological and psychological measures to better understand the effects of stimulation on performance and stress mitigation.

Acknowledgments

First of all, we want to express our sincere gratitude to our supervisors Luca Mesin and Matteo Raggi for the opportunity and for having accompanied us during the development of the thesis with their precious advice useful for improving the quality of the project and helping us grow professionally.

We would also like to thank the Polytechnic of Turin and GEA Solutions for providing us with the resources necessary to carry out our research and all the individuals who took part in the experiment without whom it would not have been possible to achieve this objective.

We would like to express a special thank you to our families and friends for their continued support even in the most difficult situations.

We sincerely thank you all.

Antonella and Aurora.

"Science explores what is,
engineering creates what has never been."
- Theodore von Kármán

Contents

List of Tables

List of Figures

Acronyms

ADHD	Attention Deficit/Hyperactivity Disorder
ApEn	Approximate Entropy
ART	Auditory Reaction Times
ATP	Adenosine Triphosphate
BB	Binaural Beats
BBT	Binaural Beats Technology
BPM	Beats Per Minute
CMS	Common Mode Sense
CRH	Corticotropin Releasing Hormones
CS	Central Sulcus
DRL	Driven Right Leg
DispEn	Dispersion Entropy
EEG	Electroencephalogram
EMG	Electromyography
EOG	Electrooculogram
FuzzyEn	Fuzzy Entropy
HFD	Higuchi Fractal Dimension
IAF	Individual Alpha Frequency
IES	Inverse Efficiency Score
KFD	Katz Fractal Dimension
LSL	Lab Streaming Layer

MAD	Median Absolute Deviations
MAE	Mean Absolute Error
M1	Primary Motor Cortex
MSE	Mean Square Error
MSE	Multiscale Entropy
NIC	Neuroelectrics Instruments Controller
SNS	Sympathetic Nervous System
PNS	Nervous System Parasympathetic
PPC	Posterior Parietal Cortex
pNN50	Percentage of NN Intervals Differing by More Than 50 ms
PSS	Perceived Stress Scale
RMSE	Root Mean Square of Successive Differences
RMSSD	Root Mean Square of Successive Differences
ROC	Receiver Operating Characteristic
SDNN	Standard Deviation of NN intervals
SE	Standard Error
SE	Spectral Entropy
SampEn	Sampled Entropy
ANS	Autonomic Nervous System
CNS	Central Nervous System
PNS	Symptom Peripheral Nervous System
SM	Stress Reduction
SOC	Superior Olivary Complex
SCWT	Stroop Color-Word Test
TSST	Trier Social Stress Test
USB	Universal Serial Bus

VAS	Visual Analogue Scale
VE	Vigilance Enhancement
VRT	Visual Reaction Times
HRV	Heart Rate Variability
HV	High Vigilance
RF	Random Forest

Chapter 1

Introduction

1.1 Nervous system

The nervous system is fundamental for the coordination and regulation of the human body's functions. It is primarily divided into two parts: the central nervous system (CNS) and the peripheral nervous system (PNS). The CNS includes the brain and the spinal cord, while the PNS consists of sensory and motor nerves [1].

1.1.1 Anatomy and physiology of the brain

In Figure 1.1 and Figure 1.2 are depicted dorsal and lateral views of the brain anatomy. Eight lobes are recognized in it, four for each hemisphere:

1. Frontal lobe;
2. Parietal lobe;
3. Occipital lobe;
4. Temporal lobe.

1.2 Cerebral cortex

The outer layer of gray matter is called the cerebral cortex (Figure 1.3). Its thickness varies from 1.5 to 4 mm and it is composed of folds formed by gyri and sulci (Figure 1.4). Within the cortex, it's possible to find the soma, which are the cell bodies of neurons, as well as unmyelinated axons. The main lobes are created by the sulci and folds, specifically, the central sulcus (CS) separates the frontal lobe from the parietal lobe, as the frontal lobe is positioned anterior to the CS, whereas the parietal lobe is located posteriorly. The gyrus anterior to the CS is called the precentral gyrus, while the one posterior is called the postcentral gyrus. The primary motor cortex (M1) is positioned along the anterior wall of the central sulcus (CS) and

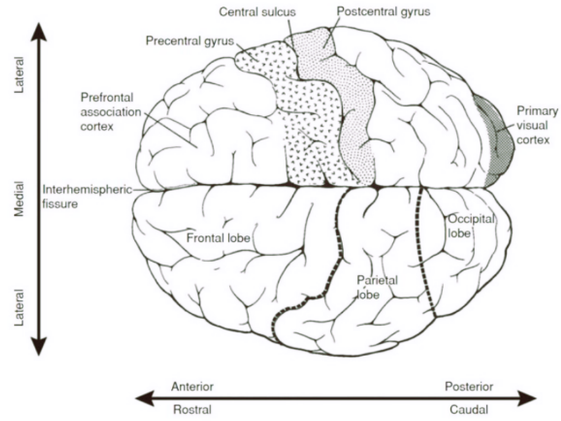

Figure 1.1: Dorsal view *(Adapted from [133])*

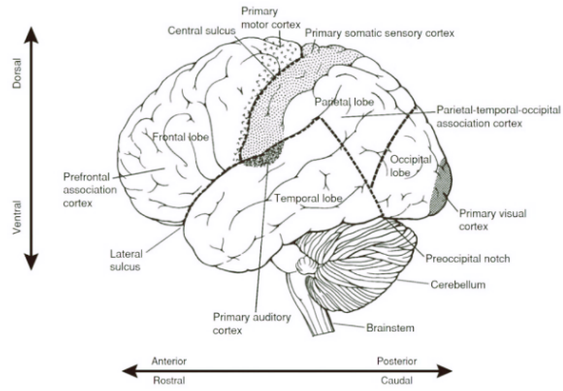

Figure 1.2: Lateral view *(Adapted from [133])*

extends along the precentral gyrus. The primary somatosensory cortex (S1), on the other hand, is located along the posterior wall of the central sulcus (CS) and extends up to the postcentral gyrus. Behind the CS are the parietal lobe and the occipital lobe. The primary somatosensory cortex (S1) is situated in the most anterior region of the parietal lobe. Further back, in the posterior parietal cortex (PPC), there is a region of multimodal association cortex that receives input from the surrounding somatosensory, visual, and auditory sensory areas. The occipital lobe, located at the posterior pole of the brain, is primarily composed of areas dedicated to vision. The temporal lobes, which are located ventrally on the sides of the brain, are crucial for auditory signal processing, advanced visual processing, and memory.

The cerebral cortex has three histologically distinguishable parts:

1. The **neocortex**: it comprises the majority of the cortex in mammals;
2. The **paleocortex**: it includes a region in the lower part of the brain that includes the olfactory cortex (but is not limited to that one);
3. The **archicortex**: a structure located deep within the temporal lobes that plays a fundamental role in the formation of new memories and spatial navigation.

1.3 Subcortical areas

The main subcortical areas of the brain that interact with the cortex and are intimately involved in motor and sensory functions include:

1. **Thalamus**: The thalamus is located below the cortex, in a deep position within the brain (Figure 1.5). It acts as the main gateway to the cerebral cortex for sensory stimuli coming

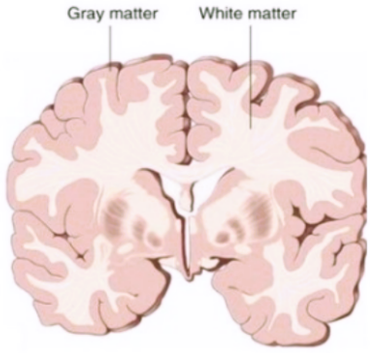

Figure 1.3: Gray matter and white matter *(Adapted from [134])*

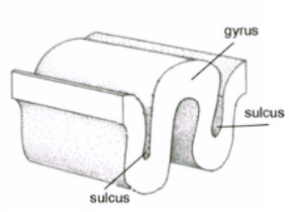

Figure 1.4: Grooves and convolutions *(Created by CristianoPR, Public domain, via Wikimedia Commons)*

from the spinal cord and other subcortical structures, such as the basal ganglia and the cerebellum. Additionally, it receives input from the cerebral cortex, indicating that the thalamus plays a complex regulatory role.

2. **Brainstem**: The brainstem is located at the base of the brain and is composed of the midbrain, the pons, and the medulla. The medulla connects to the spinal cord. Within the brainstem, there are nerve fibers ascending and descending from the spinal cord; moreover, it contains numerous motor and sensory nuclei, which are groups of neurons that further process these signals. The highest concentration of these nuclei is found in the pons.

3. **Basal Ganglia**: The basal ganglia are a group of interconnected nuclei located deep within the brain (Figure 1.6). They have close connections with the cerebral cortex and are very important for movement control.

4. **Cerebellum**: The cerebellum is located beneath the posterior part of the cerebral hemispheres. It is very important for performing smooth and well-coordinated movements, as well as for learning and adapting motor skills. Despite not having direct connections with the spinal cord, the cerebellum still exerts an indirect influence on movements through its connections with the brain and the brainstem.

1.4 Neurons and glial cells

The neuron (Figure 1.7) represents the fundamental unit of the nervous system, characterized by a cell body known as the soma, branching extensions called dendrites, and a long extension known as the axon. The dendrites are responsible for receiving signals from other neurons or sensory cells. These signals are then conveyed to the cell body for integration. The axon is responsible for transmitting the signal. It can be covered by the myelin sheath, an insulating layer produced by Schwann cells, which helps to speed up signal transmission.

Three types of neurons can be distinguished:

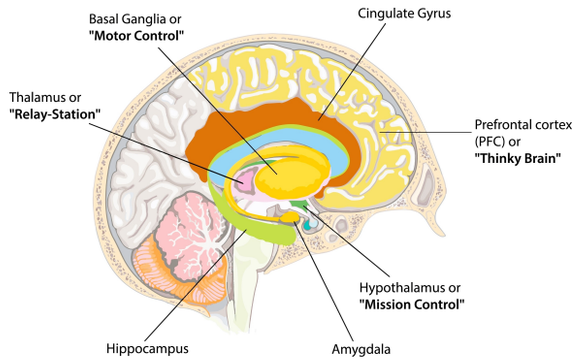

Figure 1.5: Subcortical areas

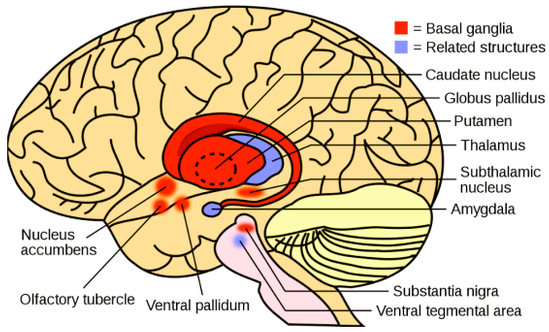

Figure 1.6: Basal ganglia

1. **Sensory neurons**: afferent neurons with long dendrites and short axons that transmit information from receptors to the central nervous system (CNS);

2. **Motor neurons**: efferent neurons with short dendrites and long axons that transmit information from the central nervous system (CNS) to effectors.

3. **Interneurons**: neurons that connect motor neurons and sensory neurons within specific regions of the central nervous system (CNS) through short dendrites and either long or short axons.

Glial cells constitute a group of non-neuronal cells that provide structural support, nourishment, and regulation of the neuronal environment within the nervous system. (Figure 1.8). Key types include:

1. Astrocytes, responsible for structural support and nutrient supply;

2. Oligodendrocytes and Schwann cells, which produce the myelin sheath to enhance the conduction of nerve impulses;

3. Microglia, which play an immune role;

4. Ependymal cells, which produce cerebrospinal fluid;

5. The terminal root that provides structural support;

6. Satellite glial cells that provide support to neurons in nerve ganglia.

1.5 Synapses

The synapse, or "gap," is the area where information is transmitted between neurons, typically located between the axon terminals and dendritic spines, although this is not always the case. There can also be synapses between axon and axon, dendrite and dendrite, and axon and cell body. The neuron that sends the signal is called the presynaptic neuron, while the one

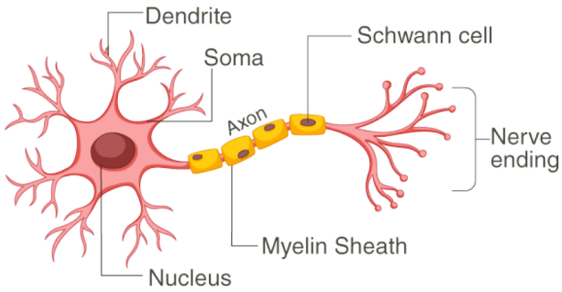

Figure 1.7: Neuron *(Adapted from [135])*

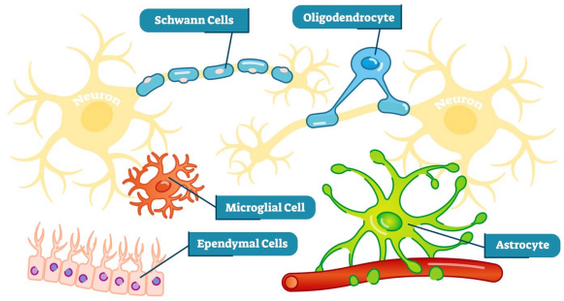

Figure 1.8: Glial cells

that receives the signal is called the postsynaptic neuron. It is important to note that these designations are relative to a specific synapse: most neurons function as both presynaptic and postsynaptic. The synapses are divided into chemical and electrical.

1.5.1 Chemical synapses

When an action potential reaches the end of the axon, it causes the depolarization of the membrane and the opening of voltage-gated sodium (Na^+) channels. Sodium ions (Na^+) enter the cell, causing further depolarization of the presynaptic membrane. This depolarization leads to the opening of voltage-gated calcium (Ca^{2+}) channels. The influx of calcium ions into the cell activates a signaling cascade that triggers the fusion of synaptic vesicles, small membrane-bound vesicles containing neurotransmitter molecules, with the presynaptic membrane. When a vesicle merges with the presynaptic membrane, it releases neurotransmitters into the synaptic cleft, the space outside the cells that lies between the presynaptic and postsynaptic membranes, as shown in Figure 1.9 (A). The neurotransmitter passes through the synaptic cleft and binds to receptor proteins located on the postsynaptic membrane. This binding with a specific neurotransmitter causes the voltage-gated ion channels present on the postsynaptic membrane to open. Neurotransmitters can cause either excitatory or inhibitory responses in the postsynaptic membrane.

After neurotransmission, the neurotransmitter needs to be removed from the synaptic cleft so that the postsynaptic membrane can reset and be able to receive a new signal. This can occur in three ways: the neurotransmitter can diffuse away from the synaptic cleft, be degraded by enzymes present in the synaptic cleft, or be recycled by the presynaptic neuron.

1.5.2 Electrical synapses

Electrical synapses (Figure 1.9 (B)) are not as prevalent as chemical synapses, and they function quite differently in terms of signal transmission. In the case of an electrical synapse, the presynaptic and postsynaptic membranes are situated very close to each other and are physically connected by channel proteins that create gap junctions. These gap junctions enable current to flow directly from one cell to another. In addition to ions that conduct the current, other molecules like ATP can also pass through the large pores of these junctions.

There are substantial differences between chemical and electrical synapses. In electrical synapses, signal transmission occurs almost instantaneously, and some of these synapses allow bidirectional signal passage. Additionally, electrical synapses are less likely to be blocked and play an important role in synchronizing the electrical activity of groups of neurons.

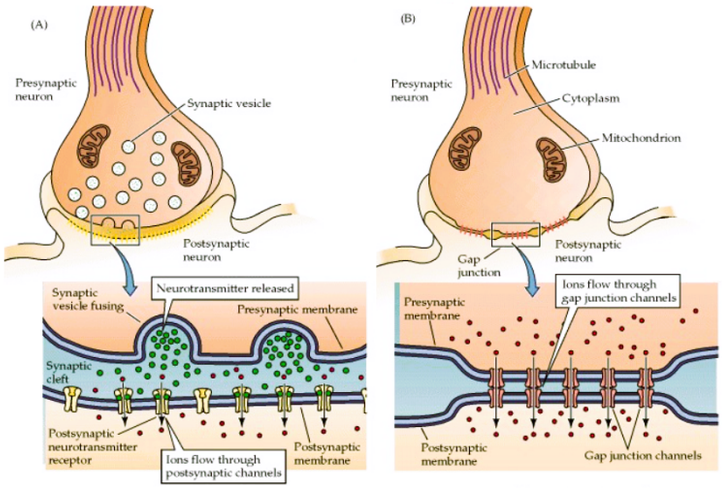

Figure 1.9: Chemical synapse (A) Electrical synapse (B)

1.6 Electroencephalogram (EEG) signal

The electroencephalogram (EEG) is a diagnostic examination that allows investigation of brain functionality by analyzing and recording its electrical activity caused by the flow of electric currents during synaptic excitations of dendrites in neurons. Recording is done using electrodes placed on the scalp, making it an important clinical tool for the study of the brain as it is non-invasive and for the diagnosis of some neurological pathologies. However, it provides signals of poor quality due to the numerous layers through which the signal is acquired [2].

1.6.1 Interpretation of EEG signals

An EEG signal is typically characterized by an amplitude ranging from 10 µV to 100 µV and a frequency band ranging from 0.3 Hz to 80 Hz. Based on their frequency, EEG signals can be classified by identifying 5 frequency bands described below and represented in the Figure 1.10:

1. **Delta Band (δ)**: Delta waves are predominant in brain regions such as the occipital lobe and parietal lobe during deep sleep. The band is characterized by slow and wide waves (20-200 μV) that occur at frequencies lower than 4 Hz. They are typically recorded in children and their presence decrease with the age. It is observed in adults during deep sleep and is unusual in awake adults. A large amount of delta activity in awake adults is abnormal and is correlated with neurological diseases. Due to its low frequency, it is easy to confuse delta waves with artifact signals, which are caused by large neck or jaw muscles.

2. **Theta Band (θ)**: Theta waves are most commonly observed in brain regions such as the temporal lobe and frontal lobe. Theta waves are found in the range from 4 to 7 Hz with amplitudes 1-100 μV. In a healthy, awake adult, only a small amount of theta frequencies can be recorded; they are more easily observable in children or adults in drowsy states, meditative states, or sleep. The theta band has been associated with meditative concentration and a wide range of cognitive processes such as mental calculation, demands of maze tasks, or conscious awareness.

3. **Alpha Band (α)**: Alpha rhythms are found in the occipital region of the brain. They occur in the range from 8 to 13 Hz and have amplitudes ranging from 10 to 200 μV. Their amplitude increases when the eyes are closed and the body relaxes, while they attenuate when the eyes open and mental effort is exerted. These rhythms primarily reflect visual processing in the occipital region of the brain and may also be related to the brain function of memory. There is also evidence that alpha activity can be associated with mental effort, measurable through the analysis of these rhythms.

4. **Beta Band (β)**: The frequency range of the beta band extends from 13 to 30 Hz, it is recorded in the frontal and central regions of the brain, and it is associated with motor activities; it has reduced amplitudes (10-20 μV). Beta rhythms are desynchronized during actual or imagined movement. They are characterized by a symmetric distribution when there is no motor activity. However, during active movement, beta waves attenuate, and their symmetric distribution changes.

5. **Gamma Band (γ)**: Gamma rhythms belong to the frequency band ranging from 30 to 100 Hz, and they also have reduced amplitudes (10-20 μV). The presence of gamma waves in the brain activity of a healthy adult is correlated with certain motor functions or perceptions. Some experiments in healthy subjects have revealed a relationship between gamma waves and maximal muscle contraction activity. This relationship is replaced by the recording of signals in the beta band during weak contractions, suggesting a correlation between cortical gamma or beta oscillatory activity and strength. Additionally, several studies have provided evidence of the role of gamma activity in the perception of both visual and auditory stimuli.

1.6.2 Signal acquisition

The EEG signal is acquired through electrodes applied to the scalp according to a standardized positioning recognized internationally. The placement of electrodes on the scalp follows the "10-20 system" standard. It is based on certain anatomical landmarks and anthropometric measurements:

1. Nasion (depression dividing the forehead and the nose);

2. Inion (bony protuberance found at the base of the skull along the midline at the rear of the head);

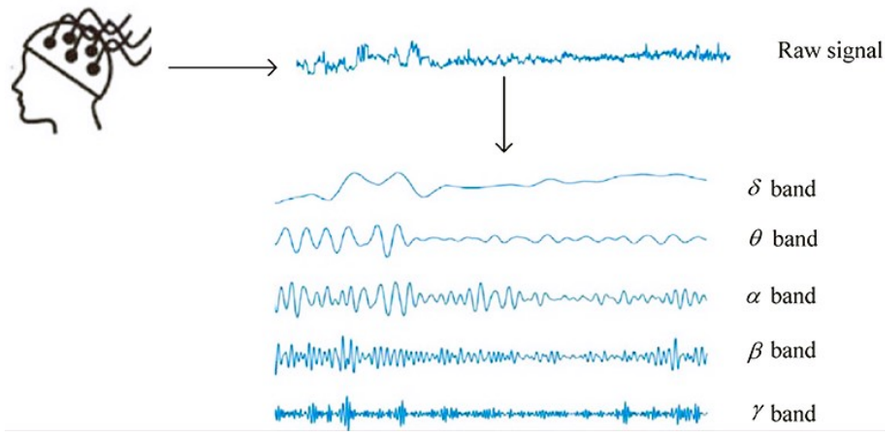

Figure 1.10: Frequency bands of EEG signal *([136])*

3. Right and left preauricular points;
4. Measurement of the distance between Nasion and Inion;
5. Measurement of the distance between the right and left preauricular points.

The individual acquisition points have a standardized name consisting of two symbols:

1. The first symbol indicates the underlying brain region:
   (a) Fp (frontal-polar);
   (b) F (frontal);
   (c) C (central sulcus);
   (d) P (parietal);
   (e) O (occipital);
   (f) T (temporal).
2. The second symbol consists of:
   (a) by the letter "z" for electrodes lying on the midline;
   (b) by an even number for electrodes located to the right of the midline and by an odd number for electrodes to the left. The number increases progressively as you move away from the midline.

In addition to the acquisition electrodes, two ear reference electrodes are also used, indicated as A1 and A2. The distances between adjacent electrodes correspond to 10% or 20% of the distance between Nasion and Inion or the distance between the preauricular points, hence the name "10-20".

The electrode placement procedure begins by measuring the distance between Inion and Nasion along the midline (lI-N) to identify the two points Fpz and Oz, at a distance equal to 10% of lI-N from Nasion and Inion, respectively. The electrodes Fz, Cz, and Pz are then placed sequentially at intervals of 20% of lI-N starting from Fpz. Subsequently, the distance between the two preauricular points A1 and A2 is measured, referred to as lA1-A2, along the transverse line intersecting Cz. For the left hemisphere, the electrodes T3 and C3 are placed sequentially at intervals of 20% of lA1-A2 starting from the midline z. The same is done on the right hemisphere with electrodes C4 and T4. Next, the distance between Oz and Fpz along the line passing through T3 is measured, and based on this measurement, Fp1 is positioned at 10% of the distance Oz-Fpz from Fpz, while F7, T3, T5, and O1 are placed sequentially at intervals of 20% of the distance Oz-Fpz starting from Fp1. The same procedure is followed for Fp2, F8, T4, T6, and O2. Additionally, along the line Fp1-O1 passing through C3, the electrodes F3, located halfway between Fp1 and C3, and P3, between C3 and O1, are placed. This is replicated for F4 and P4 on the right side. Finally, T1 and T2 are placed halfway between, respectively, F7 and T3 and F8 and T4. The electrode placement following the described standard is shown in the Figure 1.11.

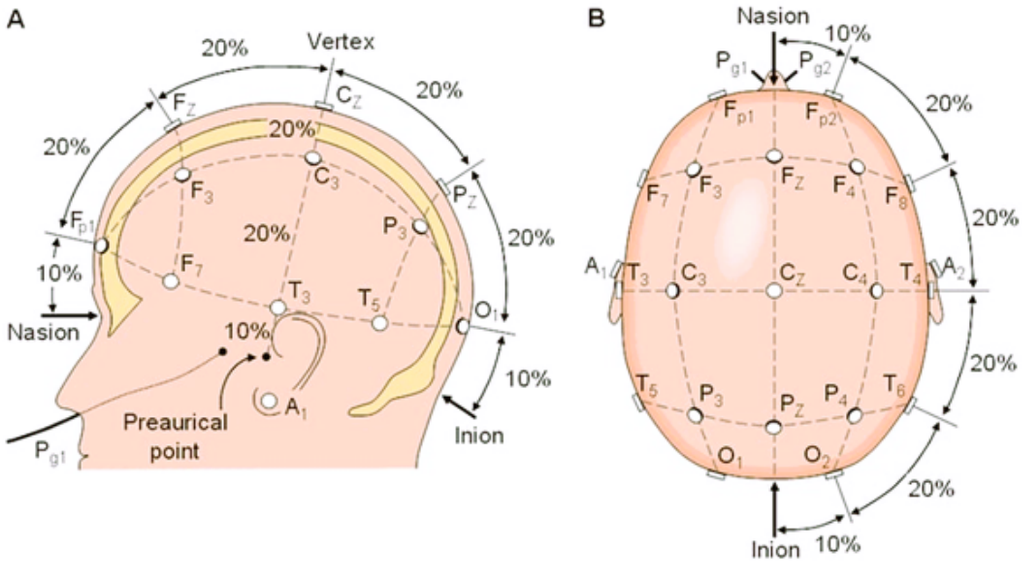

Figure 1.11: Electrode placement according to the 10-20 system: a) lateral view, b) top view. *([137])*

The electrodes cover a wide area of the skull to detect activity from multiple areas of the cortex, so a large number of electrodes are required, typically ranging from 21 for standard EEG to 256 for high-density EEG (HD-EEG). Consequently, the manual procedure (more complicated and with a higher risk of error) has been replaced by special caps that simplify the positioning of the electrodes, as shown in the Figure 1.12.

Figure 1.12: Example of a cap for EEG signal acquisition. The cap simplifies the positioning of electrodes according to the 10-10 standard.

The electrodes represent the interface between the skin and the acquisition device and have the function of transferring the potential difference generated between two points on the skin to the input of the acquisition system, converting the ionic current present in the human body into electric current. The ideal electrode is one that does not generate artifacts and does not distort the signal. It is possible to approach this ideal by carefully choosing the material of the electrodes used for signal acquisition. Generally, the most commonly used material is Ag/AgCl since electrodes made from this material respond best to these requirements as their behavior closely approximates the ideal one. The signal acquisition phase is particularly important because EEG is very sensitive to disturbances and artifacts, such as movement artifacts or

eye artifacts, and often, even though the signal is adequately processed, it is not completely clean. For this reason, it is fundamental to pay close attention during the acquisition phase, in order to limit disturbances of any nature as much as possible. Precautions to be taken for good acquisition include thoroughly disinfecting and degreasing the skin before proceeding with electrode placement, to remove any contaminations that could affect conductivity, and checking that the electrodes are not worn out. The use of a conductive gel is also very important, as it reduces the electrode-skin impedance and therefore increases conductivity, as well as the positioning of the electrodes, which must be as precise as possible. Furthermore, it is advisable to avoid recording in locations where there are electrical or electromagnetic disturbances [3].

There are different types of electrodes available in the market. There are pre-gelled electrodes (therefore disposable) or others that have a cup shape for the application of conductive gel between the electrode and the skin. The cup has a rear hole that allows the insertion of the gel after electrode placement (Figure 1.13a). Alternatively to the gel, sponges soaked in saline solution can also be used (Figure 1.13b).

However, the preparation of the skin, the application of gel, and the subsequent cleaning require a lot of time, and despite the attention paid to preparation, it could still happen that the gel leaks out, causing short circuits between adjacent channels. To avoid these problems, so-called "dry electrodes" have been developed, which rely on direct electrode-skin contact, eliminating the need for conductive gel and speeding up the placement (Figure 1.13c). Dry electrodes typically have higher electrode-skin impedance, and consequently, the electrode-amplifier system is less robust in rejecting network interference [2].

Figure 1.13: Examples of EEG electrodes: a) cup electrode, b) sponge electrode, c) dry electrode.

As already mentioned, the EEG signal is obtained from measuring the potential difference between two points. Signal acquisition can occur through monopolar (or unipolar) derivation or through bipolar derivation, as depicted in the Figure 1.14. In the first case, the signals acquired from the electrodes are referenced to the same reference point; in the second case, each EEG channel is obtained as the difference between the potentials read by two electrodes placed on the scalp, which are usually adjacent electrodes. For example, in the case of three electrodes, with one acting as the reference, the differences are measured between the potential recorded between the first electrode and the reference and that recorded between the second electrode and the reference [2].

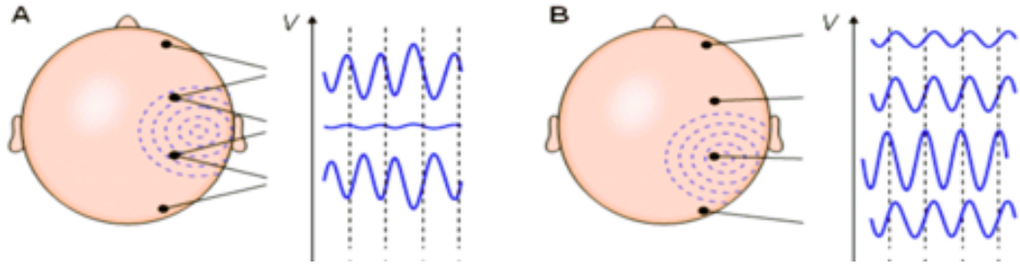

Figure 1.14: EEG Acquisition: A) Bipolar derivation, B) Monopolar (or unipolar) derivation. *([138])*

1.7 Cardiovascular system

The cardiovascular system sends blood throughout the body, adjusting speed and volume in response to various stimuli. It is composed of the heart, arteries, veins, and capillaries. This system operates in a coordinated manner to ensure adequate blood circulation to all body tissues. The regulation of the cardiovascular system results from a complex interaction between factors such as blood volume, hormones, electrolytes, drugs, adrenal glands, kidneys, and neural signals from the parasympathetic and sympathetic nervous systems [4].

1.7.1 Anatomy and physiology of the heart

The heart constitutes the functional center of the circulatory system; it is the engine that enables the transport of oxygen from the lungs to the cells of various tissues and organs for their nourishment and facilitates the exchange of carbon dioxide in the lungs. Structurally, the heart (see Figure 1.15) is a hollow organ divided into four chambers: two atria and two ventricles, each located on the left and right sides, separated by walls called septa.

Its conical shape consists of overlapping tissues:

1. The **pericardium**, a protective serous pocket surrounding the heart;
2. The **epicardium**;
3. The **myocardium**, the heart's muscular tissue;
4. The **endocardium**, lining the heart's internal walls.

The heart is composed of involuntary striated muscle tissue and has the ability to generate its own electrical impulses to trigger contraction. The sinoatrial node, located between the superior vena cava and the right atrium, acts as the "pacemaker," initiating the heartbeat and coordinating the heart's activity through the muscle fibers. Additionally, the heart is equipped with autonomic nerve fibers that form the cardiac plexus. The vagus nerve and sympathetic fibers connect the organ to the sympathetic, parasympathetic, and sensory systems, ensuring synchronized responses to stimuli from the brain.

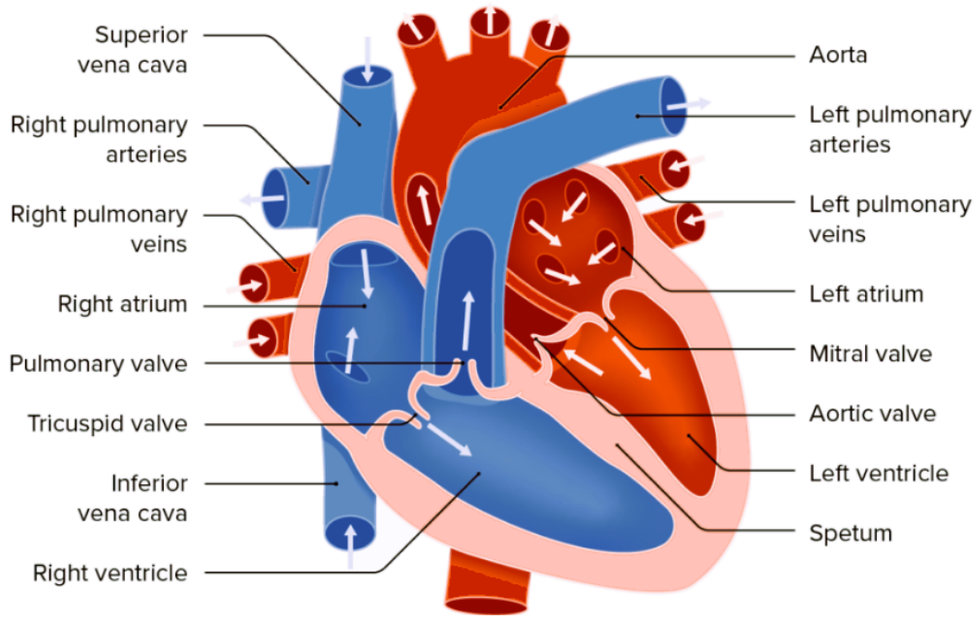

Figure 1.15: Heart's anatomy

From a functional perspective, the heart acts as a pump whose main task is to distribute oxygenated blood to the body's cells, tissues, and organs for their sustenance, and to collect carbon dioxide-laden blood to transport it to the lungs where gas exchange with oxygen occurs.

The oxygenated blood (arterial blood) travels through the body via the aorta, which is the main artery that branches into smaller arteries and capillaries. At the same time, the deoxygenated blood returns to the heart through the superior and inferior vena cava to be reoxygenated [5].

1.8 Electrocardiographic signal (ECG)

The electrocardiographic signal represents the electrical activity of the heart during contraction. It is the potential difference that can be observed through a differential amplifier between two points on the human body [2].

The ECG is a pseudo-periodic signal as the signal corresponding to one cardiac cycle repeats at more or less regular intervals over time. It is also considered pseudo-deterministic because the signal related to a cardiac cycle is composed of six basic waveforms (P, Q, R, S, T, U) that follow each other in an orderly and repetitive manner between cardiac cycles. Each of these waveforms is characteristic of specific cardiac activity, for example, the P wave is generated by atrial depolarization, while the QRS complex is generated by ventricular depolarization and the T wave by ventricular repolarization. This makes the ECG a morphologically interpretable signal.

1.8.1 Interpretation of the ECG signal

In the Figure 1.16, there's a typical ECG signal along with its corresponding nomenclature. It is possible to see the five characteristic waves of the signal in adults: P, Q, R, S, T. The U wave, which would follow the T wave, is mainly visible in pediatric age. Additionally, it is not possible to observe atrial repolarization as it is hidden by the QRS complex [2].

To interpret the signal, is necessary to analyzes the shape, amplitude, and duration of the waves. In fact, the waveform's shape, as well as the interval between two waves and the electrical level of the signal between two successive waves, are important diagnostic information. Important parameters also include the greater or lesser regularity with which cardiac cycles occur and the variability in the duration of individual cardiac cycles.
Below is a brief explanation of the characteristic features observable in an ECG [6]:

- P Wave: The P wave is produced when the sinoatrial node emits the stimulus. It represents the depolarization of the atria, which, being relatively weak, creates a small P wave. The duration of this wave varies between 60 and 120 ms, while its amplitude is at most 0.25 mV.

- QRS Complex: It is composed of three different waves: Q, R, and S. These three together represent the depolarization of the ventricles. The first of these is a negative, small wave. It corresponds to the depolarization of the interventricular septum. The R wave, on the other hand, is positive and corresponds to the depolarization of the apex of the left ventricle. Lastly, there is the S wave, which, like the Q wave, is negative and small in amplitude, representing the depolarization of the basal and posterior regions of the left ventricle. The overall duration of the QRS complex varies between 60 and 90 ms.

- T Wave: It is small in size, sometimes so small that it is not visible. It indicates the repolarization of the ventricles, which is the recovery phase of the ventricles after contraction.

- U Wave: It is only occasionally visible and appears primarily in pediatric ECGs; it represents the repolarization of the papillary muscles.

- PR Interval: It is an isoelectric line that indicates the atrioventricular conduction time, which is the interval between the beginning of atrial depolarization (start of the P wave) and the beginning of ventricular depolarization (start of the QRS complex).

- QT Interval: It represents the time required for the ventricles to depolarize and repolarize, or the duration of electrical systole. Its duration depends on the variation in heart rate but generally ranges between 350 and 440 ms. After the T wave, there is a period of electrical inactivity in the heart during which the ECG signal remains isoelectric until the next impulse.

- ST Interval: It represents the time between ventricular depolarization and repolarization, thus the interval between the end of the S wave and the beginning of the T wave. Usually,

during this phase, there is no electrical activity, so this segment is isoelectric. However, in some cardiac conditions, its amplitude can increase or decrease by up to 0.1 mV.

- RR Interval: It represents the time between two successive R waves, corresponding to the duration of the specific cardiac cycle. Normal heartbeat versus ectopic beats or other artifacts is referred to as the NN interval [132].

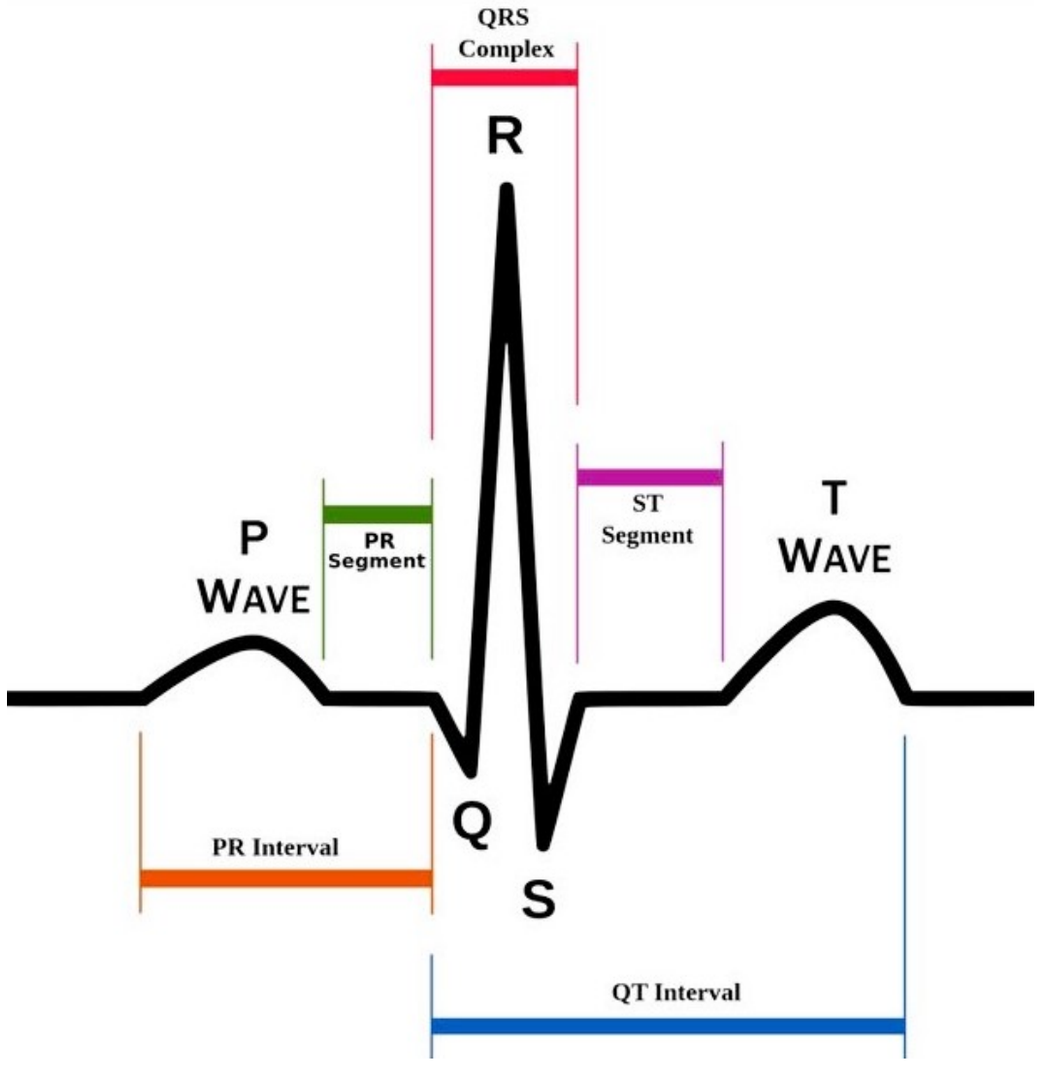

Figure 1.16: Electrocardiographic signal *(Adapted from [139])*

1.8.2 Heart rate variability (HRV)

Heart Rate Variability (HRV) is the variation in the time intervals between consecutive heartbeats. HRV is measured by analyzing the times between consecutive heartbeats, known as RR intervals. First, the R peaks are identified, and then a tacogram is created, which is a graphical

representation of these RR intervals plotted against the sequential number of heartbeats. This graph is useful for understanding heart rate variability over time and can be used to assess the condition of the autonomic nervous system.

HRV can be estimated through time domain features [7], such as the standard deviation of NN intervals (SDNN) or the root mean square of successive differences (RMSSD). Alternatively, one can move into the frequency domain and analyze the power spectral density (PSD) of the signal. Looking at the Figure 1.17, it's possible to distinguish three frequency bands: the Very Low Frequency (VLF) in the frequency range between 0.003 and 0.04 Hz, the Low Frequency (LF) between 0.04 and 0.15 Hz, and the High Frequency (HF) in the corresponding frequency range of 0.15 to 0.4 Hz. However, in this latter case, it is important to consider that a proper analysis of HRV requires signals recorded for a sufficiently long period of time. Specifically, it is necessary for the recording to be at least 10 times the length of the wavelength of the lowest frequency being investigated. If we want to provide some numbers: to evaluate the HF components (frequency below 0.15 Hz), it requires more than 1 minute of recording ($\frac{1}{0.15Hz} \times 10 = 67s$), which further increases to 4 minutes ($\frac{1}{0.04Hz} \times 10 = 250s$) for the LF components (frequency below 0.04 Hz) [127]. It's therefore evident that, in the case of real-time analysis, these parameters should be excluded.

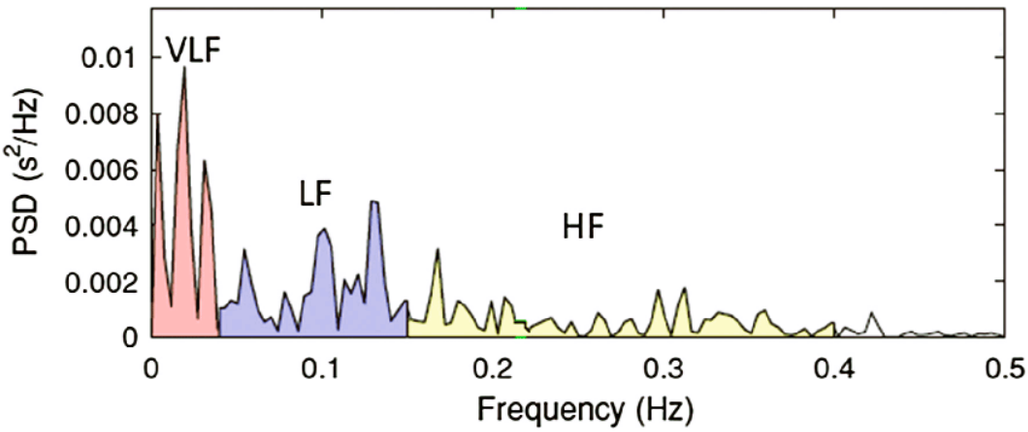

Figure 1.17: PSD estimation with FFT *([95])*

The HRV reflects how well the heart can adapt to physiological and environmental changes [8]. This is influenced by the heart rate, which in turn is regulated by the sympathetic (SNS) and parasympathetic (PNS) nervous systems. A low HRV, and thus a very regular heartbeat, indicates a reduced capacity for adaptation of the autonomic nervous system, while a high HRV indicates the prevalence of parasympathetic activity over the sympathetic one [128].

When we are stressed, our body responds by increasing the heart rate, leading to a reduced HRV. The decrease in intervals between heartbeats (RR) results in reduced values of SDNN and RMSSD, and also affects the power of the HF (which decreases) and LF (which increases) frequency bands. This complex set of changes in HRV during stress reflects activation of the

sympathetic nervous system and reduced activity of the parasympathetic system, indicating a physiological response to the stressful burden [9].

1.8.3 Signal acquisition

To collect the ECG signal, a differential amplifier is used for each observed acquisition channel. Typically, ten electrodes are used, four of which are positioned on the limbs and six on the chest, thus obtaining 12 leads (6 obtained from the electrodes placed on the limbs and the other 6 from those on the chest) [2].

The limb leads are obtained using 4 electrodes, one for each limb. Among them, the electrode of the right leg (RL) serves as a reference, while the other three electrodes sense the potential difference of the limb to which they are connected relative to the right leg. From these four electrodes, 9 possible different leads are obtained, of which 6 (those present in the Figure 1.18) are those commonly used in clinical settings:

- The standard bipolar leads, also known as I, II, and III leads, are simply derived from the potential difference measured by electrodes placed on two limbs. In the following equation, LA represents the potential measured by the electrode on the left arm, LL represents the potential measured by the electrode on the left leg, and RA represents the potential measured by the electrode on the right arm.

$$I = \text{LA} - \text{RA}$$
$$II = \text{LL} - \text{RA}$$
$$III = \text{LL} - \text{LA}$$

- The Wilson leads use the average of the potentials calculated from the electrodes on the right arm, left arm, and left leg as reference. Therefore, they consist of 3 additional leads, each obtained as the difference between the potential of an electrode and the average potential at the central node or Wilson's node. However, these leads are not used in clinical practice.

- The Goldberg leads, or augmented leads, are equivalent to those of Wilson but have an amplitude greater than 50%, which is why they are preferred over Wilson leads.

$$aVL = LA - \frac{1}{2} \times (RA + LL)$$
$$aVR = RA - \frac{1}{2} \times (LA + LL)$$
$$aVF = LL - \frac{1}{2} \times (RA + LA)$$

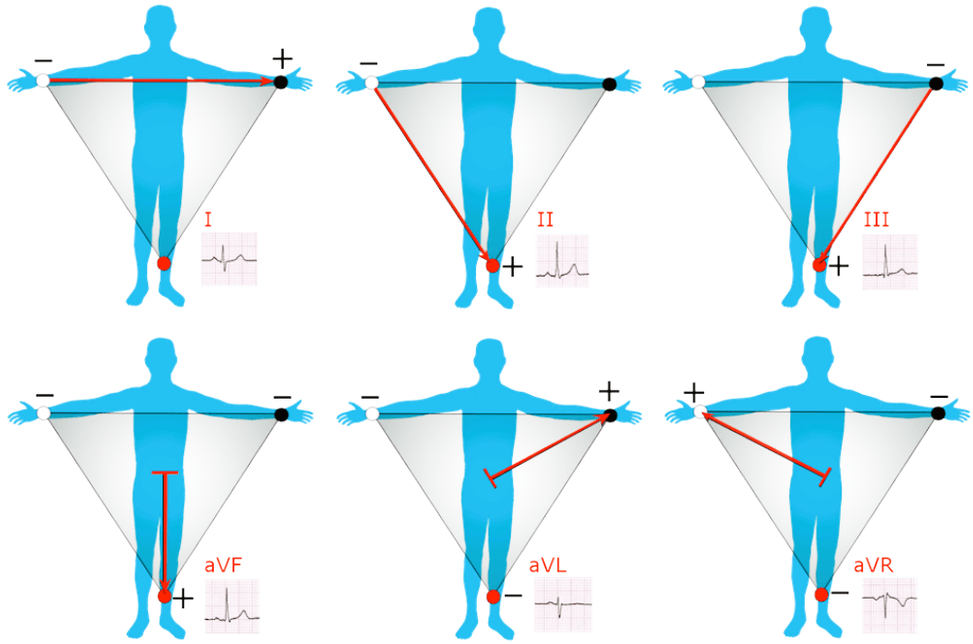

Figure 1.18: The standard bipolar leads and the Goldberg leads *(Public domain, via Wikimedia Commons)*

The six leads that are actually used are not linearly independent, but it is still advisable to observe them as they provide different perspectives on the electrical activity of the heart.

To achieve higher spatial resolution, 6 electrodes are also used on the chest following a standardized positioning as depicted in the Figure 1.19. In this case, they are referred to as precordial leads, which are named from V1 to V6.

1.9 Heart-brain connectivity

A fundamental aspect of human health is the flow of information within the body.

The nervous system uses a hierarchical method to perform this function: it starts with the central nervous system and continues with the peripheral nervous system. The central nervous system consists of the brain and the spinal cord, while the peripheral nervous system is divided into the somatic nervous system and the autonomic nervous system [129].

The autonomic nervous system (ANS) manages the body's internal balance and modulates vital functions such as breathing and heartbeat. It enables communication between the heart and brain [130].

When a person's body requires an adaptive response to a sudden change, the sympathetic nervous system quickly activates. It stimulates the necessary organs, accelerates the heartbeat, dilates the alveoli, and induces the liver to release energy.

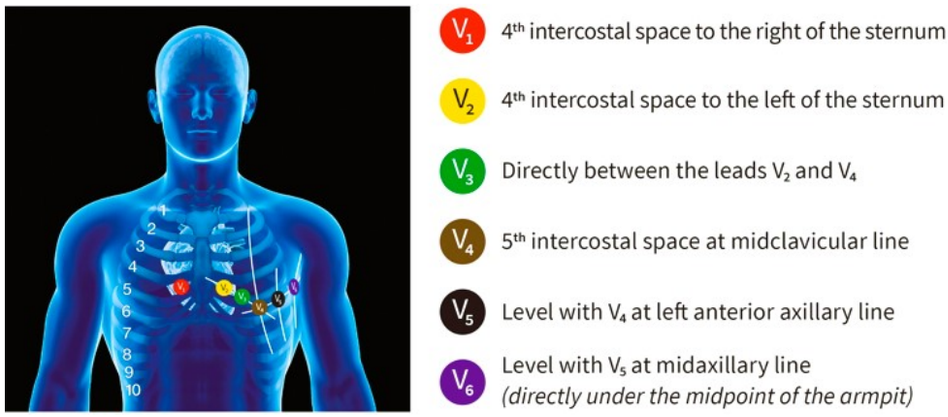

Figure 1.19: Precordial leads

At the same time, it slows down or suspends the activity of non-essential organs for body mobilization, such as the intestines. Once the stress phase is over, the other branch of the ANS, the parasympathetic nervous system, restores the body's resting state and promotes energy recovery [131].

Among the organs stimulated by this adaptive cascade, the heart is certainly the most relevant. The heart and brain are interconnected through the sympathetic cardiac nerve and the parasympathetic nerve. This innervation allows the regulation of heart rate based on the brain's signals: acceleration through the sympathetic nervous system and deceleration through the parasympathetic nervous system [130].

The vagus nerve is the main component of the parasympathetic pathway. However, the interactions between the brain and the heart are not limited to just this modulation.

The vagus nerve also facilitates the flow of information from the heart to the brain, informing the latter about the heart's functional status.

The heart is a powerful transmitter of information, very few neuroscientists have investigated the other way around, namely the possible influences of the heart on the brain. Among the first pioneers to explore these little-known areas were physiologists John and Beatrice Lacey, who in the 1960s and 1970s demonstrated how the heart sends information to the brain and strongly influences the latter in its response to the environment [10].

Subsequently, in the early 1990s, neurocardiologist J. Andrew Armor discovered what is called the "brain in the heart," an intrinsic nervous system in the heart composed of around forty thousand neurons. This system is capable of initiating physiological processes independently of the brain and is therefore referred to as the "little brain." Most of the nerve fibers in the parasympathetic branch (about 80%) are afferent, meaning that the information sent from the heart to the central nervous system is the most abundant [10].

Depending on the situations we experience in our daily lives, the heart rate reflects the adjustments the brain makes so that the body can better adapt to these situations.

These adaptations are carried out through the sympathetic and parasympathetic systems. One might ask whether this balance is always appropriate for the situation in which the person

finds themselves. In this context, the vagus nerve assumes a fundamental role. It is a specific nerve that constitutes the parasympathetic branch and originates from the brainstem, extending to the base of the brain and connecting to the main organs. It is the longest nerve in the body.

The vagus nerve is responsible for regulating the heart and other organs. In fact, it is a double nerve: information travels from the brain through one pathway and returns to it through the other [10]

1.10 Stress

Stress represents the body's reaction to stimuli that interrupt its internal balance, whether physical or psychological in nature. This reaction involves changes at the psychological, physical, and behavioral levels that allow the body to respond to the stimuli. The causes of stress can be related to physical factors, such as trauma or fatigue, but also to psychological or mental causes, such as work commitments or social pressures.

The body's response to stress is nonspecific, meaning that the same adaptation mechanisms are activated regardless of the cause of the stress. The presence of stress triggers a series of chemical mediators that activate the paraventricular nuclei of the hypothalamus, increasing alertness and preparing the body for a fight or flight reaction. At the same time, the sympathetic nervous system is also activated, and hormones such as adrenaline and cortisol are released.

The Locus Coeruleus is a brain structure located in the pons and plays a fundamental role in the body's response to stress. This structure releases norepinephrine, a neurotransmitter that prepares the brain to react to new or unexpected stimuli, thus increasing alertness and attention.

The nerve pathways of the sympathetic nervous system are those that release norepinephrine and act quickly to activate visceral organs such as the heart and lungs, while inhibiting non-essential functions such as digestion. Additionally, the release of adrenaline and cortisol further enhances the body's ability to cope with emergency situations.

When stress persists for a long time, the response to it further develops: the hypothalamic-pituitary-adrenal (HPA) axis is activated, leading to the production of cortisol, a hormone that mobilizes the energy resources needed to sustain the stress response. The hypothalamic nuclei that produce corticotropin-releasing hormone (CRH) and the locus coeruleus that releases norepinephrine are interconnected in both directions by bundles of nerve fibers, so CRH and norepinephrine stimulate each other. Additionally, the locus coeruleus is directly activated by the amygdala.

Stress also encompasses the concept of allostasis, which is the adaptation of the body by modifying physiological parameters (such as heart rate and hormone levels) in response to external stimuli. This mechanism allows the organism to adapt to circumstances by establishing a new functional equilibrium.

In summary, cognitive stress, caused by mental and emotional pressures, triggers a complex neuroendocrine response involving the brain and the nervous system, preparing the body to handle challenging situations [39]

Chapter 2

Machine Learning Algorithms

Machine Learning is a field of study within artificial intelligence that deals with creating systems that learn or improve performance based on the data they use. Machine learning is based on two main methods: classification and regression [26]. Classification involves distinguishing the class membership of a particular observation; regression is the process of estimating the relationships between a dependent variable and one or more independent variables. So, in the first case, the machine learning algorithm returns a categorical output, while in the second case, a continuous output is obtained.

Algorithms are the engines that power Machine Learning. The two main types of machine learning algorithms currently used are: supervised machine learning and unsupervised learning. The difference between these two types is defined by the way each algorithm learns data to make predictions:

- **Supervised learning**: this method learns to generate an output relative to an input based on input-output pairs provided to it as examples. The input dataset is divided into training and test datasets. The former is used to teach the algorithms certain methods that they will then use on the test dataset to train themselves. These algorithms therefore require external support as they learn from a set of data that is already labeled and has a predefined output. Among them, the Support Vector Machine (SVM) is included.
- **Unsupervised learning**: in this method, learning is not based on examples provided by a data scientist, but it is the algorithm that interprets the data and then returns the correct outputs, refining based on its own errors. Unsupervised machine learning involves training based on unlabeled data for which a specific output has not been defined. These algorithms are primarily used for feature reduction and clustering, as in the case of K-Means clustering algorithms.

In the following subsections, a brief overview of the machine learning methods used in some stress-related literature studies reported below will be provided.

2.1 Support Vector Machine (SVM)

Support Vector Machines (SVM) are supervised learning models capable of executing both classification and regression [27]. Input data belonging to two different classes are nonlinearly mapped by the algorithm into a multidimensional feature space and then a linear decision surface is constructed. Typically, the margin is considered as the hyperplane, which is drawn in such a way that the distance between the margin and the classes is maximized, thus minimizing the classification error (see Figure 2.1).

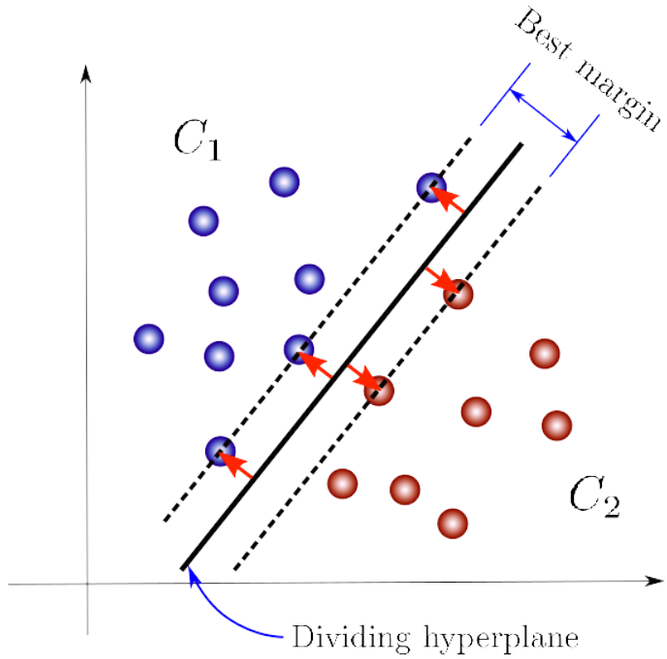

Figure 2.1: SVM binary classification example.

In addition to performing linear classification, SVMs can efficiently perform a non-linear classification using what is called the kernel trick, implicitly mapping their inputs into high-dimensional feature spaces. In practice, it adds additional features obtained by combining the original elements, thus increasing the dimensionality of the space (see Figure 2.2).

As mentioned initially, this machine learning method can also be implemented as a regressor (SVR) [43], which is particularly useful in scenarios where it is desired to predict continuous values rather than classify data into categories. In SVR, it's going to search for the function that best approximates the training data while minimizing the error and keeping it within a tolerance range.

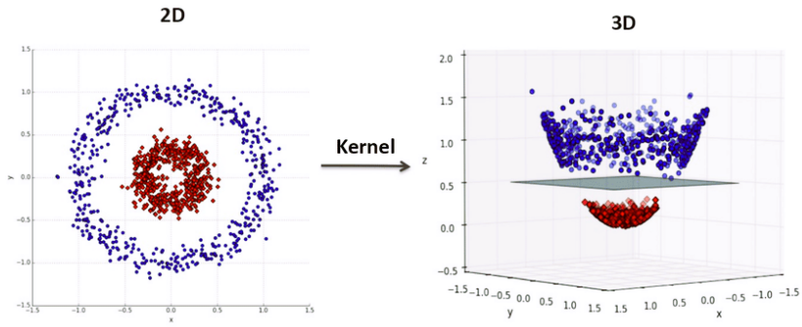

Figure 2.2: Illustration of the kernel trick applied to a two-dimensional non-linear classification problem. *(Adapted from [120])*

2.2 Random Forest

The Random Forest (RF) is based on the use of several decision trees (DT) which is, in turn, a supervised learning approach used for classification and regression.
From the main node consisting of the entire data set, several "child" trees are generated using random replicas (bootstraps) of the data present in the "parent" node. This process is repeated recursively on each subset thus derived recursively and ends when the subset in a node has the same values as the target label or when further subdivisions no longer lead to an improvement in the model's performance. The risk is that, growing a tree too much can lead to overfitting of the data, but the use of RF helps to mitigate this problem by aggregating the predictions of individual trees.
This machine learning tool can be used both as a classifier, returning an output equal to the class selected by the majority of the trees with which it was trained, and as a regressor through which the average prediction of the individual trees is returned. It also uses dimensionality reduction methods [44].
To overcome the problem of overfitting, different techniques are used including bootstrap aggregation (or bagging) and Random features subset. In the case of bagging, each tree of the forest is composed only with a subset of the original data set, obtained by random sampling with replacement. With this method it is possible to select the same sample multiple times during the creation of the subset. After training each tree on its respective subsets, the results of the various trees are then combined. In the second case, instead, each tree is trained using a different subset of the original dataset. In this way, a single tree could overfit the data of its subset, but the entire forest as a whole does not [45].

2.3 LASSO

LASSO regression (Least Absolute Shrinkage and Selection Operator) is a supervised learning technique used that, starting from the complete model, chooses a subset of independent variables that minimizes the prediction error for a quantitative response variable. This technique

is able to automatically select the relevant features thanks to the L1 penalty applied in the cost function. The L1 norm is particularly effective in managing multicollinearity and in reducing the risk of overfitting in regression models. This happens because this penalty tends to reduce the regression coefficients of some independent variables towards zero, thus eliminating the less significant or redundant ones [41].

Mathematically, given a value λ, a non-negative parameter, LASSO solves the problem [50]:

$$\min_{\beta_0,\beta} \left(\frac{1}{2N} \sum_{i=1}^{N} (y_i - \beta_0 - \mathbf{x}_i^T \beta)^2 + \lambda \sum_{j=1}^{p} |\beta_j| \right) \tag{2.1}$$

where N is the number of observations, y_i is the response to observation i, $\mathbf{x}_i$ is a vector of length p to observations i, λ is a non-negative regularization parameter corresponding to a value of Lambda, and β_0 and β are a scalar and a vector of length p, respectively.

As λ increases, the number of non-zero components of β decreases. This L1 penalty process is essential to reduce model complexity and prevent overfitting.

2.4 Clustering K-Means

K-means (Figure 2.3) is an unsupervised learning algorithm that solves the clustering problem [26]. Given a certain dataset, this algorithm classifies it into a certain number of clusters using an iterative method. This method involves defining k centers, one for each cluster; then all the points in the dataset are assigned to the nearest center until all points have been assigned. At this point, k new centroids are calculated, corresponding to the centroids of the clusters obtained previously. This process is repeated until the most accurate clustering is achieved, which corresponds to minimizing the total intra-group variance.

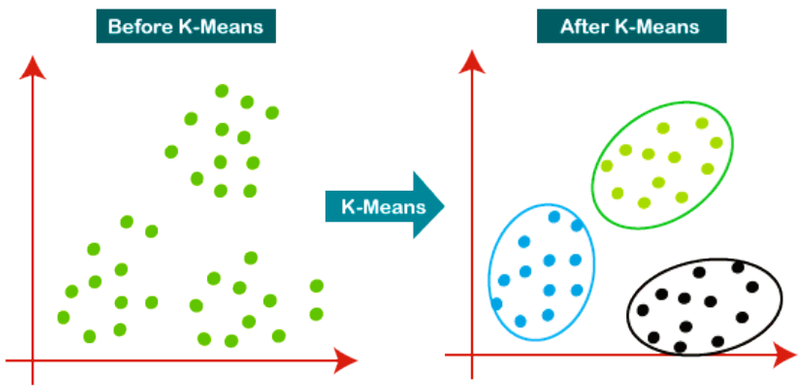

Figure 2.3: Clustering K-Means example

One method used to evaluate the stress level of subjects is certainly to use questionnaires, but also the physiological parameters of the person are useful to detect stress. In this regard, machine learning methods are often used to identify the stress state of a subject using the

physiological data recorded during stressful situations [36]. Among the most used algorithms for this purpose it is possible to identify the Support Vector Machine (SVM), the K-Nearest Neighbors Classifier, the Random Forest (RF) and the Lasso regressor, all of which have a high accuracy.
In [36] a collection of movement data and physiological characteristics of 15 subjects from the WESAD dataset was used, obtained from a device worn on the chest and a device worn on the wrist. For the training of the classification algorithms, the principal component analysis (PCA) was first applied with a number of components equal to 20, subsequently, different machine learning techniques were used and compared, including the aforementioned ones. Both a three-class classification was carried out, in which the individual is identified as amused, normal or stressed; and a two-class classification in which he is identified only as stressed or not stressed. The results showed that the accuracy reached 81.65% for the three-class classification and up to 93.20% in the case of binary classification.

Ravindar Ahuja and Alisha Banga [37] used machine learning algorithms to detect mental stress in 206 university students. They found that SVM had the best performance, demonstrating an accuracy of 85.71%, followed by RF with an accuracy of 83.33%.
In a study that detected stress levels based on EEG signals [38] the k-nearest neighbor (k-NN) algorithm produced an overall accuracy of 73.38% for classification.
In [40] the two researchers assessed the emotional state of 25 subjects through physiological markers, including EEG and ECG, and compared some regression algorithms used for their prediction. Among the analyzed algorithms there are also RF, Support Vector Regression (SVR) and the Lasso model. Emotions were distinguished on the basis of valence and arousal values and the comparison was based on regression metrics including the R^2 score, the mean square error (MSE) and the root mean square error (RMSE). According to the experimental results, the RF regressor was found to be the best as it performed well both on real-time data and in terms of regression metrics. Specifically, the training time was 3.19 s and the prediction time was 0.137 s, while, regarding the regression metrics, RF outperformed the other algorithms with an R^2 of 0.84, the MSE of 0.27 and the RMSE of 0.52, demonstrating good performance also on the dataset. Overall, it produced the best compromise between accuracy and speed among all the regressors analyzed in this study, thus also compared to SVR and Lasso.
At the University of Pisa, the Lasso regressor was used to identify potential biomarkers of physiological stress in human sweat, comparing them with physiological parameters typically associated with stress, such as heart rate (HRV), electrodermal activity and thermal imaging during a color-word Stroop test [41]. Before performing the regression, they normalized both chemical and physiological signals based on the relative resting session.
Another Italian study also used the Lasso regressor in a stress context [42]. In detail, this work aimed to compare the performance of LASSO versus that of the ordinary least squares (OLS) estimator in detecting cardiovascular, respiratory and cerebral interactions during different levels of mental stress. The results showed that, of the two methods, LASSO was the one that highlighted the role of brain activity and its connection with heart rate and breathing.

Chapter 3

Adaptive neurostimulation and binaural beats

Adaptive neurostimulation is an innovative techniques in the field of neurophysiology that allows modulation of brain electrical activity by leveraging the subject's feedback to adjust the parameters being evaluated. This approach is referred to as closed-loop method and, because it performs real-time analysis, it is very useful in studying the nervous system due to the inherently dynamic nature of neural activity. If the same stimulus is provided but with a different physiological state, the physiological effects observed can be completely different. Closed-loop brain stimulation techniques can therefore modulate or adapt the output of therapeutic stimulation in real-time in response to the local physiological environment [11].

Closed-loop neurostimulation offers two primary advantages over traditional open-loop administration. Unlike open-loop systems, which operate based on a fixed program regardless of the condition of the subject and only collecting information or measure results after the stimulation process is complete, closed-loop neurostimulation dynamically adjusts based on real-time feedback. The advantages are:

1. Increased likelihood of reaching the desired state due to enhanced stimulation efficacy, minimizing the possibility of undesirable side effects;

2. The stimulus generator works more efficiently by activating only when needed, such as when the brain shows abnormal activity or impaired function, synchronizing each stimulus with the patient's current brain state [12].

These treatments can be used for therapeutic purposes, in case of pathologies, but also for improvement purposes in healthy subjects [13].

3.1 A closer look to adaptive neurostimulation

In adaptive neurostimulation, stimulation parameters are dynamically adjusted to optimize the effect of stimulation in real-time. Stimulation is governed by a device or algorithm that

dynamically adapts to variations in the patient's brain electrical activity, thus offering more accurate and targeted treatments. The subject undergoes stimuli of various types, such as visual, auditory, and electrical, which are modulated based on brain activity or other physiological parameters, such as heart rate variability. This type of neurostimulation is very useful when the physiological or clinical effects of neuromodulation treatment are unpredictable. In this way, it's possible to monitor these effects to optimize treatment parameters relative to the effects themselves [12].

User-adaptive neurostimulation is a very promising technique because it allows for the creation of highly specific therapy that is tailored to the individual needs of the patient and can vary based on their response to stimuli. Moreover, especially when using acoustic stimulation, it is possible to treat unconscious individuals or those with altered mental states who are therefore unable to engage in any mental effort.

This technique is useful for treating neurological disorders and conditions, as well as for rehabilitation purposes, such as following traumatic brain injury or stroke. However, it can also be used in healthy individuals to enhance cognitive processes.

3.1.1 Adaptive neurostimulation using binaural beats

Binaural beats are an auditory effect that occurs when each ear is exposed to two tones at different frequencies. This effect creates the perception of a third tone whose frequency is equal to the difference between the two original tones. Binaural beats are widely used for neural stimulation because they are perceived within the frequency range of approximately 1-30 Hz, which corresponds to EEG signals [14]. Their use is based on the hypothesis of brainwave synchronization or "neural entrainment," according to which periodic external stimuli lead to the synchronization of brainwaves with the rhythm of the stimulus. Studies in the most applied fields refer to neuroscientific research that states that binaural beats induce systematic changes in EEG parameters.

Over the years, several studies have outlined the limitations of binaural beats:

1. Licklider et al [15] showed that for a binaural beat to be perceived, the two frequencies must be within a maximum of 1000 Hz, since the human ear cannot detect sounds with frequencies higher than 1 kHz.

2. From the study [16], it is evident that binaural beats seem to be perceived better at carrier frequencies – that is, the frequencies of the two tones presented – of around 400 Hz.

3. From the study by Perrott and Nelson [17], it is inferred that the maximum difference between the two tones should be around 30 Hz; beyond this, the two tones are perceived separately, although this threshold seems to depend on the stimulation technique.

The superior olivary complex (SOC) is found to be an important structure for sound integration and is identified as the primary neuroanatomical structure involved in the perception of binaural beats [18]. In this study, the auditory capacity of the subjects was tested through tonal audiometry [19]. The tones were presented via headphones to ensure that exposure to each of the two frequencies was limited to one ear only.

3.1.2 Studies on stress treatment with binaural beats

Several studies employ binaural beats (BB) to mitigate stress induced by respective stress protocols. Stress conditions alter the value of various EEG and ECG parameters, which will be discussed further in subsequent chapters. There are several studies analyzing the influence of binaural beats on stress, different studies analyze the influence of stimulation in different frequency ranges. Here, we delve into a few of the consulted studies for this project as examples.

Studies utilizing the beta band:

1. A study conducted at the American University of Sharjah developed a protocol to evoke four different mental states: rest, control, stress, and stress reduction [20]. Stress was induced through cognitive tests with time constraints, while mitigation was achieved through binaural beat stimulation. Spectral power density maps showed differences between mental states, with stress predominantly affecting the temporal region. An improvement in temporal activity was observed during stress mitigation.

2. At the same University the four mental states (rest, control, stress and stress mitigation) were examined by inducing mental stress using the time-constrained Stroop Color-Word Test (SCWT) and mitigating using 16 Hz binaural beat stimulation [21]. Results showed increased connectivity between frontal and parietal regions during stress compared to rest and control states. Similarly, during stress mitigation, increased connectivity between frontal regions was observed, indicating that binaural beats improve cognitive attention and reduce stress.

3. Katmah et all developed a study in which they evaluated the effect of 16 Hz binaural beats on cognitive vigilance and stress by subjecting participants to the Stroop Color-Word Test to induce stress, followed by 10 minutes of auditory stimulation with 16 Hz binaural beats [22]. Results showed a significant increase in target detection accuracy by 21.83% ($p < 0.001$) and a reduction in mental stress. Analysis indicated that binaural beats improved connectivity in the left dorsolateral and ventrolateral prefrontal cortex, mitigating the effects of stress on information flow between the two brain hemispheres.

Studies utilizing the theta band:

1. A 2017 study compared the effects of music embedded in theta brain wave frequency using binaural beat technology (BBT) versus music alone on the cardiovascular stress response in post-deployment military personnel [23]. The study found significant differences in heart rate variability (HRV) at both low and high frequencies ($p = 0.01$). During acute

stress testing, those exposed to BBT music showed reduced sympathetic responses and increased parasympathetic responses, while those who listened to music alone had the opposite effect.

2. A study conducted at a private Midwestern University employed the Trier Social Stress Test (TSST) and divided participants into intervention and control groups [24]. The intervention group was exposed to pink noise, carrier tones, and embedded binaural beats (BB), whereas the control group listened to pink noise and carrier tones without the BB component. Perceived stress was evaluated using a visual analog scale (VAS), while HRV was recorded. Results showed that the intervention group, listening to BB, exhibited greater parasympathetic dominance during TSST compared to the control group, suggesting that exposure to binaural beats may attenuate stress responses to acute psychological stressors.

3. E. Krasnoff and G. Cavaliere recruited subjects seeking relaxation due to stress [25]. This study revealed that measured brainwave activity indicates that binaural beats (BB) objectively induce a state of relaxation. This was evidenced by various scores obtained from EEG readings, including increased positive outlook and relaxed brain, along with scalp topographic maps. Additionally, most subjects showed improvements in microcirculation and cardiovascular scores.

Studies utilizing the alpha band:

1. A binaural beat generation internet page highlights how listening to binaural beats, through the phenomenon of *frequency following response*, can induce a subject's brain frequency towards a desired state by applying an external stimulus [76]. In particular, if the external stimulus consists of binaural beats with a frequency belonging to the alpha band, the subject's brain wave frequency tends to synchronize with that range. This state is associated with conditions of relaxation while maintaining a certain alertness.

   The study also highlights that listening to binaural beats in the theta and alpha bands not only promotes relaxation and meditation, but also improves learning abilities, helping to reduce the time needed to acquire new skills.

2. A study carried out between 2005 and 2007 analyzes the effect of Binaural Beats on various groups of subjects, with particular attention to their ability to influence the state of consciousness and psychophysical well-being [104]. In particular, it was evaluated whether listening to binaural beats at 10 Hz could induce a state of relaxation. The 39 participants were divided into different groups: subjects without pathologies (16 participants); children with behavioral disorders (9 participants); adolescents with anxiety disorders, depression or borderline diagnoses (4 participants); and adults with borderline diagnoses (3 participants) or neurotic disorders (6 participants).

   Each subject listened to a soundtrack containing Binaural Beats for 10 consecutive sessions. Psychophysical and behavioral reactions were monitored and recorded to evaluate the effect of listening.

For non-pathological subjects, relaxation or awakening was generally observed, with listening difficulties only in the youngest children. Among children with behavioral disorders, some showed a positive reaction such as relaxation, while others could not tolerate listening. Adolescents with neurotic disorders appreciated listening more, reporting benefits such as relaxation and rest. Adults with borderline diagnoses had difficulty concentrating on listening, with some experiencing discomfort and agitation. Finally, adults with neurotic disorders completed the sessions, reporting positive feelings such as serenity and relaxation.

3. In a study published in 2018, 40 young subjects were assessed for auditory reaction times (ART), visual reaction times (VRT), and short-term memory in three different conditions: no stimulation and stimulation with constant alpha and gamma binaural beats [80]. For ART and VRT, the tests consisted of clicking a computer key as soon as they heard a 1000 Hz beep or as soon as they saw colored circles. For working memory, the task consisted of memorizing a numerical sequence and remembering whether a certain number displayed on the screen was part of that sequence. The results showed statistically significant differences for ART and VRT in the conditions with binaural beats compared to the one without stimulation, indicating an improvement in attention through entrainment with alpha and gamma binaural beats. Working memory, on the other hand, did not show values with statistical difference despite having better scores in the presence of stimulation.

4. J. Kraus and M. Porubanova conducted a study in which 50 university students were divided into two groups: both groups listened to the sound of the sea and, in one of the two groups, this sound was superimposed with stimulation with alpha BBs [85]. Stimulation with BB was carried out before subjecting the subjects to the task. The task used was the AOSPAN task which consists in responding to a mathematical expression by evaluating whether the proposed result is true or false, then a sequence of letters is displayed, with each letter shown for 800 ms and, at the end of the presentation of this sequence, a matrix of letters appeared and the participant had to remember the order in which these letters had been presented. The final analyses revealed an improvement in attention and working memory in subjects to alpha binaural beat stimulation compared to the control group.

Chapter 4

Materials and Methods

4.1 Research question

The aim of this study is to develop a closed-loop system capable of modulating binaural beat (BB) stimulation in real time, with the aim of reducing the detected stress level and improving users' performance. The experimental question underlying this research is whether stimulation with binaural beats adapted to the subject's stress state can actually improve performance and positively influence the stress level, compared to stimulation with binaural beats at a constant frequency.

To achieve this goal, the project is divided into three fundamental phases:

1. Creation of a protocol capable of inducing both stress and relaxation in the subjects, so that the model can learn from data of different nature;
2. Development of a model capable of estimating the stress level in real time;
3. Devising a method to adapt binaural beat stimulation based on the estimated stress level.

Furthermore, the study aims to compare the effectiveness of adapted stimulation with that of constant binaural beats, in order to determine which of the two strategies leads to better results in terms of stress reduction and performance improvement. A key aspect of the research is to evaluate whether adapted stimulation can improve users' performance regardless of the difficulty level of the task performed.

4.2 Instrumentation and communication protocols

The equipment utilized in this study comprises the 8-channel Enobio device from Neuroelettronics for capturing EEG and the ECG signals from the participants, NIC2 software that allows the communication between the Enobio and the authors' personal computers.

4.2.1 Enobio 8

The Enobio system in Figure 4.1 comprises a portable and wireless device tailored for monitoring EEG signals, along with additional functionalities for EOG and ECG monitoring. Operating within a bandwidth of 0 to 125 Hz, a sampling rate of 500 SPS and an ADC with a dynamic resolution of 24 bits (0.05 μV), it provides robust data acquisition capabilities [28].

Included in the Enobio kit are essential components such as the Enobio Necbox, serving as the core device that can be attached to the neoprene cap via a velcro patch. The 8-channel connector, despite its name, consists of 10 cables - 8 for active signal monitoring and 2 for reference signals (CMS and DRL). Each cable terminates with connectors compatible with the electrodes utilized for signal acquisition (see Figure 4.2).

The Enobio system also allows for the recording of ECG signals, which requires additional accessories: an extension for electrode (Figure 4.3) and adhesive electrodes in Figure 4.4 that are also used for CMS and DRL references.

For further information on the system it's possible consult the technical file at the following link: `https://www.neuroelectrics.com/solutions/enobio/8/`

In this study, 7 channels are dedicated to EEG signal acquisition and one for ECG monitoring via a wrist extension cable, while adhesive disposable electrodes were employed for reference, positioned behind the ears at the mastoid bone level.

Figure 4.1: 8-channel Enobio *([28])*

Figure 4.2: Channels connector *([28])*

Figure 4.3: Electrode extension

Figure 4.4: Adhesive electrode

4.2.2 NIC 2 Software

The Neuroelectrics Instruments Controller (NIC) software [29], specifically NIC2, serves as a comprehensive interface for managing Enobio and Starstim devices from a computer. It facilitates EEG signal monitoring and experiments involving transcranial electrical stimulation, offering various connection modes including USB cable, Bluetooth, and Wi-Fi.

Once connected, NIC2 provides extensive control over signal processing and visualization. Users can enable TCP/IP protocol for data transmission to external software like Matlab, and configure line noise filters at either 50 Hz or 60 Hz. Moreover, visualization filters can be set to display signals within specific frequency bands (figure 4.5).

The software allows for the inclusion a maximum of 9 markers during experiments, each corresponding to keyboard buttons 1 to 9, facilitating later segmentation of data. Users can create detailed acquisition protocols specifying step names, durations, and channel configurations. The software supports multiple file formats for data storage, including .easy, .edf, .nedf, and .sdeeg, with the option to transmit data via Lab Streaming Layer (LSL) for real-time analysis (Figure 4.6).

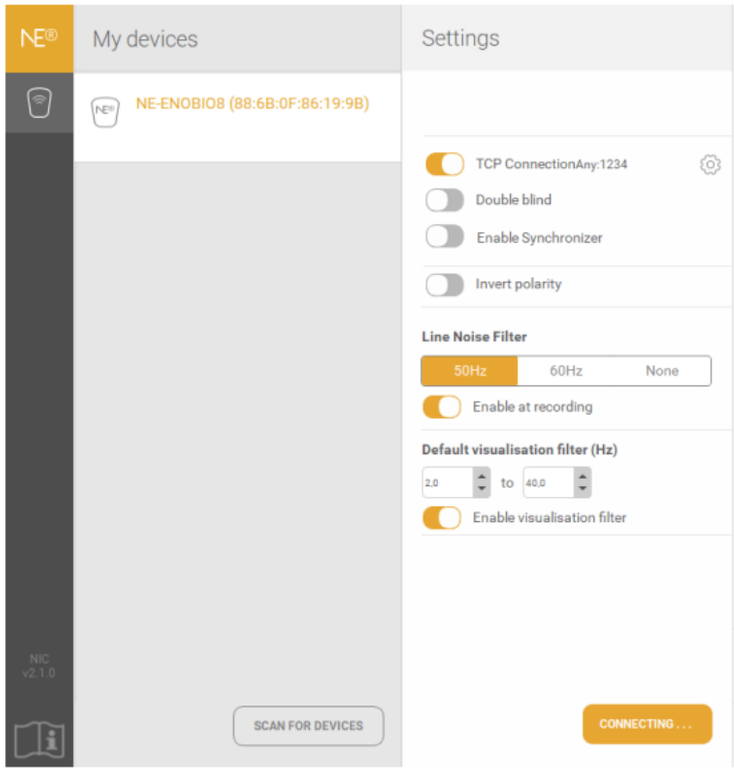

Figure 4.5: NIC2 settings

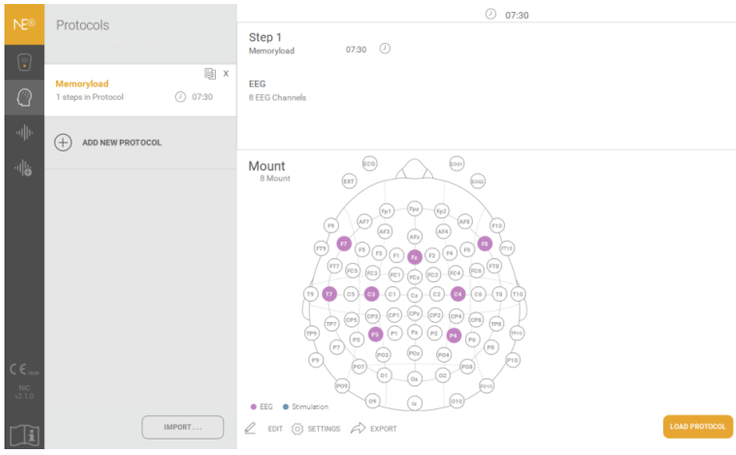

Figure 4.6: NIC2 protocol

During acquisition, NIC2 provides a liveview panel for monitoring EEG signals and stimulation experiments. Users can adjust visualization parameters such as channel reference, time window, and voltage scale. Additionally, quality assessment of EEG signals is facilitated through a quality index (QI), with each channel color-coded based on signal quality: green for excellent, orange for good, and red for poor (Figure 4.7).

Figure 4.7: NIC2 channels

Overall, NIC2 offers a user-friendly graphical interface, simplifying interaction with Enobio device. It provides comprehensive control over signal acquisition, processing, and visualization, enhancing the efficiency and accuracy of EEG experiments and analyses. The protocol can be initiated, halted, and renamed at the top of the screen.

4.2.3 Matlab Toolkit

For EEG signal processing, both offline and in real-time, Matlab was used. Specifically, the following libraries were employed: the EEGLAB plugin and MatNIC, used respectively for the import of the signal recorded through the Enobio hardware and for communication with the NIC software.

MatNIC is a tool developed by Neuroelectrics used to run NIC2 while in real time and remotely using Matlab [30]. TCP/IP, which stands for Transmission Control Protocol/Internet Protocol, is a set of communication protocols used to connect network devices on the Internet [31]. In our study, Matlab acts as the client, initiating the connection, while NIC2 functions as the server, waiting for incoming connections. Once the connection is established, data can be transmitted bidirectionally across the network. In our study, the TCP/IP connection is used for loading and initiating EEG, ECG and stimulation protocols. TCP/IP is also used for communication between Matlab and Python where Matlab acts as the client and Python functions as the server.

For the NIC real-time interaction with Matlab the Lab Streaming Layer (LSL) connection

were used. The LSL is a flexible set of libraries and software tools to synchronize multi-modal times, stream real-time data, and stimulate. As a prerequisite, LSL necessitates that all software that communicates data from and to an external device should be on the same network with the device that is running the LSL server [32]. The LSL connection in this experiment is utilized for EEG signal recording and sending markers from the LSL server to NIC2.

4.3 Experimental Protocol

Here is a brief description of the protocol used in this study. The individual parts are explained in more detail in the following subchapters. The participant is made to sit on a chair in front of a white wall to avoid distractions. He is asked to fill out two questionnaires: the perceived stress scale (PSS) and a questionnaire regarding the activities carried out in the last 24 hours. Once the questionnaire has been filled out, the subject is asked to adjust the brightness of the computer, put on headphones and is asked to adjust the volume so as to isolate himself from the environment, being careful not to set the volume too high so that it does not bother him later and the subject is subjected to two hearing tests to evaluate the quality of the subject's hearing and to the evaluation of the subject's hearing perception threshold. Once these procedures are completed, the participant is made to wear the equipment and the electrodes are positioned. The subjects were asked not to keep their eyes closed during the entire duration of the experiment, to move as little as possible and not to speak from the moment the experiment began. The protocol consists of four acquisitions:

1. **Calibration**: this was the first acquisition performed for each subject, useful for extracting all the features specified in subsection 4.4.2 and training the chosen regressor model;

2. **Stimulation with constant binaural beats**: this condition consists in repeating the experiment by subjecting the subject to listening to binaural beats at a constant frequency;

3. **Stimulation with adapted binaural beats**: this condition consists in repeating the experiment by subjecting the subject to listening to binaural beats at a adapted frequency in real time based on his/her stress level;

4. **Absence of stimulation**: this phase serves as a control condition, useful for verifying that any improvements in performance or stress management are actually due to stimulation and not to external reasons.

The order in which each subject was subjected to the last three conditions was randomized to avoid bias problems. Each acquisition is structured as follows:

- **Task test**: each subject was asked to perform a short and simplified simulation of the mathematical task, so that they could understand how it was most comfortable to position themselves to provide answers with the keyboard buttons;

- **Baseline** (3 minutes): relaxation phase useful to normalize all the data acquired and in order to restore the state of relaxation before subjecting the subject to the new condition;
- **Evaluation of self-perceived stress**: the subject is asked to evaluate his/her state of stress using the visual analogue scale (VAS) with a range ranging from -4 to +4, -4 indicates "very relaxed", 0 is "neutral", +4 "very stressed";
- **Countdown**: a 3-second video with a countdown is shown in order to make the subject understand that the mathematical task is about to begin;
- **Mathematical task** (5 minutes): the subject finds himself/herself answering mathematical expressions through multiple choice with a time limit;
- **Self-perceived stress assessment**: the subject is asked again to assess his/her state of stress through the VAS.

The structure of the protocol with the choice of alternating task phases with relaxation phases and the timing adopted for the duration of each phase refers to studies given below in which the stress of the subjects was investigated: [52]; [53]; [54];[55]; [56] and [57]. Participants are warned that they will have to repeat the experiment four times but they are not told that the conditions vary from one acquisition to the next. In order to further increase the stress of the participants, they were said that they would be recorded during the entire execution of the protocol with a video camera positioned immediately above the computer screen, and the video would then be sent to experts to analyze the correlation between facial expressions and stress. Stress is in fact a condition that also depends greatly on the psychological condition of the subject as suggested by numerous studies on stress such as [46], [47], [48] to name a few. Only at the end of the experiment were the subjects informed that, in reality, no recording had been started.

4.3.1 Questionnaires

As previously mentioned, all subjects were asked to fill out two types of questionnaires. The first questionnaire, the Perceived Stress Scale (PSS) [49] is a classic stress assessment tool developed in 1983 and still widely used to assess feelings and perceived stress [99]. The questionnaire concerns the feelings and thoughts developed by the subject in the last month. It consists of 10 questions to which one of the following answers can be provided:

- 0: never;
- 1: almost never;
- 2: sometimes;
- 3: fairly often;
- 4: very often.

This test allows to classify the subject into three stress classes:

1. low stress: scores ranging from 0-13;
2. moderate stress: scores ranging from 14-26;
3. high perceived stress: scores ranging from 27-40.

The second questionnaire [74] instead deals with the subject's conditions over a shorter period of time, in particular the subject was asked questions about carrying out certain activities in the last 24 hours. The first part of the questionnaire was the same for all subjects, the second part of the questionnaire instead concerned the female population, as it concerned the menstrual cycle and pregnancy.

The two questionnaires had two different purposes. The first is useful in order to know the starting stress level of the subject before being subjected to the experiment. The second instead was useful in order to adopt exclusion criteria to exclude from the dataset subjects who for external reasons would have introduced a bias in the study. As for the exclusion criteria, reference was made to [74], among those applied in this study we cite: caffeine consumption in the hours preceding the experiment that would have influenced both the electroencephalographic characteristics, but above all the electrocardiographic ones, drug consumption in the 24 hours preceding the experiment, excessive alcohol consumption in the 24 hours preceding the experiment, the intake of psychotic drugs and if the subject at the time of the experiment was in the menstrual phase. A total of 40 subjects were acquired, consisting of 21 males and 19 females, all university students. However, the application of these exclusion criteria, combined with signal acquisition problems that occurred during some recordings, led to the elimination of half of the participants. The final dataset consists of 20 subjects, including 14 males and 6 females. These are university students: the average age is 24.75 years with a standard deviation of 1.89; the average height is 172.15 cm with a standard deviation of 9.69 and the average weight is 68.35 with a standard deviation of 13.64. Nobody is a night worker; 10 of them practiced sports in the 24 hours before the experiment and 3 subjects are smokers.

It is possible to view the two questionnaires in appendix B and appendix C

4.3.2 Hearing test

To assess the hearing ability of the subjects, they were made to wear headphones and were subjected to a test to ensure that the hearing quality of the subject was appropriate for the experiment since the stimulation provided is an auditory type stimulation with a different frequency between the two ears. To do this, a hearing test was used obtained from the website of the Italian audiological center Audire composed of a pure tone with increasing frequency. For each subject, the two ears were tested separately and they were asked to stop the video when they could no longer hear the sound. All participants stopped the video after the 16 kHz threshold, as expected given the average age of the sample. They stopped the video at the same frequency when analyzing both ears, indicating that the hearing was equivalent for both. Consequently, all subjects in the study passed the hearing test. The test used and the

instructions for use are reported at the following link: `https://www.youtube.com/watch?v=nnJGKHZ5yUw`

4.3.3 Perception threshold and use of brown noise to mask binaural beats

A second hearing test was performed to define the subject's auditory perception threshold. During the experiment, in order to isolate the subject from the surrounding environment, they were made to listen to relaxing music with brown noise superimposed in the case of acquisitions with stimulation. Brown noise, in fact, serves to mask the binaural beats so that the subject does not notice them [51]. In order to estimate the subject's perception threshold, they were asked to adjust the volume of the device so that listening to the music with brown noise superimposed was high enough to isolate them from the environment but not so much as to cause annoyance. Once the volume of the device was set, pure tones were superimposed on the music plus noise using a python code developed by us for this project that was able to reproduce three seconds of sound at a modulated volume between 0 and 1. The volume of the first tones sent to the subject were high enough to ensure that the subject could distinguish them from the underlying music. The volume was decreased in 0.01 steps until the subject no longer reported hearing the sound. The perception threshold thus identified was used to adjust the volume of the binaural beats specifically for each subject. For this purpose, various tests were carried out to identify the best condition: initially, 0.5 dB was added to the hearing threshold of the subject, the purpose behind this idea was to ensure that the brain perceived the stimulus. However, all the tested subjects revealed that they recognized the presence of the binaural beats compared to the condition without stimulation. In order to make the binaural beats inaudible in line with [51] it was decided to subtract 0.5 dB from the hearing threshold of the subject. This choice turned out to be the optimal one since the binaural beats were not heard by the participants, but, at the same time, they led to positive effects on attention as reported in chapter 5.

4.3.4 Baseline

The baseline phase consists of a light image with a darker cross in the center (Figure 4.8).

This choice is useful in order to focus the subject's gaze on the screen, avoiding that he looks around, compromising the state of relaxation that is hoped to be achieved in this phase [52]. The baseline phase lasts 3 minutes. This choice was dictated both by the above-mentioned studies and for experimental reasons. Since there are different opinions in the literature about how long this phase should last, in this study we tried to find the optimal duration for the experiment in question starting from the suggestions in the literature and making numerous attempts based on the feedback from the subjects acquired during the pilot tests and on the results provided by the regressor, concluding with the minimum duration so that the subject did not feel bored but such that it was possible for the regressor to recognize the difference between the two phases. As already anticipated in the introduction of this chapter, the baseline phase

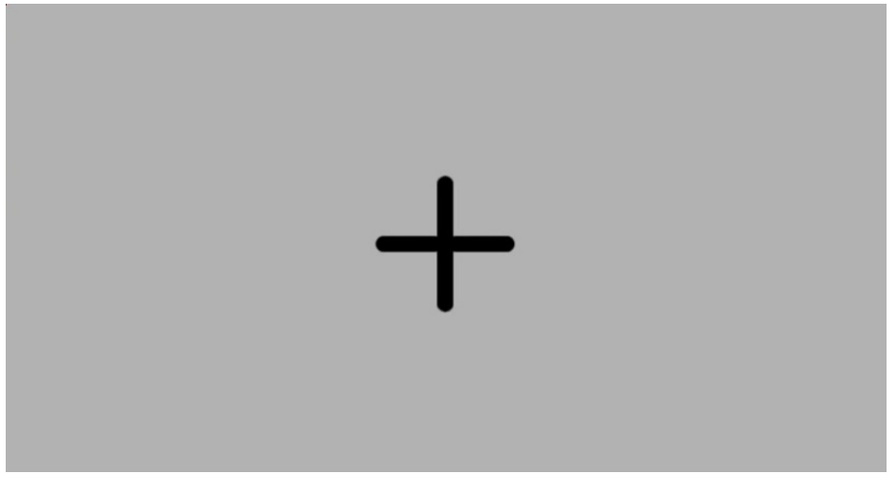

Figure 4.8: Baseline screen

recorded during calibration was used to normalize the metrics of the four acquisitions before performing the regression [58]. The data were normalized using the z-score normalization:

$$z = \frac{x - \mu}{\sigma} \tag{4.1}$$

Where:

- z is the normalized value (z-score)
- x is the original value of the data
- μ is the mean of the distribution
- σ is the standard deviation of the distribution

4.3.5 Math task

As a stress-inducing phase, it was chosen to subject the subjects to the resolution of mathematical expressions. Numerous studies can be found in the literature on methodologies for inducing controlled stress in subjects and, among the most widespread methodologies, the Trier Social Stress Test TSST [47], the Stroop Color and Word test (SCWT) [60] or even mathematical tests [61] such as successive subtractions [62], the MIST test [63] and mathematical calculations [52] are cited. By comparing with the literature, taking into account the resources available in this study and the experimental question to be answered, a 5-minute arithmetic test was developed.

This test requires answering a series of mathematical calculations within a certain time limit. The timer for each question is displayed on the screen (Figure 4.9).

The subject was shown a multiple choice calculation lasting 3 seconds. On the screen, participants could also see the number of correct and incorrect responses they were giving. Additionally, feedback on the best result achieved by participants in the study up to that day

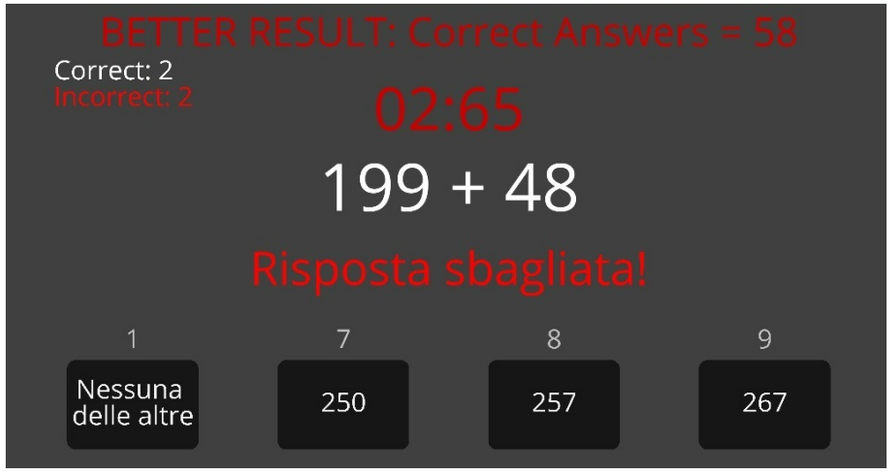

Figure 4.9: Math task screen

was provided. This was intended to increase competitiveness among the participants and thus make the protocol more stress-inducing. The mathematical task was divided into two levels of difficulty, in fact, three minutes of the five minutes had a higher level of difficulty and 2 minutes had a lower level of difficulty. This choice was made to evaluate how binaural beats behave when the task is difficult. The structure of each question in the two difficulty levels varies depending on the type of operation and was chosen so that the variation in difficulty was perceived but, at the same time, the 3 seconds made available were sufficient to elaborate an answer so as to avoid the subjects answering randomly.
In the easy task part:

- **Sums and subtractions**: the first value of the operation was a two-digit number between 60 and 90 to which a number between 6 and 15 was added/subtracted;
- **Multiplications**: the multiplicand was a number between 2 and 9 and the multiplier was between 5 and 10;
- **Divisions**: the dividend was between 2 and 8 and the divisor between 5 and 11.

To increase the difficulty, in the difficult part of the task:

- **Adding and Subtracting**: the first value was a three-digit number between 100 and 400 and the second was a number between 20 and 99;
- **Multiplications**: the multiplicand became a number between 9 and 13 and the multiplier between 7 and 20;
- **Divisions**: both the dividend and the divisor were numbers between 6 and 12.

In all these cases, the digits composing the equation were chosen randomly by the python code developed specifically but with a unique seed for each experimental condition (calibration, stimulation with constant binaural beats, stimulation with adapted binaural beats and no

stimulation) so as to ensure that all subjects were subjected to the same mathematical operations in the various stimulation conditions, guaranteeing reproducibility between subjects and also allowing the repeatability of the study.

Every time the subject answered incorrectly, the message "Incorrect answer!" was displayed on the screen, or "Not given" if no answer was provided within the 3 seconds available. The error message was also displayed in 30% of the questions chosen for each recording as an additional stress stimulus so as to be able to analyze the results of this strategy.

4.3.6 Self-reported stress

To assess the level of stress perceived by the subjects during the experiment, they were asked to self-assess their state of stress both at the end of the relaxation phase and once they had finished the mathematical task. This assessment was carried out using the Visual Analogue Scale (VAS), a tool widely used in psychology and clinical settings to measure subjective states, such as pain or stress.

The Visual Analogue Scale is a psychometric scale that allows to subjectively quantify a personal experience. It typically consists of a horizontal line, on which the subject indicates the perceived level of a certain sensation or state. The ends of the line represent the extreme limits of the experience, such as "absolutely absent" at one end and "maximum present" at the other [64].

In the context of this experiment, the VAS was used as a stress self-assessment tool. Participants were asked to select a value from those available on the line to indicate their stress level, with values ranging from -4 to +4 as in Figure 4.10.

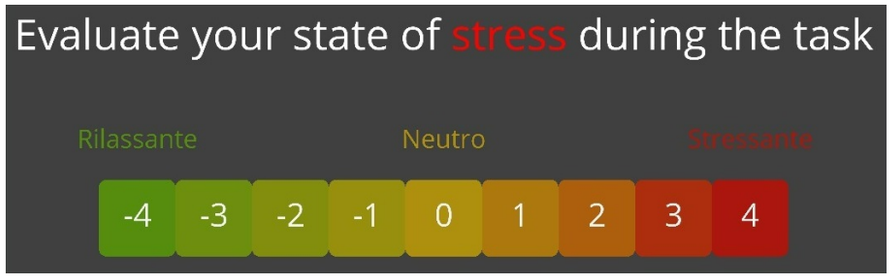

Figure 4.10: Stress auto-assessment screen

In particular:

- -4 corresponds to "very little stressed";
- 0 indicates a "neutral" state;
- +4 represents the state of "very stressed";

VAS was chosen for this study because of its ease of use and its ability to provide a discrete but detailed measure of stress, thus allowing to detect variations in the emotional state of the subjects.

4.3.7 Electrode placement

The correct positioning of the electrodes is crucial to ensure accurate acquisition of the physiological signals necessary for the analysis. In the present study, the choice of the electrode positions for the acquisition of the electroencephalographic signals was made following an in-depth analysis of the studies in the literature, some of which are reported: [52], [65], [66],[67].

Electrodes were placed in correspondence with the frontal (Fp1, F3, Fz, F4, Fp4) and parietal (P3, P4) regions to better capture the brain activity related to the cognitive processes involved in the mathematical task and to the state of relaxation.

In addition to the standard EEG electrodes, two specific electrodes were used:

- DRL (Driven Right Leg): Placed on the right ear, the DRL was used as a reference to reduce common mode noise and therefore to improve the signal-to-noise ratio for both EEG and ECG signals;
- CMS (Common Mode Sense): Placed on the left ear, the CMS detected the common mode signal of the subject's body for both systems, EEG and ECG. This signal was used to improve the overall quality of the recording, reducing common interference between the electrodes.

For recording the electrocardiographic (ECG) activity, an electrode of the Enobio was used that was placed on the left wrist. This electrode detected the main cardiac electrical activity, working in combination with the DRL and CMS electrodes.

4.4 Signal Preprocessing and Analysis

This section illustrates the main signal processing and analysis steps, which are essential for extracting meaningful information from raw data. Starting from preprocessing, which aims to improve signal quality by reducing noise and distortions. Next, feature extraction is discussed to identify and quantify the relevant characteristics of the signal. Finally, the problem of outlier detection and elimination is addressed, which is essential to ensure the robustness of the analyses.

A specially designed Matlab code has been developed to perform these operations, which allows to automate and optimize the various processes. The code starts with the preparation of the environment, implements filtering algorithms, feature extraction techniques for identifying significant features, and methods for detecting and managing outliers, ensuring an accurate and reliable analysis.

4.4.1 EEG and ECG filtering

Signal preprocessing is a very important step in preparing raw data before they are analyzed. This subsection describes the techniques used for filtering and segmentation of the EEG and ECG signal with the aim of improving the signal quality and simplifying the extraction of

meaningful information. The developed Matlab code implements these techniques, which ensure efficient and accurate pre-processing.

Appropriate filtering has been applied on both EEG and ECG signals to reduce noise and isolate the relevant frequency components for further analysis. The EEG filter masks are shown in Figures 4.11 and 4.12, the ECG filter masks are shown in Figures 4.13 and 4.14

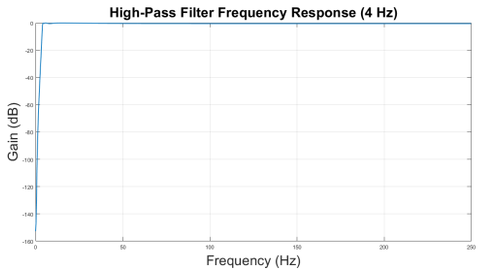

Figure 4.11: EEG high-pass filter

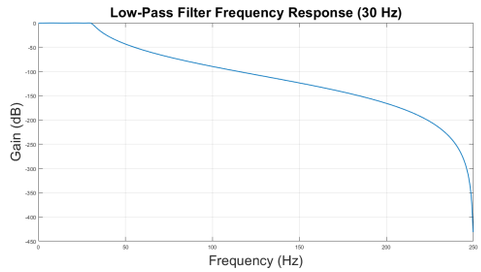

Figure 4.12: EEG low-pass filter

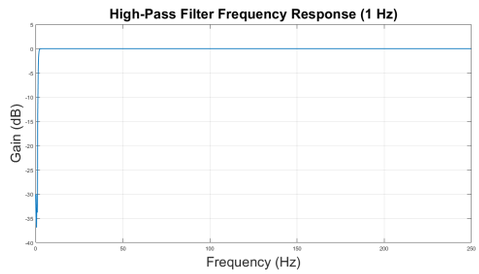

Figure 4.13: ECG high-pass filter

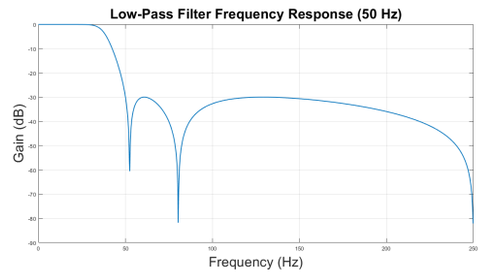

Figure 4.14: ECG low-pass filter

- **EEG Signal Filtering**: The EEG signal is filtered using a high-pass filter with a cutoff frequency of 4 Hz and a low-pass filter set to a cutoff frequency of 30 Hz. Both filters are designed using a first-order Chebyshev filter with 0.5 dB of passband ripple and a 40 dB attenuation. This configuration allows to keep only the components of interest, minimizing low- and high-frequency interference;

- **ECG Signal Filtering**: The ECG signal is filtered using a high-pass filter with a cutoff frequency of 1 Hz and a low-pass filter with a cutoff frequency of 50 Hz. Second-order Chebyshev filters were used for both filters, with a passband ripple of 1 dB and a 30 dB attenuation. The goal of this filtering is to maintain the physiological components of the ECG and reduce low-frequency interference, such as baseline motion, and unwanted high frequencies.

- **Signal Segmentation**: Once filtered, the EEG and ECG signals are segmented based on the markers used during recording to identify the baseline and mathematical task phases of the subjects.

4.4.2 Feature extraction

The main goal of this study is to improve the performance of subjects under stress states through the use of binaural beats at a constant frequency equal to the individual alpha frequency of the subject or by adapting the frequency of the binaural beats to the stress state of the subject over time. For this purpose, a regressor has been developed, whose threshold identifies the stress state of the subject. In order to implement such an index, it is essential to extract significant features from the EEG and ECG data. In this study, the electrocardiographic signal and the electroencephalographic signal were acquired, for which 7 channels were used. In total, after a careful analysis of the literature ([101],[102],[117],[118],[100],[52],[121]) about the most significant features to extract to discriminate the state of stress from that of relaxation, 23 features were extracted from the EEG and 4 from the ECG for a total of 160 features (multi-channel features). Each of these will now be described in detail.

Regarding the features extracted from the electroencephalographic signal:

- **Mean**: calculates the mean value of the EEG signal of a given signal segment. Its mathematical formula is:
$$\mu = \frac{1}{n}\sum_{i=1}^{n} x_i \tag{4.2}$$
  - n is the total number of samples in the epoch;
  - x_i represents each sample in the epoch;

- **Median**: represents the central value of the data of an epoch of the EEG signal when the data are sorted in ascending order.

- **Variance**: measures the dispersion of the values with respect to the mean.
$$\sigma^2 = \frac{1}{n}\sum_{i=1}^{n}(x_i - \mu)^2 \tag{4.3}$$

- **Standard deviation**: expresses the dispersion of the EEG signal values in units of the same magnitude as the signal.
$$\sigma = \sqrt{\sigma^2} \tag{4.4}$$

- **Minimum value**: lowest value within the epoch of the EEG signal.
$$\text{Min}(x) = \min(x_1, x_2, \ldots, x_n) \tag{4.5}$$

- **Maximum value**: The highest value within the EEG signal epoch.
$$\text{Max}(x) = \max(x_1, x_2, \ldots, x_n) \tag{4.6}$$

- **Range**: The difference between the maximum and minimum values of an EEG signal epoch.

$$\text{Range}(x) = \text{Max}(x) - \text{Min}(x) \tag{4.7}$$

- **Kurtosis**: A measure of the relative flatness of an EEG signal epoch distribution.

$$\text{Kurtosis}(x) = \frac{\frac{1}{n}\sum_{i=1}^{n}(x_i - \mu)^4}{\sigma^4} \tag{4.8}$$

- **Skewness**: measure of the symmetry of the distribution of an epoch of the EEG signal with respect to the mean.

$$\text{Skewness}(x) = \frac{\frac{1}{n}\sum_{i=1}^{n}(x_i - \mu)^3}{\sigma^3} \tag{4.9}$$

- **25th Percentile**: value below which 25% of the sorted data of the EEG signal epoch fall.

$$P_{25}(x) = x_{\left(\frac{n+1}{4}\right)} \tag{4.10}$$

- **75th Percentile**: value below which 75% of the sorted data of the EEG signal epoch falls.

$$P_{75}(x) = x_{\left(\frac{3(n+1)}{4}\right)} \tag{4.11}$$

- **Mobility**: measures how rapidly the signal changes over time.

$$\text{Mobility} = \sqrt{\frac{\text{var}\left(\frac{dx(t)}{dt}\right)}{\text{var}(x(t))}} \tag{4.12}$$

- **Complexity**: measures the irregularity and complexity of the signal over time.

$$\text{Complexity} = \sqrt{\frac{\text{Mobility}\left(\frac{dx(t)}{dt}\right)}{\text{Mobility}(x(t))}} \tag{4.13}$$

- **Power ratios**:

  Power ratios between different frequency bands are a useful indicator to understand cognitive mechanisms related to stress. Power ratios provide a more precise view of brain dynamics than single frequency bands [116].

  - *Power ratio* β/α: The ratio of power in the beta band to that in the alpha band of the EEG signal.

$$\frac{P_\beta}{P_\alpha} \tag{4.14}$$

    An increase in this ratio is often associated with increased alertness and mental tension. During stressful situations, Beta activity tends to increase, indicating greater

cognitive effort, at the same time, Alpha activity, which typically reflects a state of relaxation, tends to decrease.

- *Power ratio* β/θ: The ratio of power in the beta band to that in the theta band of the EEG signal.

$$\frac{P_\beta}{P_\theta} \tag{4.15}$$

High values of this ratio are often observed during tasks that require high attention and mental effort, and a significant increase is associated with conditions of acute stress.

- *Power ratio* θ/α: The ratio between the power in the theta band and that in the alpha band of the EEG signal.

$$\frac{P_\theta}{P_\alpha} \tag{4.16}$$

A low Theta/Alpha ratio may suggest a condition of reduced stress, where states of calm and relaxation prevail. On the contrary, in conditions of stress or prolonged cognitive effort, an increase in Theta activity with respect to alpha activity is often observed, thus increasing the ratio.

- **Spectral Entropy (SE)**:

Spectral entropy measures the complexity or unpredictability of a signal, such as a brain wave, by analyzing the distribution of the signal's energy across different frequencies. This concept is based on Shannon entropy, which quantifies the information or uncertainty in a system.

A signal is analyzed by examining its power spectrum, which shows how the signal's energy is distributed across different frequencies. This spectrum is then normalized to resemble a probability distribution, where the sum of all probabilities equals one. Spectral Entropy is calculated using the following formula:

$$H = -\sum_{m=1}^{N} P(m) \log_2 P(m), \tag{4.17}$$

where $P(m)$ is the probability associated with each frequency m, and N is the total number of frequencies.

Spectral Entropy allows us to compare different signals or systems. Higher SE values indicate a more complex or less predictable signal, such as white noise, which has all frequencies uniformly distributed [110].

In this study, SE is used to analyze EEG signals during cognitive tasks, helping to assess the level of brain engagement and distinguish between states of concentration and rest. SE is therefore useful for building predictive models that attempt to interpret and classify different mental states.

In Matlab, there is a function `pentropy` that calculates the Spectral Entropy of a signal over time. This function makes it easier to visualize entropy variations over time, providing an indication of the complexity of the signal at various times.

- **Approximated Entropy modified**:

  The approximated entropy modified is an improved method for measuring the complexity of brain signals (EEG). The original method, called Approximate Entropy (ApEn), was useful for studying EEG signals, but it had some limitations due to its sensitivity to various parameters, such as sampling frequency and epoch length, which could lead to inconsistent results.

  To overcome these problems, the Modified Approximate Entropy [119] was developed, which optimizes the original method to make it more stable and reliable. The main modifications include:

  - *Adjusted delay time:* The delay time between signal points is adjusted to better match the specific frequency of the EEG signal. This prevents the signal from being sampled too many times, preventing distortions in the results.
  - *Dynamic tolerance level:* The tolerance, which determines how close the points must be to be considered similar, is chosen dynamically to ensure an adequate number of recurrent points, making the complexity measure more reliable.
  - *Vector Smoothing:* Some vectors in lower dimensions are eliminated to maintain stability, ensuring that the computation remains consistent.
  - *High-pass Filter:* A filter is used to remove low-frequency trends, so that the analysis focuses only on frequencies that are relevant to the specific EEG signal.
  - *Theiler Window:* A technique is introduced to prevent points that are too close in time from being considered similar, reducing false indications of complexity.

  Modified Approximate Entropy makes it more precise to study the complexity of EEG signals, especially during cognitive tasks. This method improves the ability to understand how brain activity changes in response to different cognitive loads, providing more stable and reliable information than the original method.

- **Fuzzy Entropy (FuzzyEn)**:

  Fuzzy entropy is an evolution of traditional complexity measurement techniques and is designed to be less sensitive to noise and data variations than Approximate Entropy (ApEn) and Sampled Entropy (SampEn).

  FuzzyEn evaluates how similar parts of a temporal signal are using a fuzzy function that assigns a more gradual degree of similarity than a simple equality comparison. This approach reduces sensitivity to small changes in the data, making the complexity measure more robust and reliable.

Fuzzy Entropy is particularly useful for the analysis of physiological signals, such as EEG, where the presence of noise and the need for reliable measurements are critical factors [111].

- **Multiscale Entropy (MSE)**:

  Multiscale entropy is an advanced method for assessing the complexity of temporal signals, which extends the concept of entropy to different time scales. This approach is particularly useful for analyzing biological signals, such as EEG, which exhibit characteristics across multiple time scales, from rapid oscillations to slower variations.

  The basic idea of MSE is to compute the entropy of the signal not only at the original time scale, but also on coarse-grained versions of the signal, representing the signal at different temporal resolutions. This process allows capturing the intrinsic complexity of the signal at multiple levels, providing a more complete view of its dynamics [112].

- **Higuchi Fractal Dimension (HFD)**:

  The Higuchi fractal dimension is a useful tool for analyzing the complexity of temporal signals, such as EEG, and for understanding brain activity. It measures the irregularity or complexity of a signal and can reveal subtle changes associated with different cognitive states.

  To calculate HFD, a time series is segmented into sub-sequences:

$$(X(1), X(2), \ldots, X(N)) \tag{4.18}$$

  From these, new series are formed for each initial time m and time interval k, creating k new series:

$$X_{mk} = X(m), X(m+k), X(m+2k), \ldots, X\left(m + \left\lfloor \frac{N-m}{k} \right\rfloor \cdot k\right) \tag{4.19}$$

  Where m ranges from 1 to k. For each value of k, the length $L_m(k)$ is given by the normalized sum of the absolute differences between consecutive points of the signal distant k units from each other:

$$L_m(k) = \left(\sum_{i=1}^{\left\lfloor \frac{N-m}{k} \right\rfloor} |X(m+ik) - X(m+(i-1)k)| \right) \times \frac{N-1}{\left\lfloor \frac{N-m}{k} \right\rfloor \cdot k} \tag{4.20}$$

  The HFD is then calculated as:

$$FD = -\frac{\log L_m(k)}{\log k} \tag{4.21}$$

  Where $L(k)$ is the calculated length and k is the time interval [113].

- **Katz Fractal Dimension (KFD)**:

  The Katz fractal dimension is an important method for analyzing the complexity of EEG signals, allowing us to assess the structural complexity of neural oscillations [114]. The KFD calculates the fractal dimension as a scalar index that reflects the shape and dimensionality of the EEG wave. Generally, fractal dimensions range between 1 and 1.5, where lower values indicate simpler waves and higher values indicate more complexity.

  The KFD is calculated using the total length of the signal L, the sum of the distances between consecutive points, and d, the maximum distance from the origin point of the wave to the farthest point:

$$L = \sum_{i=1}^{N-1} \text{dist}(i, i+1) \tag{4.22}$$

$$d = \max \text{dist}(1, i) \tag{4.23}$$

  The fractal dimension (FD) is then determined by the logarithmic ratio between L and d:

$$FD = \frac{\log(L)}{\log(d)} \tag{4.24}$$

  For EEG analysis, it is essential to normalize the scale, using an average interpoint distance a to adjust the FD calculation:

$$FD = \frac{\log(L/a)}{\log(d/a)} \tag{4.25}$$

- **Alpha asymmetry**:

  Alpha asymmetry is a measure used to analyze the differences between alpha brain waves (8-13 Hz) in the two hemispheres of the brain. This measure is useful for understanding asymmetries in brain activity, which can provide information about emotions, attention, and other psychological states.

  Alpha waves are associated with a state of relaxation and calm, however, asymmetry between alpha waves in the two hemispheres can reflect different psychological states, for example, greater alpha activity in one hemisphere than the other may indicate a predisposition toward specific emotional or cognitive states.

  To calculate Alpha Asymmetry, the following procedure was adopted:

  - *Calculation of Alpha Power*: In this study, the powers were calculated by Fourier transform in the channels F3, F4, Fp1 and Fp2.
  - *Determination of Asymmetry*: calculated as the ratio between the difference and the sum of the alpha power in the left hemisphere and that in the right hemisphere.

$$A = \frac{P_{\mathrm{L}} - P_{\mathrm{R}}}{P_{\mathrm{L}} + P_{\mathrm{R}}} \tag{4.26}$$

where P_{L} is the power of alpha waves in the left hemisphere and P_{R} is the power of alpha waves in the right hemisphere.

– *Interpretation*: A positive value of A indicates greater alpha power in the left hemisphere than in the right, while a negative value indicates greater power in the right hemisphere. These values can be related to various psychological or cognitive conditions, for example, higher alpha activity in the right hemisphere is often associated with greater emotional reactivity or stress [115].

The features extracted from the electrocardiographic signal were:

- **Beats Per Minute (BPM)**: represents the number of heartbeats per minute, calculated as:

$$\mathrm{BPM} = \frac{60}{\mathrm{RR}_{\mathrm{average}}} \tag{4.27}$$

where $\mathrm{RR}_{\mathrm{average}}$ is the average interval between consecutive heartbeats (in seconds). BPM is a fundamental indicator of heart rate, used to evaluate the body's response to different stimuli.

- **Root Mean Square of Successive Differences (RMSSD)**: measure of heart rate variability that reflects short-term variations. It is calculated as:

$$\mathrm{RMSSD} = \sqrt{\frac{1}{N-1}\sum_{i=1}^{N-1}(\mathrm{RR}_{i+1} - \mathrm{RR}_i)^2} \tag{4.28}$$

where RR_i is the interval between consecutive heartbeats and N is the total number of intervals. The RMSSD is particularly sensitive to parasympathetic variations.

- **Standard Deviation of NN intervals (SDNN)**: The SDNN represents the standard deviation of the NN intervals (intervals between consecutive normal heartbeats). It is calculated as:

$$\mathrm{SDNN} = \sqrt{\frac{1}{N}\sum_{i=1}^{N}(\mathrm{RR}_i - \mathrm{RR}_{\mathrm{average}})^2} \tag{4.29}$$

where $\mathrm{RR}_{\mathrm{average}}$ is the average interval of the NNs. The SDNN is used to assess the overall heart rate variability.

- **Percentage of NN intervals that differ by more than 50 ms (pNN50)**: The pNN50 measures the percentage of consecutive pairs of NN intervals that differ by more than 50 milliseconds. It is calculated as:

$$\mathrm{pNN50} = \frac{\text{Number of pairs with difference} > 50 \text{ ms}}{N-1} \times 100 \tag{4.30}$$

where N is the total number of intervals. The pNN50 is an indicator of heart rate variability and vagal tone.

To identify the R peaks from the ECG signal in order to calculate the metrics mentioned above, we used the Pan-Tompkins algorithm [124] [125]. This algorithm is capable of detecting the QRS complex in real-time through signal processing and adapting to possible irregularities in the heart rhythm. Specifically, it utilizes filters, including a band-pass filter between 5 and 15 Hz and a derivative filter to highlight the QRS. Subsequently, the signal is squared and averaged to reduce noise. The filtering varies according to the sampling frequency of the signal to best suit its characteristics. The algorithm also performs a series of checks to ensure the correct identification of the R peaks. Among these is the verification that the detected peak is actually related to the QRS complex and not a T wave with particularly high amplitude. In this regard, if a peak is detected after the heart's refractory period but within 360 ms from the previous QRS complex, the mean slope of this waveform is evaluated and compared with that of the immediately preceding R peak: if the current wave's slope is less than half that of the previous wave, it is assumed to be a T wave and is thus discarded. Additionally, if no peak is detected within a sufficiently long time interval, the algorithm realizes it has missed a QRS and initiates a search, thereby limiting the number of false negatives. The minimum time interval from which the algorithm starts to look for the QRS complex is 1.66 times the current RR interval, given that physiologically, the time between two consecutive heartbeats cannot vary faster than this. To reduce false positives, the algorithm also eliminates all those peaks identified as possible QRS complexes but that actually occurred during the heart's refractory period, i.e., within 200 ms of the last detected QRS, since physiologically, the ventricles cannot be depolarized during this time despite the presence of a stimulus. In the Matlab code used in this thesis [126], an additional check is performed to identify noise: a peak with a latency less than both 360 ms and half the average RR interval is considered noisy. Below are the two images obtained by the Pan-Tompkins algorithm for a subject of this study. They show the results of the signal processing (Figure 4.15) and the identification of the QRS complexes (Figure 4.16).

To ensure temporal coherence between EEG and ECG epochs, an approach was adopted that uses 5-second windows with a 4-second overlap for both signals. This means that the features were extracted from 5-second segments, but updating the calculation every second. This method allows obtaining a feature value every second, but based on the data collected in the previous 5 seconds, ensuring greater continuity and reliability in the measurements. This methodology was applied both to the features extracted from the ECG and to the entropy measures.

For all other features, in order to respect the computational constraints and allow real-time processing within the 10 seconds available between the presentation of successive stimuli, a different calculation method was implemented. In this case, the 5-second window was divided into 10 sub-intervals of half a second each. Features were then computed for each sub-interval, and the results were then averaged to obtain a single representative value for the entire 5-second window. The same 4-second overlap was maintained in this approach. This approach allows for

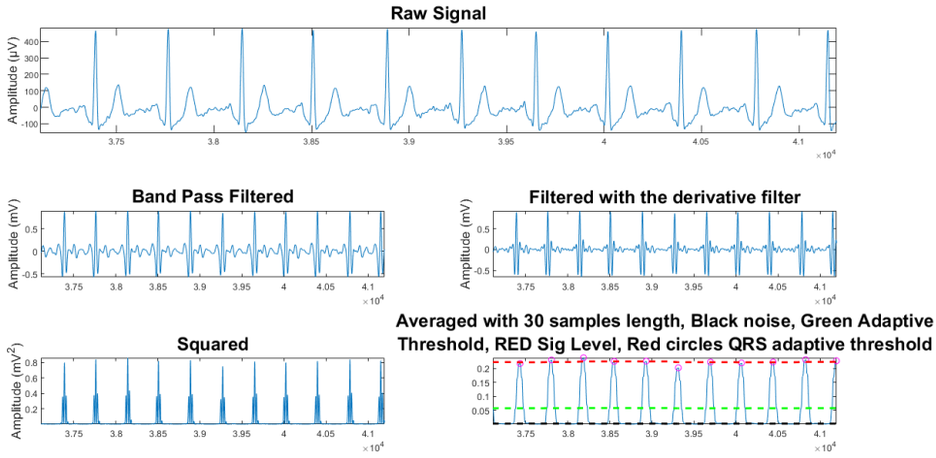

Figure 4.15: Signal processing

a reduction in computational load, while maintaining signal integrity and estimation accuracy.

4.4.3 Outlier detection and elimination

For the analysis of the data, the presence of outliers can significantly impact the results, making it difficult to interpret correctly. An outlier is an observation that deviates significantly from the majority of the data, suggesting that it may have been generated under different conditions or by a different process. In EEG or ECG data, outliers can arise from a variety of factors, such as external interference, subject motion artifacts, or technical issues with the equipment.

To address this issue, `Matlab` provides the `isoutlier` function, which is particularly useful for identifying and removing outliers, using, among others, the Median Absolute Deviations (MAD) method. The MAD method is effective for handling outliers in data that may not follow a normal distribution. This method calculates the median of the absolute deviations from the median of the data, providing a measure of variability. An observation is generally considered an outlier if it is more than three times the median absolute deviations (MAD) from the median [68].

The `isoutlier` function in `Matlab`, when configured to use the MAD method, identifies outliers by evaluating how much the data deviates from the median in terms of the MAD. The command to use the MAD method is:

```
TF = isoutlier(A, 'median')
```

In this command, `A` represents the input dataset. The `'median'` specification instructs the function to use the MAD method to detect outliers. The function then returns a logical array `TF` of the same size as `A`, where `true` indicates an outlier.

In this analysis for EEG and ECG data, the `isoutlier` function was used with the MAD method to pre-process the data. This step was crucial to maintain the integrity of the dataset.

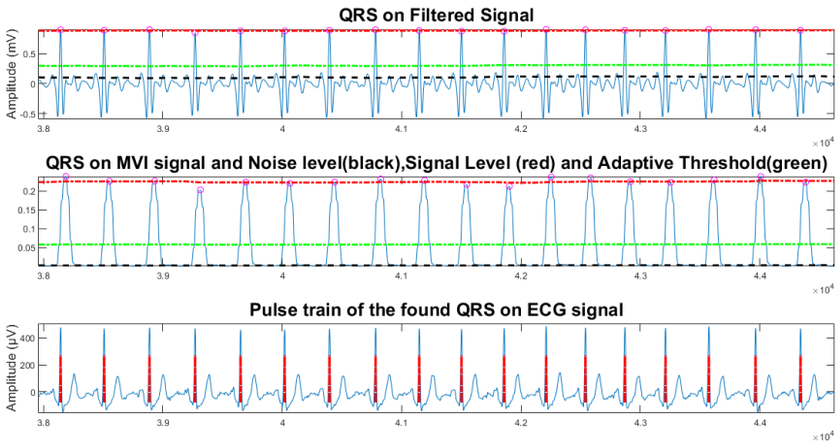

Figure 4.16: Identification of QRS complexes

By effectively identifying and eliminating outliers, the reliability of subsequent analyses, including the calculation of various complexity measures and the interpretation of signals in relation to cognitive states, was improved.

4.5 Model training

This section describes the process of preparation and training a Random Forest-based regression model. In particular, EEG feature selection was performed using the Fisher Ratio to choose the most relevant features; ECG features were added to these and then the Random Forest model was trained.

4.5.1 Feature selection: Fisher ratio

The Fisher Ratio is a technique used to select the most relevant features for a specific problem, since it is able to distinguish between different conditions by measuring how much a given feature is discriminant between two classes. It helps to identify the most relevant features by evaluating the ratio between variance between classes and variance within classes, improving the classification accuracy. In particular, the formula it adopts is the following[33]:

$$\mathrm{FR} = \frac{(\mu_1 - \mu_2)^2}{\sigma_1^2 + \sigma_2^2} \tag{4.31}$$

where μ_1 and μ_2 are the means of the distributions considered and σ_1 and σ_2 are their variances.

In this context, the Fisher Ratio is applied to the features extracted from the signals to identify the most discriminating ones between the two classes: relaxation and stress. First, all the

features are normalized with respect to those of the baseline. Subsequently, the Fisher Ratio is calculated for each feature, excluding those of the ECG. The features are ordered according to the Fisher Ratio and the best 25 are selected, which will then be used to train the regressor together with those of the ECG. The choice to use only 25 features was made following experimental tests that led to identifying the minimum number of features that would allow for a regressor with excellent performance at the same time. In this method, the ECG features were not considered for two main reasons:

1. The features calculated for the EEG are much higher than those of the ECG, so for the former it is necessary to make the feature selection while it is not for the latter since there are only 4 features;

2. One of the objectives of this thesis is to evaluate the relevance of the ECG on the study that was carried out, therefore it was chosen to include these characteristics for the training of the Random Forest regardless and then evaluate later whether the regressor considered them more or less important compared to the 25 EEG characteristics selected by the Fisher Ratio;

4.5.2 Comparison between regressors

To evaluate which regressor to use, experimental tests were performed comparing three different models: Random Forest, SVM and LASSO. Initially, for Random Forest and SVM, tests were performed on the same subject to evaluate the best parameters to use to have a good regression. Calibration was used as the training set and stimulation with constant binaural beats as the test set. The choice of the best regressor was based on the values of the regression metrics.

As for the Random Forest, with the same number of trees (Tree = 300), the kfold with k = 20 was chosen because both k = 20 and higher values of k (such as k = 22, k = 21, k = 25, k = 30) allow for excellent regression metrics on the training set, but these metrics relating to the test set worsen when using k values greater than 20. Similarly, even lower values, such as k = 5, k = 10, K = 15 had worse performances than k = 20. With the same Kfold (k = 20), different combinations were evaluated by varying the number of trees to train (Tree = 50, Tree = 100, Tree = 200, Tree = 250, Tree = 300, Tree = 350, Tree = 400) and the best was 300 because it is the one with the best metrics for the test set in addition to having excellent values also in the training set. As for the SVM, various kfolds were evaluated (with k = 5; k = 10; k = 15; k = 20), but, with the same number of evaluations of the objective function, the kfold with k = 5 was better; with the same kfold (k = 5), the number of evaluations of the best objective function is 50 because compared to the other values explored (10, 30, 40) it had better performances on the test set.

Once the parameters to be used for the Random Forest and the SVM were identified, we moved on to making comparisons between regressors: to evaluate which is the best regressor we carried out pilot tests with 3 subjects. For each regressor, two signals were used (one as a

training set and one as a test set). These signals are related to the same subject and were acquired 5 minutes apart from each other. The following parameters are taken into consideration for the comparison between the regressors:

1. Execution time in the training set;
2. Regression metrics in the training set for the i-th subject;
3. Regression metrics in the test set for the i-th subject;

The regression metrics considered are:

- The coefficient of determination R^2: measures how well the data are explained by the proposed model. More precisely, it represents the variation of the dependent (or response) variable that can be attributed to the variation of the independent variable through the regression model. Values of R^2 close to 1 indicate a good ability of the model to predict the observed data, while values close to 0 indicate a poor prediction ability. The formula is as follows:

$$R^2 = 1 - \frac{\sum_{i=1}^{n}(y_i - \hat{y}_i)^2}{\sum_{i=1}^{n}(y_i - \bar{y})^2} \tag{4.32}$$

  Where: y_i is the observed value; $\hat{y}_i$ is the value predicted by the model; $\bar{y}$ is the mean value of the observations and n is the number of observations.

- Mean Square Error (MSE): measures the average of the squared errors, or the difference between the observed value and the predicted value. A low MSE indicates that the predicted values are very close to the observed values. The formula is given by:

$$\text{MSE} = \frac{1}{n}\sum_{i=1}^{n}(y_i - \hat{y}_i)^2 \tag{4.33}$$

- Root Mean Square Error (RMSE): It is simply the square root of the MSE. So the formula is as follows:

$$\text{RMSE} = \sqrt{\text{MSE}} = \sqrt{\frac{1}{n}\sum_{i=1}^{n}(y_i - \hat{y}_i)^2} \tag{4.34}$$

- Mean Absolute Error (MAE): It measures the average of the absolute differences between the observed values and the predicted values. Unlike MSE and RMSE, it does not consider the variability of the errors (squared error). The formula is:

$$\text{MAE} = \frac{1}{n}\sum_{i=1}^{n}|y_i - \hat{y}_i| \tag{4.35}$$

  In the MSE, RMSE and MAE formulas y_i is the observed value; $\hat{y}_i$ is the value predicted by the model and n is the number of observations [107].

The tables 4.1 and 4.2 show the results obtained for the training set and the test set respectively.

Regarding the execution time on the training set, the LASSO is the best; followed by the Random Forest and finally by the SVM which has a significant gap. The execution time was then also evaluated in the test set which confirmed these trends. Regarding the regression metrics on the training set, the best is the SVM, followed by the Random Forest which however is slightly distant from the first and lastly the LASSO. Regarding the regression metrics on the test set, it is not possible to draw up a ranking because each regressor was the best for a subject.

At the end of these comparisons it was concluded that using the Random Forest seems to be the most appropriate choice because:

1. It has acceptable execution times (unlike the SVM);
2. It has excellent performances on the training set, in fact, it distances itself by very little (by a negligible value) from the performances of the SVM (unlike the LASSO)
3. It has good performance in the first subject test set and acceptable performance in the third subject test set.

Subject	**Regressor**	**Execution time** [s]	R^2	**MSE**	**RMSE**	**MAE**
First Subject	Random Forest	15.466234	0.972243	0.029451	0.171614	0.068339
	SVM	47.039248	0.973696	0.024345	0.156503	0.110739
	LASSO	4.892293	0.833969	0.160632	0.400789	0.307492
Second Subject	Random Forest	14.956177	0.971093	0.030248	0.173921	0.064958
	SVM	61.625078	0.980553	0.019584	0.139942	0.102218
	LASSO	0.991465	0.86636	0.133645	0.36557	0.259642
Third Subject	Random Forest	15.169868	0.980188	0.022306	0.149353	0.069244
	SVM	39.735030	0.986955	0.013951	0.118116	0.096379
	LASSO	0.584839	0.896795	0.103207	0.321259	0.251579

Table 4.1: Results of the different regressors for each subject: signal used as Training Set

LASSO also seems to be a good choice because it has almost immediate execution times and, despite having worse regression metrics than the other two regressors, they are still good values. However, Random Forest was preferred because it has better metrics than LASSO at the expense of only 10/15 seconds more of execution. On the other hand, SVM is excluded because its execution times are too long for a real-time analysis.

Subject	Regressor	Execution time [s]	R^2	MSE	RMSE	MAE
First Subject	Random Forest	17.325162	0.925041	0.076936	0.277374	0.110972
	SVM	48.742034	0.867815	0.139054	0.372899	0.261187
	LASSO	6.496140	0.84465	0.229811	0.479387	0.393876
Second Subject	Random Forest	16.387945	0.030775	1.076992	1.037782	0.936256
	SVM	63.274152	0.00027	1.062387	1.030721	0.956555
	LASSO	2.867452	0.045509	2.183324	1.477607	1.209763
Third Subject	Random Forest	16.978458	0.77821	0.245377	0.495355	0.263995
	SVM	41.174620	0.837531	0.185154	0.430296	0.291163
	LASSO	1.974201	0.7614	0.270749	0.520335	0.387069

Table 4.2: Results of the different regressors for each subject: signal used as Test Set

4.5.3 Regression: Random Forest

In this thesis, a regressor was chosen rather than a classifier to calculate the stress level, since a continuous output index was needed to modulate the parameters for neurostimulation. After various analyses in which three regressors were compared, it was decided that Random Forest was the most appropriate choice because it has excellent performance metrics and also appropriate execution times for real-time analysis.

Random Forest is a supervised learning algorithm that is based on the construction of multiple decision trees during training and returns the average of the individual predictions of the trees. In the context of this thesis it was used for the modulation of binaural beats in real time.
The Random Forest regressor model was trained using the features extracted from the first recording made on the i-th subject, i.e. the calibration one (without stimulation), normalized with respect to the baseline and selected by the Fisher Ratio with the addition of the 4 ECG metrics. In total, the Data set was therefore composed of 29 features. First, cross-validation was performed, which is useful when a limited amount of data is available to obtain a reliable estimate of the model's performance. Cross-validation was in fact performed to avoid potential overfitting of the model to the training data and was implemented using k = 20 because from the analyses carried out it turned out to be the best value in terms of regressor performance. 300 trees were trained, obtaining excellent regression metrics. To speed up the training process, the parallel pooling process was also used, which allowed the simultaneous use of 4 cores.
Figure 4.17 and the table next to it (table 4.3) show the training of the Random Forest regressor of a subject taken as an example and the related regression metrics. In the Figure 4.17 the blue circles are the true labels which have been set equal to -1 for the relaxation condition which goes from the beginning to 180 seconds and to +1 for the stress condition which begins immediately after relaxation and continues for 5 minutes. The red stars are the predictions of the Random

Forest regressor. The pink dashed lines divide the images into three stress regions: high stress (between +1 and +0.3); medium stress (between +0.3 and -0.3) and relaxation (between -0.3 and -1).

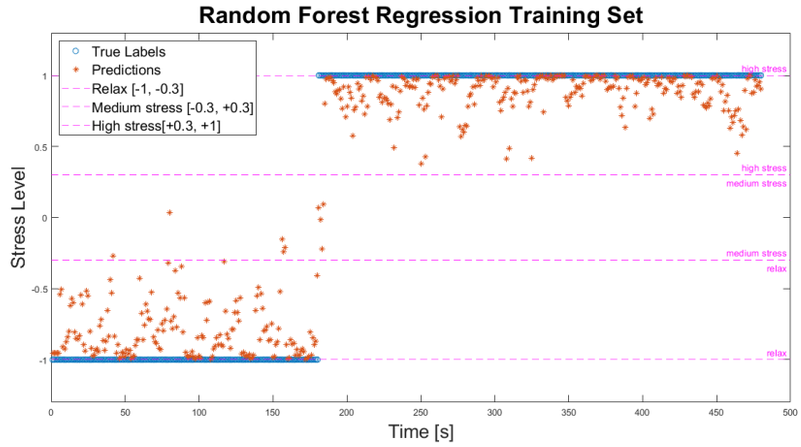

Figure 4.17: Random Forest regression Training Set

R^2	MSE	RMSE	MAE
0.971349	0.028971	0.170209	0.070865

Table 4.3: Regression metrics

A limitation of our study is the fact that we do not have a ground truth that allows us to accurately distinguish the stress phases from the relaxation phases. In the study of stress, cortisol is generally used but, for our experimental conditions, it was not possible to collect cortisol from the subjects, therefore, to train the Random Forest, we decided to force it by considering the entire baseline phase as relaxing (the labels were set equal to - 1) and the entire mathematical task phase as stress-inducing (the labels were set equal to + 1). The 20 models obtained with the KFold were ordered based on the Mean Absolute Error (MAE) values and of these, the first 3 models that obtained the best performance were selected in order to create a more robust regression. The total predictions are obtained as the average of the predictions of the three best models.

Furthermore, an associated classifier was developed to distinguish between relaxation states and activity states. This classifier uses an optimal threshold determined by maximizing the separability between the active and relaxed states, to do this the ROC (Receiver Operating Characteristic) curve was used. This method tries to find the threshold that optimally compromises the number of false positives and the number of true positives by looking for the point on the ROC closest to the ideal ‘(0,1)‘ where the false positive rate is zero and the true positive rate is one. Specifically, the optimal threshold was found using the point closest to the top left

corner of the ROC plot (i.e. the point [0,1]). To do this, the Euclidean distance between the point ‘(0,1)‘ and the point ‘(X(i), Y(i))‘ in the ROC curve was calculated for each threshold T. The Euclidean distance formula used is the following:

$$\text{distance} = \sqrt{(X(i) - 0)^2 + (Y(i) - 1)^2} \tag{4.36}$$

Where:

- $X(i)$ is the false positive rate corresponding to the threshold $T(i)$.
- $Y(i)$ is the true positive rate corresponding to the threshold $T(i)$.
- 0 is the ideal false positive rate.
- 1 is the ideal true positive rate.

This Euclidean distance measures how close the point $(X(i), Y(i))$ is to the ideal point $(0, 1)$ in the ROC curve. The goal is to minimize this distance to find the threshold that best balances the true positive rate and the false positive rate.
Predictions below this cutoff are like a signed value of -1, while those above are set to +1, which represents a high stress level. Another threshold is added corresponding to the average value of predictions during the task phase, indicative of a high stress level. Finally, the average threshold between the general optimal and the high stress threshold is calculated. This is the final threshold that represents an average level of stress of the user and is the one that will then be used as a reference in the modulation of the parameters for the neurostimulation. Figure 4.18 shows the regressor with the addition of the thresholds calculated for the subject.

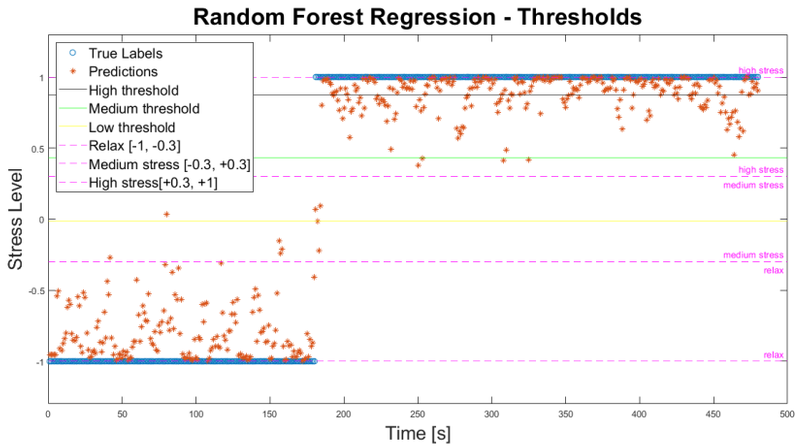

Figure 4.18: Random Forest regression with thresholds

4.6 Neurostimulation Methodology

In this study, it was decided to adopt neurostimulation through the use of *alpha binaural beats*. This stimulation modality works by exploiting the phenomenon of brain entrainment, where the difference in frequency between two tones presented separately to each ear creates a third frequency perceived by the brain, thus synchronizing neuronal activity within a predefined interval [14], [76]. Since the intent of this study is to promote a state of relaxation in the subjects, the binaural beats used to modulate brain waves were those in the alpha band, which is commonly associated with a state of alert relaxation and an optimization of cognitive abilities, attention and information processing speed [76], [104], [81], [82]. Following the indications given by studies [16] and [17], the carrier frequency of the BBs was chosen to be 400 Hz and the maximum difference between the two tones never exceeded 30 Hz.

Two distinct configurations were used: a constant frequency configuration and an adaptive configuration, which modifies the frequency of the binaural beats in real time in response to the user's stress state. These configurations were tested to understand which of the two was more effective in mitigate the stress and improving the subject's performance during the mathematical task.

4.6.1 Constant Binaural Beats

Stimulation with constant frequency binaural beats represents a more traditional approach to neurostimulation, in which the difference in frequency between the tones presented remains unchanged for the entire duration of the activity. In this study, the frequency of the binaural beats was kept within the alpha band (8-13 Hz).

In this configuration, the tone sent to the left ear was fixed at 400 Hz, while the tone sent to the right ear differed by a predetermined frequency equal to the individual alpha frequency (IAF) summed to 400 Hz. The IAF, a term first introduced by Klimesh in 1999 [107], represents the highest frequency in the Alpha band and is obtained by examining the frequency spectrum between 8 and 13 Hz to identify the one with the maximum power. In this study it was calculated during calibration for each subject, as the average of the IAF value estimated in channels P3 and P4 [108]. This stimulation modality was used to evaluate its effect in working conditions without dynamic adaptations to the cognitive needs of the user, providing an important reference for comparing the effectiveness of adaptive neurostimulation.

4.6.2 Adapted Binaural Beats

Unlike the constant frequency configuration, the stimulation with adaptive binaural beats exploits the ability to modulate the frequency of the tones in real time based on the brain response of the user. In this configuration, the initial frequency of the binaural beats was set equal to the IAF value calculated during the calibration phase. During the activity, the tone sent to the left ear was maintained at 400 Hz, while in the right ear, a frequency value adapted based on the stress level of the subject determined by the regression model was added to the carrier frequency of 400 Hz. The frequency modulation occurred with intervals of 10 seconds, so as to

use an epoch long enough to be considered informative for what concerns the ECG, but keeping the duration of the interval short enough to not introduce too much delay, as it is precisely a real-time modulation.

This dynamic modulation process, implemented through an optimization algorithm, allowed to adapt the stimulation to the user's cognitive condition in real time, thus improving the effectiveness of neurostimulation. A detailed explanation of how the algorithm works will be provided below, and the flowchart of the algorithm's operation can be found in Figure 4.19.

1. **Start of the process**: The process starts with the sending of the IAF, in the case of the first stimulus sent, or of the previous stimulus after the first 10-second interval;

2. **Threshold check**: The algorithm checks whether at least 60% of the Random Forest (RF) predictions of the user's stress state are higher than a predefined threshold. This threshold has been estimated as the average between the threshold that maximizes the distinction of the two conditions (stress-relax) and the average value of the RF predictions during the task phase being calibrated.

    - **Condition not satisfied**: The algorithm sends the previous stimulus again, and the cycle restarts without changing the frequency.
    - **Condition satisfied**: If 60% of the predictions are above the threshold, the algorithm proceeds by comparing the current number of predictions above the threshold with the previous number:
        - **Greater**: If the current number of predictions above the threshold is greater than the previous cycle, the algorithm checks whether the last modulation increased or decreased the frequency.
            * **Last modulation increased the frequency**: The algorithm decides to decrease the frequency by 2 Hz, reversing the direction.
            * **Last modulation decreased the frequency**: The algorithm decides to increase the frequency by 2 Hz, reversing the direction.
        - **Less**: If the current number of predictions above the threshold is less than the previous cycle, the algorithm checks the last modulation direction again:
            * **Last modulation increased frequency**: The algorithm reduces the frequency by 1 Hz, keeping the same direction.
            * **Last modulation decreased frequency**: The algorithm increases the frequency by 1 Hz, keeping the same direction.
        - **Equal**: If the current number of predictions above the threshold is equal to the previous cycle:
            * **Last modulation increased frequency**: The algorithm continues to increase the frequency, but by a smaller amount (0.5 Hz), indicating that the direction is correct.

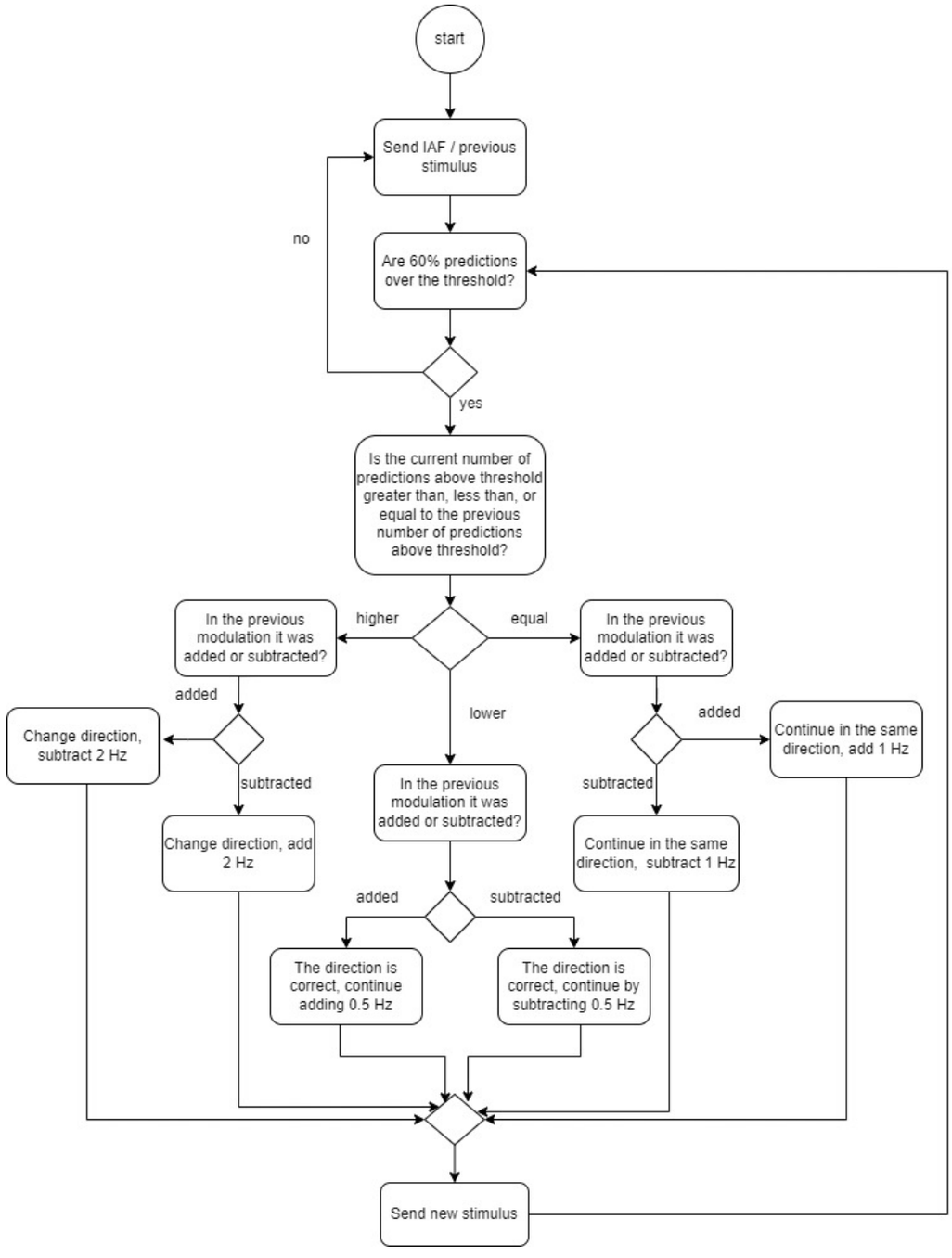

Figure 4.19: Flowchart of the operation of the frequency modulation algorithm

- **Last modulation decreased frequency**: The algorithm continues to decrease the frequency, but by a smaller amount (0.5 Hz), indicating that the direction is correct.

3. **Sending the new stimulus**: After determining the new frequency to use, the algorithm sends the new stimulus to the user and the cycle begins again.

This process continues iteratively: it modulates the frequency of the binaural beats to optimize the user's cognitive performance and seeks a convergence towards a frequency that maximizes performance and decreases stress. The algorithm is designed to be adaptive, it corrects the direction of the modulation in response to changes in the regressor predictions.

4.7 Performance evaluation metrics

Performance evaluation metrics are essential tools for quantifying the effectiveness and accuracy of individual or group performance. In this chapter, we will focus on the performance evaluation of a group of 20 subjects who performed a mathematical task. These metrics provide an objective basis for comparing the performance of participants under the different experimental conditions envisaged in this study. The main metrics used to evaluate such performance are: Accuracy, Reaction Time (RT) and Inverse Efficiency Score (IES).

4.7.1 Accuracy

Accuracy is a metric that measures the proportion of correct answers provided by participants compared to the total number of questions in the task. In the context of a mathematical task, Accuracy reflects the subject's ability to correctly solve the proposed problems. It is defined as:

$$\text{Accuracy} = \frac{\text{Number of correct answers}}{\text{Total number of trials}} \tag{4.37}$$

This metric is a direct measure of correct performance and provides an immediate indication of the subject's ability to complete the assigned task successfully. It is particularly useful for identifying how accurately participants understand and solve mathematical problems.

4.7.2 Reaction Time (RT)

Reaction Time (RT) measures the time it takes a participant to respond to a question after it has been presented. In the context of a mathematical task, RT can provide information about how quickly the subject processes and solves problems. It is commonly measured in milliseconds (ms).

This metric is an indicator of the subject's cognitive processing speed. Shorter reaction times may indicate greater alertness, while longer times may suggest difficulty or uncertainty in the solution process. RT can vary significantly between subjects and conditions. In the context of this study, the average reaction time was calculated for each subject taking into account only the questions to which the correct answer was provided.

4.7.3 Inverse efficiency Score (IES)

To combine the effect of accuracy and reaction time, as suggested by Townsend and Ashby, it's possible to use the Inverse efficiency Score (IES) [75] which combines information on the speed

and accuracy of responses in a single metric. The IES is particularly useful for considering both the speed and the accuracy of responses, avoiding that a high speed compensates for a low accuracy or vice versa. It is calculated as:

$$\text{IES} = \frac{\text{average RT}}{1 - \text{PE}} = \frac{\text{average RT}}{\text{Accuracy}} \tag{4.38}$$

- **average RT**: It represents the average reaction time for each participant calculated on the responses to which he/she answered correctly.
- **PE (Proportion of Errors)**: It is the proportion of incorrect answers compared to the total number of trials.
- **Accuracy**: It is the proportion of correct answers compared to the total number of trials.

The IES considers both precision and speed and therefore allows to obtain a balanced measure of the subjects' performance. A low IES indicates that the subject responded quickly and with a low number of errors, suggesting a high efficiency in the task. This metric is particularly useful in contexts where it is important not only to respond correctly, but also to do so quickly.

4.8 Statistical test

In data analysis, it is essential to apply adequate statistical methods to draw valid and reliable conclusions. Different techniques are used to evaluate hypotheses and compare groups, depending on the characteristics of the data and the assumptions made on the statistical models. In this chapter, we will explore some of the most commonly used statistical tests: the Shapiro-Wilk test for testing normality of data, the ANOVA for comparing means between multiple groups, the t-test for comparing two correlated or independent groups, the Friedman test for nonparametric analyses on multiple paired groups, and the Wilcoxon test for comparing two correlated conditions.

These tests provide useful tools for analyzing and interpreting data and for determining whether observed differences are statistically significant and whether research hypotheses can be accepted or rejected. Choosing the most appropriate test for the data depends on the specific characteristics of the data and the type of hypothesis to test.

4.8.1 Shapiro-Wilk Test

The Shapiro-Wilk test [69] is a statistical method used to test the normality of a data distribution. Introduced by Samuel Shapiro and Martin Wilk in 1965.

This test is based on comparing the order of the values observed in the sample with the values expected if the data were normally distributed. In essence, the test measures how much the observed data differ from an ideal normal distribution.

The test calculation is based on a statistic W, defined as:

$$W = \frac{\left(\sum_{i=1}^{n} a_i x_{(i)}\right)^2}{\sum_{i=1}^{n}(x_i - \overline{x})^2} \tag{4.39}$$

where:

- $x_{(i)}$ are the ordered values of the sample,
- $\overline{x}$ is the mean of the sample,
- a_i are constant coefficients that depend on the expected values of a normal distribution and on the sample covariance.

The statistic W takes values between 0 and 1, where values closer to 1 indicate a greater conformity to normality.

The Shapiro-Wilk test is a hypothesis test in which the null hypothesis (H_0) states that the data are normally distributed. Therefore:

- If the p-value associated with the statistic W is greater than a pre-specified significance level (for example, $\alpha = 0.05$), the null hypothesis is not rejected, indicating that there is insufficient evidence to say that the data are not normal.
- If the p-value is less than α, the null hypothesis is rejected, suggesting that the data does not follow a normal distribution

4.8.2 ANOVA (Analysis of Variance)

ANOVA [70], or Analysis of Variance, is a statistical technique used to compare means between distinct groups. Introduced by Ronald Fisher in 1925, ANOVA is a powerful tool for identifying whether there are significant differences between group means by analyzing the overall variability of the data.

This statistical test is based on the concept of breaking down the total variance observed in the data into two main components:

- **Between-group variance (or explained variance)**: represents the variation between the means of the different groups and measures how much the means of the groups differ from each other.
- **Within-group variance (or residual variance)**: represents the variation within each group and measures how much the data within a single group differ from the mean of the group itself.

The F statistic used in ANOVA is calculated as the ratio of the explained variance to the residual variance:

$$F = \frac{\mathrm{MS}_{\text{between groups}}}{\mathrm{MS}_{\text{within groups}}} \tag{4.40}$$

where:

- $MS_{\text{between groups}}$ is the mean of the squares between groups,
- $MS_{\text{within groups}}$ is the mean of the squares within groups.

A large value of the F statistic indicates that the variance between groups is large compared to the variance within groups and therefore suggests that at least one of the group means is significantly different from the others.

The null hypothesis (H_0) in ANOVA states that all group means are equal. The alternative hypothesis (H_1), on the other hand, suggests that at least one mean differs from the others.

- If the p-value associated with the F statistic is less than a pre-specified significance level (for example, $\alpha = 0.05$), the null hypothesis is rejected. This indicates that there are significant differences between the group means.
- If the p-value is greater than α, the null hypothesis is not rejected, so it cannot be said that the group means are different.

There are several variations of ANOVA, each suited to specific situations:

- **One-way ANOVA**: Used for compare the means of three or more groups based on a single independent factor.
- **Two-way ANOVA**: Used for examine the effect of two independent factors on the means of a group. This model also allows to analyze the interaction between the two factors.
- **Repeated measures ANOVA**: Used when the same subjects are subjected to different conditions, allowing to analyze the variance due to differences within the same subjects.

ANOVA is a powerful method that allows to analyze multiple groups simultaneously, but it also has some limitations:

- It requires that the data meet certain assumptions, including normality of group distributions and homogeneity of variances.
- It does not provide any indication of which specific groups differ from each other. If the ANOVA indicates that there are significant differences, additional post-hoc tests must be performed to identify exactly which groups are different.

4.8.3 T-test

The t-test [71] is a statistical method used to compare the means of one or two samples and determine whether the observed differences between the means are statistically significant. Developed by William Sealy Gosset in 1908 under the pseudonym "Student", the t-test is widely used to analyze small sample sizes and to test hypotheses about a population mean or the difference between the means of two populations.

There are three main variations of the t-test, each suited to specific scenarios:

- **One-sample t-test**: Used to compare the mean of a single sample to a reference value or a known population mean.
- **Independent samples t-test**: Used to compare the means of two independent groups, for example to test whether the observed difference between two treatment groups is significant.
- **paired samples t-test**: Used when data are paired or correlated, such as repeated measurements on the same sample before and after a treatment.

The t-test is based on comparing the observed difference between the means of the samples with the expected difference under the null hypothesis (H_0). The null hypothesis usually states that there is no difference between the means (for the two-sample t-test) or that the sample mean is equal to a reference value (for the one-sample t-test).

The test statistic t is calculated as:

$$t = \frac{\overline{X}_1 - \overline{X}_2}{\text{SE}} \tag{4.41}$$

where:

- $\overline{X}_1$ and $\overline{X}_2$ are the means of the samples,
- SE is the standard error of the difference between the means.

The standard error SE depends on the variance of the samples and their size. The larger the difference between the means relative to the variability of the data, the greater the absolute value of the t statistic.

The value of t obtained is compared with a critical value derived from the Student t distribution with a given number of degrees of freedom: if the absolute value of t exceeds the critical value, the null hypothesis is rejected, indicating that there is a significant difference between the means.

- **p-value**: Associated with the t-test is the p-value, which represents the probability of observing a difference between the means equal to or greater than that found if the null hypothesis were true. If the p-value is lower than a pre-established level of significance (for example, $\alpha = 0.05$), the null hypothesis is rejected.

The t-test is based on some fundamental assumptions:

- **Normality**: It is assumed that the data follow a normal distribution, especially for the one-sample t-test and the independent-samples t-test.
- **Equal variances (homogeneity of variances)**: For the independent-samples t-test, it is assumed that the variances of the two groups are equal (when this assumption is not met, the corrected version of the test, called Welch's t-test, can be used).
- **Independence**: The observations within the samples must be independent of each other.

4.8.4 Friedman test

The Friedman test [72] is a nonparametric test used to compare the means of three or more related groups or measured under different conditions. Introduced by Milton Friedman in 1937, this test is particularly useful when the data do not satisfy the assumptions required for repeated measures ANOVA, such as normal distributions.

The Friedman test is based on the ranking of data within each group. The observed values are in fact ordered and ranked within each block or subject. The null hypothesis (H_0) of the Friedman test states that the group means are equal, while the alternative hypothesis (H_1) suggests that at least one of the group means is different.

The Friedman test analyzes the differences between the mean rankings of the groups, rather than the differences in the original means of the data. The Friedman test statistic is calculated as follows:

$$\chi_F^2 = \frac{12}{nk(k+1)} \left(\sum_{j=1}^{k} R_j^2 - \frac{k(k+1)^2}{4} \right) \tag{4.42}$$

where:

- n is the number of blocks (or subjects),
- k is the number of groups or treatments,
- R_j is the sum of the rankings for the j-th group.

The χ_F^2 statistic follows a chi-square distribution with $k-1$ degrees of freedom.

The calculated value of the χ_F^2 statistic is compared to a critical value from the chi-square distribution with $k-1$ degrees of freedom. If the χ_F^2 statistic is greater than the critical value, the null hypothesis is rejected, indicating that significant differences exist between the groups.

- **p-value**: The p-value associated with the χ_F^2 statistic represents the probability of obtaining a test statistic equal to or greater than that observed under the null hypothesis. A p-value less than a pre-specified significance level (for example, $\alpha = 0.05$) suggests that at least one of the group means is significantly different.

The Friedman test has several advantages:

- It does not require that the data follow a normal distribution.
- It is particularly useful in case if repeated measures or paired data, such as in experimental designs where subjects are exposed to multiple conditions.

However, it also has some limitations:

- It does not provide specific information about which groups differ from each other. For reject the null hypothesis, it's necessary to perform post-hoc tests to determine specific differences between pairs of groups.
- It is less powerful than repeated-measures ANOVA when the assumptions of the latter are satisfied.

4.8.5 Wilcoxon test

The Wilcoxon test [73] is a nonparametric test used to compare two groups of paired or related data, and is particularly useful when the data do not satisfy the assumptions required for the paired-samples t-test. This test is also called the Wilcoxon signed-rank test, and is used to determine whether there are significant differences between the means of two related groups.

The Wilcoxon test is based on the analysis of differences between pairs of observations within each subject or observation unit. These differences are ranked in order of magnitude, ignoring the sign. The test evaluates whether the sum of the ranks of the positive differences is significantly different from the sum of the ranks of the negative differences.

To apply the test, these are the steps:

- Calculate the differences between the paired values for each subject.
- Sort the differences by absolute value and assign the ranks.
- Add the ranks of the positive differences (W^+) and the ranks of the negative differences (W^-).
- Check if the Wilcoxon test statistic W is the smaller of W^+ and W^-.

The Wilcoxon test statistic W is compared to the critical values of a Wilcoxon distribution table, which depend on the sample size. If W is less than the critical value then the null hypothesis is rejected, which suggests that there are significant differences between the two means.

- **p-value**: The p-value associated with the Wilcoxon test statistic represents the probability of obtaining a statistic that is equal to or more extreme than that observed under the null hypothesis. A p-value less than a pre-specified significance level (for example, $\alpha = 0.05$) indicates that the differences between the groups are significant.

The Wilcoxon test offers several advantages:

- It does not require that the data follow a normal distribution.
- It is particularly useful when the data do not satisfy the assumptions of the t-test.

However, it also has some limitations:

- It does not provide detailed information about effect sizes, unlike parametric tests that can provide estimates of the difference between means.
- It is less powerful than parametric tests when the assumptions of parametric tests are satisfied.

Chapter 5

Results and discussions

This chapter will present in detail the results that emerged from the analysis of the data collected during the acquisition phase, with particular attention to the effects of the neurostimulations examined. The main objective is to provide a complete and detailed description of the results obtained during the study, focusing on the effectiveness of neurostimulations in mitigating stress and improving cognitive performance.

The empirical results and experimental observations will illustrate how the neurostimulation intervention influenced the participants' stress levels and their performance capabilities. In particular, the following will be discussed in detail:

1. The adaptation of real-time stimulation;
2. The comparison of the data collected during the acquisition sessions without stimulation with those obtained during the two different types of neurostimulation used during the experiment;
3. The comparison between the two types of stimulation in order to identify which of the two produced the most significant improvements.

Through statistical analysis of the data and interpretation of the results, key differences between the experimental conditions will be highlighted, also discussing possible explanations for the observed variations. This chapter aims to contribute to the understanding of the effectiveness of neurostimulations as a tool for stress mitigation and cognitive performance enhancement.

5.1 Real-time regression results

As explained in more detail in paragraph 4.6.2, the stimulation adaptation was formulated as a function of the predictions of the Random Forest regressor. In particular, based on the number of predictions that exceeded a specific threshold for each subject, the frequency could remain unchanged, increase or decrease by 0.5 Hz, 1 Hz or 2 Hz.
The Fisher Ratio method was adopted for feature selection. This approach allowed to precisely identify the most significant features and EEG channels for distinguishing between relaxation and task execution phases. Through an in-depth analysis of the selected features

using the Fisher Ratio, it was possible to determine which electroencephalographic parameters contributed most to the discrimination between these two states, highlighting the EEG channels that showed the greatest relevance in the differentiation of brain activities associated with relaxation compared to those involved in cognitive tasks.

5.1.1 Binaural modulation

A fundamental part of this thesis work was to ensure that the frequency of binaural beats adapted to the subject's stress level. To do this, the output of the Random Forest regressor was used: it was trained using the signal acquired from the subject during the calibration phase and then the model thus obtained was used in the real-time frequency modulation phase.

Summarizing what was explained in chapter 4, during the calibration phase a specific threshold for the subject was calculated, obtained as the average between the optimal threshold deriving from the ROC curve and the average value of the regressor predictions in the task phase. Subsequently, in the real-time phase, the stimulation frequency was adapted according to the subject's stress level: if, during a 10-second acquisition interval, 60% of the predictions were above the predefined threshold, the frequency of the binaural beats was modified. The direction and amplitude of this modification depended on the comparison with the number of predictions above the threshold in the previous 10 seconds.

The following are the outputs of the stimulation frequency modulation based on real-time predictions. As an example, two subjects were considered in which the frequency adaptation had particularly different trends.

As can be observed in Figures 5.2 and 5.4, in both cases during the relaxation phase (baseline) the frequency did not change and remained constant and equal to the IAF value calculated for each subject in the calibration phase. In Figures 5.1 and 5.3 show the predictions of the random forest which in fact during the baseline phase are mostly in the medium stress range [-0.3; +0.3] and complete relaxation [-1; -0.3]. The constancy of the stimulation frequency during the baseline phase demonstrates the stable and relaxed state of the subject. As soon as the mathematical test begins, the predictions of the Random Forest show an immediate reversal of the trend towards the high stress range [+0.3 to +1], indicating a significant increase in stress levels in response to the task. This increase in stress is reflected in the stimuli sent to the subjects, which show a frequency variation (-2 Hz), indicating that the right frequency to reduce stress was not immediately identified. During the task phase, a clear difference can be noted between the two subjects: in User3, the stimulus sent changes continuously throughout the duration of the task, while in User15, after an initial phase of variation, it stabilizes. In Figure 5.2, relating to User3, halfway through the difficult task, the stimuli seem to find the right direction of variation, as the steps in the frequency modulation become smaller (1 Hz) and continuously increasing, culminating in a step of 0.5 Hz and reaching a value of 12.5 Hz, after which, however, instead of stabilizing, the stimulus returns to a step of 2 Hz in the opposite direction and then reduces the amplitude of the jump again. Even in the simplest task phase, the pattern is chaotic, with the stimuli initially descending towards lower frequencies, even going below the IAF value, and then rising back up to 12 Hz. The variable trend in this

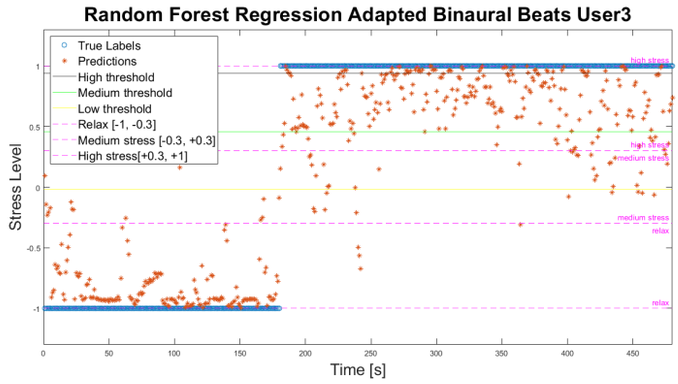

Figure 5.1: Random Forest Regression Test Set Adapted Binaural Beats User3

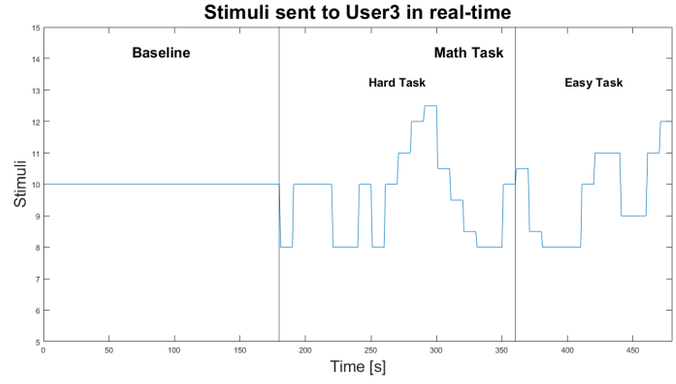

Figure 5.2: Stimuli sent to User3 in real - time

phase reflects the variations in stress levels. The Random Forest predictions (Figure 5.1) show that the subject always remains highly stressed and tends to move into the medium stress zone [-0.3 to +0.3] only in the simplest task but not significantly. This variability in the trend of the stimuli in the simple task phase suggests that, although the overall stress may be lower, there is still significant variability in the subject's response to stress, requiring continuous adjustments of the stimuli. Figure 5.4, on the other hand, shows that User15, after an initial exploration phase, received stimuli with a frequency that stabilized around an optimal value different from the IAF. This contributed to the reduction of the subject's stress during the different phases of the mathematical task. This is confirmed by the random forest predictions graph, where it's possible to see an increasing shift of the predictions towards the medium stress zone with some of them even reaching the relaxation range during the simple task.

The sudden change in the predictions and the large variations in the frequency at the end of the baseline show the initial difficulty in finding an effective frequency for stress reduction. As time passes, however, the trends of the stimuli sent to the two subjects differ: for User15 the system manages to adapt, while for User3 the pattern remains irregular. This suggests that the real-time adaptation of binaural stimuli can have a significant impact on stress management, in fact in the case of User3, the algorithm did not identify an optimal frequency, resulting in

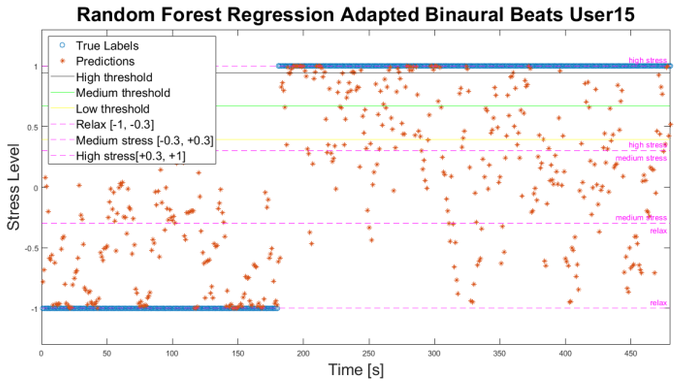

Figure 5.3: Random Forest Regression Test Set Adapted Binaural Beats User15

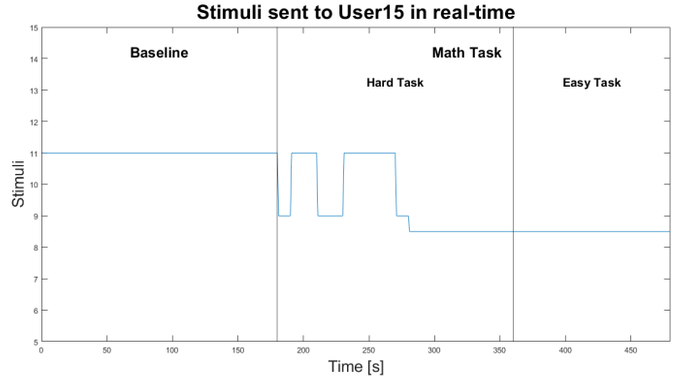

Figure 5.4: Stimuli sent to User15 in real - time

a constant state of stress, while for User15, once the optimal frequency was found, the stress decreased, suggesting that the personalization of the stimuli is crucial for the effectiveness of the treatment.

Going into more detail about the output of the stimulation adaptation algorithm, Figure 5.5 compares the average of the predictions of the Random Forest between the phase in which the algorithm was searching for the optimal stimulation and the seconds in which the frequency stabilized considering all subjects. It can be noted that during the period in which the stimulation remained constant, the average of the predictions is in the medium stress range [-0.3; 0.3] and tending towards the relaxation range [-0.3; -1], unlike those relating to the period in which the optimal frequency is searched for, which are instead in the high stress area [+ 0.3; 1]. This result was predictable considering the functioning of the algorithm developed in this thesis to evaluate the need or not to modify the stimulation (see chapter 4).

Appendix A shows the images of the remaining subjects analyzed in this study. It was observed that for some of them the frequency of binaural beats never changed, remaining constant at the IAF value calculated during the calibration phase for the entire recording time. In these cases, the stability of the frequency could indicate that the initial IAF value was already optimal for maintaining a state of relaxation or controlled stress. Other subjects, however, showed

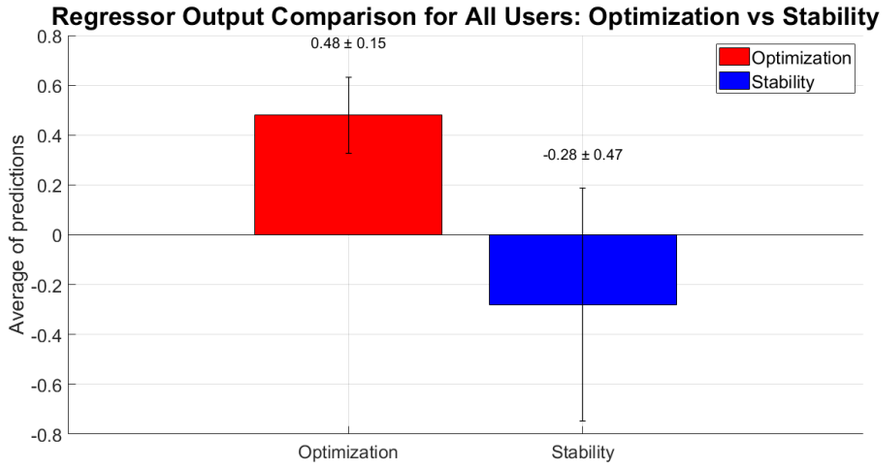

Figure 5.5: Regressor output comparison: optimization vs stability

variations in frequency not only during the mathematical task, but also during the baseline phase. This behavior could be attributed to the fact that the algorithm used to adapt the frequency of binaural beats could more successfully identify optimal changes for some subjects than others, depending on the complexity of their stress profile. Frequency stability or variations during the baseline phase suggest that individual and environmental factors, together with the effectiveness of the algorithm, play a crucial role in the effectiveness of the treatment.

These observations highlight the dynamic interaction between stress levels and adaptive stimuli and show the potential use of regulated binaural beats to manage stress in real time.

From the analyses carried out, it was noted that the frequency of binaural beats stabilized after an initial exploration for some subjects, while for others it never stabilized or never changed; for some subjects, however, it varied even during the baseline phase. These observations demonstrate that each subject has a unique behavior, reinforcing the importance of adapting stimulation and treatment to the individual specificities of the subjects themselves.

5.1.2 Predominantly selected features

The Random Forest regressor was trained using 29 features, of which 25 are the EEG features selected by the Fisher Ratio for each specific subject and 4 are the ECG features.
As part of this thesis, a general ranking of the EEG features that were most selected by the Fisher Ratio was drawn up. This process allowed us to identify the most relevant features considering the entire population of subjects studied. By aggregating the importance ratings from all subjects, we were able to draw up a general ranking of the EEG features (Figure 5.6). The features are listed in decreasing order of occurrence, that is, based on how many times each feature in any channel was among the most relevant according to the Fisher Ratio in distinguishing stress from relaxation in the various subjects during the calibration phase. In

total, there are 24 features calculated each on 7 channels, with the exception of alpha asymmetry which are calculated only in the frontal channels.

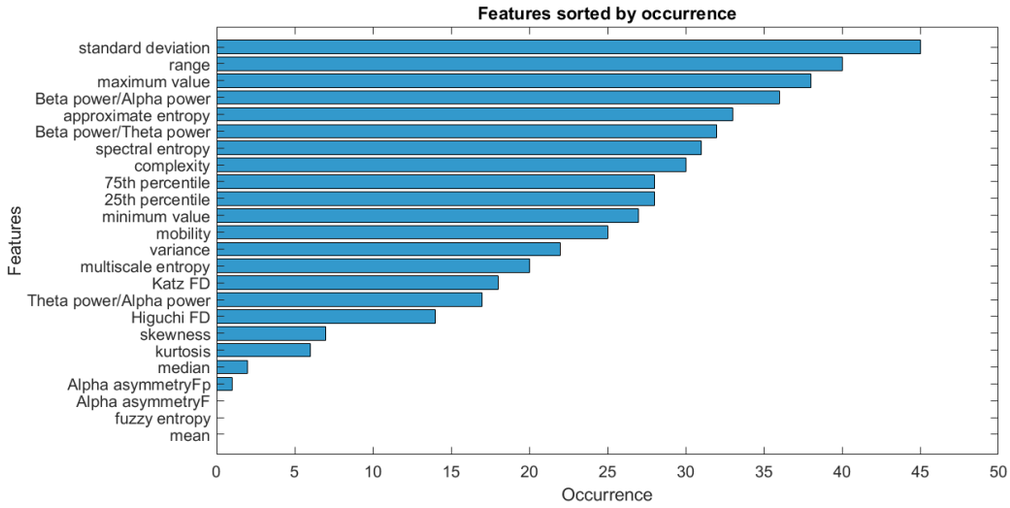

Figure 5.6: Estimated features from the EEG

The Standard Deviation was found to be the most recurrent, being selected 45 times. The standard deviation measures the dispersion of the data around the mean, indicating the intrinsic variability of the EEG signal. Next are the range with 40 occurrences and the maximum value with 38 occurrences. The best three features are therefore all features over time. Among the features least selected by the Fisher Ratio, which therefore resulted less relevant for the purposes of stress detection via EEG in this study, are the alpha asymmetry calculated between Fp1 and Fp2 which was selected as relevant only in one case. And in particular the alpha asymmetry calculated between F3 and F4 and the Fuzzy Entropy were surprisingly never selected in any case. Even if these features may be relevant in other contexts, in this study they did not show significance for stress detection and did not provide any contribution to the model's predictions. The recurrence ranking of the EEG signal channels reported in Figure 5.7 was also drawn up. This allows us to identify the positions of the EEG electrodes that provide the most significant data. Also in this case the ranking was drawn up in terms of occurrence, that is, the number of times each channel was among the most relevant.

In this study, the parietal channels P3 and P4 are the most significant for the assessment of stress. The parietal region is more activated during cognitive processes such as attention, numerical and spatial processing, information processing and during complex tasks such as arithmetic operations [123], this result could derive from a probable crosstalk phenomenon. At the same time, these results highlight a bilateral distribution of the relevance of the parietal regions, suggesting to carry out more in-depth studies on the critical role of the parietal areas in the context of stress analysis. The channels Fp2 and Fp1, located in the right and left fronto-polar region, also show a high importance. The frontal area is known for its involvement in cognitive and behavioral control [123]. The relevance of the channels Fp1 and Fp2

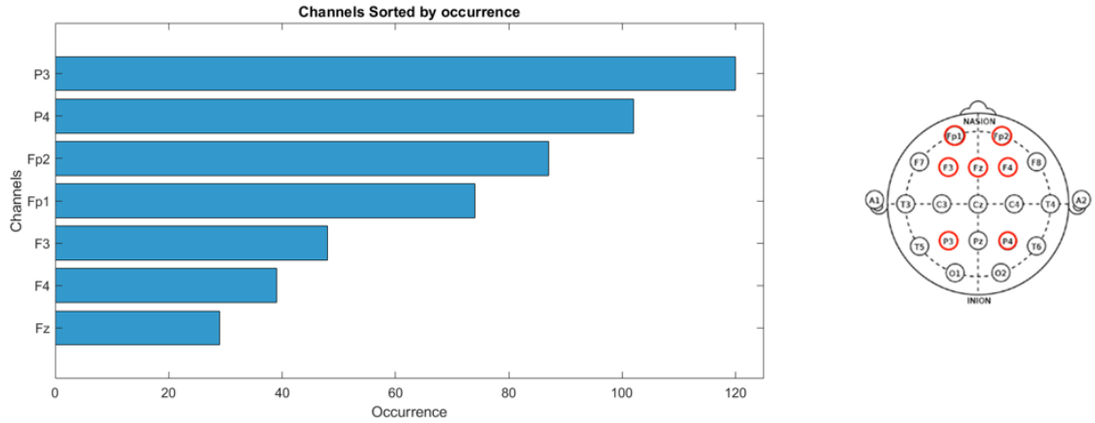

Figure 5.7: Rank selected channels

highlights the involvement of the frontal regions in the interpretation of stress signals in this study. Slightly less important are the F3 and F4 channels, located in the right and left frontal region. The Fz channel, located in the midline of the frontal region, was the least relevant among those examined. This suggests that, although the frontal regions are overall relevant, there is variability in the specific locations involved in stress detection.

An interesting aspect to explore is the distribution of the importance of EEG channels between the right and left hemispheres of the brain. The analysis of individual channels allows us to identify whether there is a predominance of relevance in one of the hemispheres.
For example, a study [93] has shown that, in the frontal area, the right hemisphere of the brain becomes dominant compared to the left hemisphere with the onset of stress as it is more associated with the processing of negative emotions. At the same time, however, the analyses carried out in the anterior temporal, lateral frontal, central, posterior temporal and parietal areas did not have significant results regarding the asymmetry in relation to affective reactivity, or an individual's emotional response to stimuli.

Alpha power asymmetry and interhemispheric asymmetry indicate mental stress [94], so several studies have relied on this data for the assessment of stress. Among these, a 2021 study [96], demonstrated that, during the relaxation phase, the amplitude of the alpha frequency is symmetrical between the two hemispheres in the frontal area of the brain. This amplitude tends to shift towards the right hemisphere during stress situations, thus generating asymmetry as indicated by the alpha asymmetry metrics calculated between the Fp1 and Fp2 channels, and F3 and F4 whose values have become more negative. In [100] in which mental stress was correlated with a noisy work environment, the use of 16 electrodes placed in the frontal area revealed an increase in stress-related cortical activity in the right frontal lobe and alpha asymmetry, with the right lobe predominance, was found between electrodes F3 and F4, but not between F7 and F8 during the Montreal Imaging Stress Task (MIST). The study [105] focused on evaluating

dispersion patterns for the detection of negative stress from electroencephalographic signals using EEG recordings taken from a public data set and performed with 32 channels positioned in the frontal, central and parietal areas of the scalp. The channels that showed the greatest statistical significance were those of the right frontal and left parietal areas. This result was also confirmed by the average values of dispersion entropy (DispEn) calculated in the calm and stress conditions, in which the largest differences between the two emotional states were obtained in the right frontal, central and left parietal regions. Furthermore, several studies have highlighted a coordinated behavior between the frontal and parietal areas of the brain in calm and stress situations. For example, it has been observed that when the frontal lobe of one hemisphere is activated, this activation is compensated by the activation of the parietal lobe of the opposite hemisphere [106].

To summarize, physiologically, an increase in cortical activity in the right hemisphere of the frontal area of the brain is expected following the processing of negative emotions such as stress, as found in the studies cited above and in others such as [98]. It also emerged that the area of the brain considered is crucial to detect which hemisphere is more activated depending on the type of emotion and that the right frontal area and the left parietal area are the most informative to distinguish the state of stress from that of relaxation.

The results of this study regarding the number of occurrences of the channels used in the two hemispheres are reported in the table 5.1. The Fz channel was not reported as it is located in the central area of the scalp.

Right hemisphere		**Left hemisphere**	
Fp2	87	**Fp1**	74
F4	39	**F3**	48
P4	102	**P3**	120
Tot:	228	**Tot:**	242

Table 5.1: Data comparison between the right and left hemispheres occurence.

As reported in table 5.1, with 242 occurrences, overall the left hemisphere of the brain shows a slight prevalence compared to the right hemisphere (228 occurrences). However, analyzing the different areas of the brain in more detail, it is noted that the channels of the left frontal area (Fp1 and F3) actually have a lower number of occurrences than their respective ones in the right hemisphere (Fp2 and F4), showing a prevalence of the right hemisphere in the frontal area compared to the left, while in the parietal area there is a greater number of occurrences in the left hemisphere. These results are in line with those of the studies cited above.

For a more detailed visualization, a heatmap was created that represents the importance of the channel-feature pairs. In this matrix, each element represents the occurrence of selection of

a specific feature for a given channel, allowing a clear visualization of the most relevant channel-feature combinations. The heatmap in Figure 5.8 provides a visual and intuitive representation of the brain regions in combination with specific feature types that have a greater impact on stress detection according to the Fisher Ratio in this study. Darker colors (red) indicate greater occurrence, while lighter colors (yellow and white) indicate less occurrence.

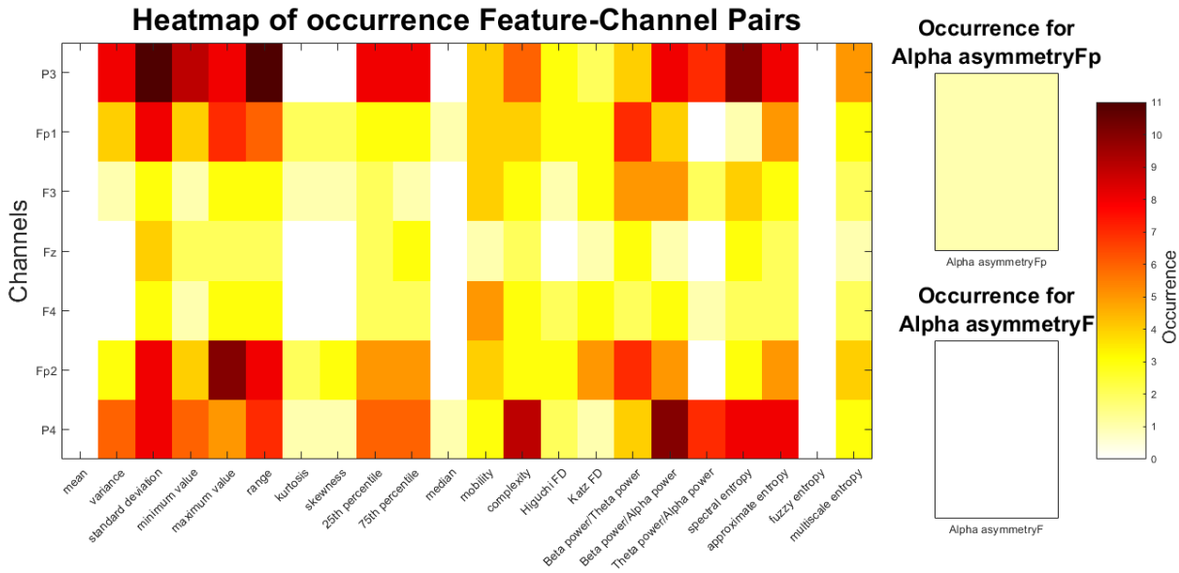

Figure 5.8: Heatmap channel-feature pairs

Analyzing the heatmap, it is possible to make some significant observations: the P3 channel shows a high frequency for many features, in particular the standard deviation and the range that both record 11 occurrences. This confirms its importance as a dominant channel, already highlighted in the channel occurrence ranking and the importance of these two features. The P4 channel also shows high values for the same features but in a less pronounced way: 8 occurrences for the standard deviation and 7 for the range. For this channel, the other metrics with the highest number of occurrences are beta/alpha power ratio with 10 occurrences, the complexity with 9 occurrences and the approximate entropy and the spectral entropy both with 8 occurrences. Also for the P3 channel the spectral entropy is important having been selected for half of the subjects. The beta/alpha power ratio and the approximate entropy instead both have 8 occurrences in this channel.

In the frontal channels the number of occurrences decreases, this is in line with what was said above. Specifically, for the Fp1 channel the standard deviation is the most recurring (8 occurrences), followed by the maximum value and the beta/theta power ratio both with 7 occurrences. In the Fp2 channel the maximum value has 10 occurrences but the standard deviation and range (both 10 occurrences) and the beta/theta power ratio with 7 occurrences are also important.

It is interesting to note that the spectral entropy, which for the parietals was among the most important metrics with 10 occurrences in P3 and 8 in P4, in the fronto-polar channels its relevance decreases: the color detachment is very evident especially in the left hemisphere, between P3 and Fp1 in which it was selected only once.

Moving to analyze the F3 and F4 channels, the maximum number of occurrences was 5, which was reached by the mobility in F4 and by the beta/alpha and beta/theta power ratios in F3. The occurrence of the various features further decreases in the Fz channel, with many of them never being selected. The only most significant metric of this channel is the standard deviation with 4 occurrences. The Fz shows the least relevance in the heatmap, confirming its low importance already found in the channel ranking. The features associated with Fz in this study generally have a low occurrence, assuming that the frontal medial position does not capture significant information for stress in the analyzed EEG data.

The colored map confirms that the alpha asymmetry between F3 and F4, the mean and the Fuzzy Entropy were not selected in any channel and, thanks to the heatmap, this observation adds an additional detail: in addition to the aforementioned, there are some channel-feature pairs that present zero occurrences. In the P3 channel, in addition to the features already mentioned, kurtosis, skewness and median were not considered important; the median in particular was selected only in the Fp1 and P4 channels but in a slightly significant way; just as in P3, kurtosis and skewness were not considered important even in the F4 and Fz channels and in the latter the Higuchi fractal dimension is also added. The theta/alpha power ratio has never been selected in the channels Fp1, Fp2 and Fz.

This analysis highlighted that some EEG features, such as standard deviation, range, maximum value, spectral entropy and approximate entropy, are particularly relevant to identify stress in this study. Instead, other features such as alpha asymmetry, skewness and Fuzzy entropy did not demonstrate relevance. This highlights how crucial it is to carefully choose the features for certain applications and to use reliable methods such as the Fisher Ratio to evaluate them. The study on the importance of EEG channels showed that parietal regions (P3 and P4) are crucial to recognize stress, followed by frontopolar regions (Fp1 and Fp2), indicating that brain areas involved in mental and behavioral processes influenced the detection of stress in the analyzed individuals. The lower relevance of F4, F3 and Fz channels, although presenting a certain frequency, suggests that the crucial information to detect stress could be concentrated mainly in the parietal and frontal-parietal regions.

One of the objectives of this thesis was also to evaluate the importance of the contribution of the ECG signal in the context of stress detection, as already done in other studies ([88], [91], [52]) and compare it to that of the EEG.

To analyze this aspect, the evaluation of the importance of the features through the Out-Of-Bag Permutation was used, which is one of the most used methods to understand how

much each feature contributes to the overall performance of the Random Forest model. During the construction of the Random Forest, for each tree, a random subset of the dataset is built through sampling with repetition (bootstrap sampling). Each decision tree is trained on a subset of samples and the training examples that are not used in the training of a particular tree are called "Out-Of-Bag" (OOB) samples. To assess the importance of each feature in the dataset, we permute its values across OOB samples and then evaluate the importance of a variable by measuring the drop in model quality when this variable is randomly applied. We measure how the model's performance (i.e., OOB error) changes after the feature permutation [35]. The rationale is that if a feature is important, then permuting it should have a significant negative impact on the model's prediction performance. If the feature is unimportant, then the permutation will have little or no impact on performance. The difference in performance between the model with the permuted feature and the original model (without the permutation) is an estimate of how important that feature is. The greater the performance decrease after the permutation, the greater the importance of the feature. In summary, permuted feature importance assesses the impact that perturbing a single feature has on the model's performance, using samples that were not seen by that particular tree during training. This strengthens the robustness of the method, as the importance is evaluated on data not used to build that specific tree, reducing overfitting and providing a more reliable estimate [34].

To evaluate the importance of the ECG in stress detection and compare it with that of the EEG, we analyzed how the Random Forest model positioned the four ECG features in the importance ranking with respect to the total of 29 features used to train the model. Subsequently, a general ranking was drawn up considering all the analyzed subjects. Figure 5.9 shows the distribution of the importance positions assigned to each ECG feature by the Random Forest model. In particular, it highlights how many times each single feature was classified in a given position within the different model runs, thus providing a clear indication of their relative importance in the overall analysis.

The root mean square of successive differences (RMSSD) plot shows a rather varied distribution of occurrences. Interestingly, this feature often occupies the top positions: it appears frequently in the first five positions (13 occurrences in total), indicating that this feature is among the most important features in stress detection. This suggests that short-term heart rate variability is a significant indicator of stress. The beats per minute (BPM) plot shows a different distribution: occurrences are few in the top positions and are more concentrated in the last positions (12 occurrences in the last two positions), indicating that mean heart rate is not among the most important features in stress detection when compared to EEG features. The standard deviation of NN intervals (SDNN) plot shows a moderately varied distribution: it appears occasionally in the top positions, but has a broader distribution than RMSSD. This suggests that long-term heart rate variability has a moderate significance in stress detection and is not as significant as RMSSD. The pNN50 plot shows a clearly skewed distribution towards the bottom positions. This implies that the percentage of successive NN intervals that differ by more than 50 ms is not considered a particularly important feature by the Random Forest model for stress recognition.

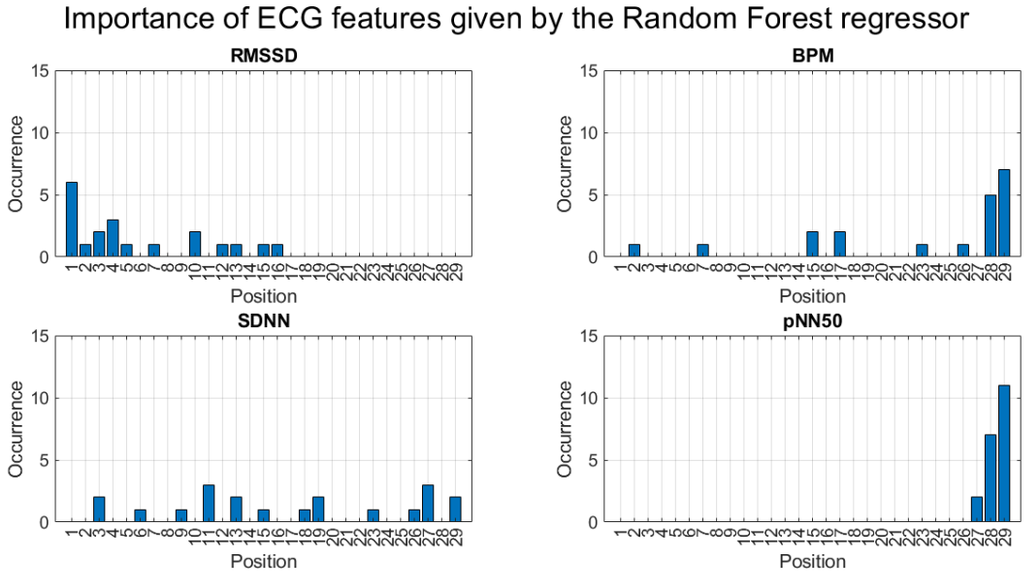

Figure 5.9: Relevance of ECG features

The results indicate that EEG-derived features are generally more relevant than ECG-derived features in the context of stress detection. For the ECG, the RMSSD emerges as the only feature with a weight comparable to the top EEG features, often being found in the top positions. The other ECG features (BPM, SDNN, pNN50) show limited importance, often occupying the bottom positions in the ranking. The analysis performed suggests that EEG signals play a significantly more relevant role than ECG signals in stress identification, with the exception of RMSSD. This result is plausible considering that EEG is much more informative than ECG considering a signal recording of the same duration. The comparative evaluation between the features suggests that EEG signals provide more detailed and sensitive information about stress states, making their inclusion essential for accurate stress detection and analysis.

5.2 Statistic analysis results

This section is dedicated to the presentation of the results obtained from the statistical analyses on the data collected during the experiment. The aim of this phase is to examine in depth how the different stimulation conditions influence the cognitive and physiological performance of the participants. Through a detailed evaluation of the data, the specific effects of each stimulation condition will be explored, in order to clarify the underlying mechanisms and their implications. The results obtained will offer critical insights to understand the effectiveness of the different experimental conditions and could help direct future research and practical applications.

Mental stress is one of the elements that significantly influence health problems in contemporary societies [77] and is becoming increasingly debilitating in everyday life. People under stress tend to worsen their cognitive functions with negative impacts on work and study. Acute mental stress in fact leads to the deterioration of creativity, problem solving, decision making and working memory [78], in addition to a decrease in attentional resources or reduced activity in the evaluation of responses [92]. Furthermore, some studies suggest that psychological stress shifts the balance of attention from a task-oriented mode to a sensory vigilance mode, modulating in particular the processes of selective attention, resulting in faster reaction times but less accurate responses [59].
The deterioration of performance under stress has been demonstrated by various studies, including a research [100] in which it was highlighted that the stress caused by a noisy work environment led to the worsening of performance in the execution of the Montreal Imaging Stress Task (MIST) compared to the silent and mentally stress-free environment. As regards the trend of reaction times under stress, however, the results of the studies are often discordant: the research [122], for example, goes against the idea arising from the study cited above. In this case, the subjects who were subjected to a mental calculation task had lower reaction times in neutral conditions compared to the stress condition, while maintaining an error rate with no significant differences between the two conditions.
The use of binaural beats to help relieve anxiety and stress is becoming more widespread as various studies show that they help to induce sleep, increase relaxation, improve memory and alertness [79].

This thesis focused mainly on evaluating the influence of alpha binaural beats on the performance of subjects subjected to a stressful condition based on what has also been done in other studies. Brain activity within the alpha rhythm has been associated with alertness, working memory, information processing speed and relaxation [81], [82], [76], [104].
In a study published in 2018 [80] for 40 young subjects, auditory reaction times (ART), visual reaction times (VRT) and short-term memory were evaluated in three different conditions: no stimulation, stimulation with constant alpha and gamma binaural beats. The results highlighted statistically significant differences for ART and VRT in the conditions with binaural beats compared to the one without stimulation, indicating an improvement in attention through entrainment with alpha and gamma binaural beats. Working memory, on the other hand, does not present values with a statistical difference despite having better scores in the presence of stimulation. Also in [85], an improvement in attention and also in working memory was detected, in subjects subjected to stimulation with alpha binaural beats compared to the control group. More recently, in 2022, a study [86] was conducted to evaluate the effectiveness of binaural beats (BB) in improving mental alertness and reducing psychological stress at work. In this regard, the experimental protocol consisted of four cognitive conditions: high alertness (HV), alertness enhancement (VE) through binaural beats, mental stress (MS), and stress relief (SM) through stimulation. Stimulation with binaural beats resulted in a reduction in reaction time to stimuli and increased accuracy in the Stroop Color-Word Test, revealing that they can

be used to increase alertness and mitigate stress. At the University of Dayton, a thesis [87] was carried out in which the subjects faced mathematical calculations of varying complexity subjected to different binaural tones, detecting an improvement in both speed and accuracy compared to the condition without auditory stimulation in all levels of difficulty.

The analyses carried out in this thesis in terms of accuracy, reaction time and inverse efficiency score (IES) are reported in the subsections below.

5.2.1 Total task

For the analysis of the data of the experimental phase, an in-depth exploration of the differences between the performances of the subjects subjected to three different stimulation conditions was carried out by analyzing three main aspects: accuracy of the responses, reaction times and inverse efficiency score (IES). These parameters were examined through statistical tests with the aim of precisely delineating the impact of the stimulations on the participants' behavior: from the Shapiro-Wilk test, accuracy and reaction time appear to have a Gaussian distribution, while the IES does not, consequently for the first two the Anova and the Student t-test were used for the post-hoc analysis and for the IES the Friedman test and the Wilcoxon test.

- **Analysis of accuracy**

  The accuracy of the responses represents a crucial parameter to understand how the different stimulations influence the subjects' ability to respond correctly. For this analysis, a repeated measures ANOVA was used, which highlighted a statistically significant difference between the subjects but not between the stimulation conditions as can be read in the table 5.2. This result suggests that, although there are substantial individual differences in response accuracy, these differences are not influenced by the applied stimulations.

Source	**Sum Sq.**	**d.f.**	**Mean Sq.**	**F**	**Prob > F**
Subject	1.20623	19	0.06349	239.97	0
Stimulation	0.00041	2	0.00021	0.78	0.4651
Error	0.01005	38	0.00026		
Total	1.2167	59			

Table 5.2: Analysis of Variance (ANOVA) results.

  To confirm these results, a post-hoc analysis was performed (using the multiple comparison test, multcompare in Figure 5.10) and the data distributions were examined using boxplots. The boxplots in Figure 5.11 clearly show the absence of significant differences between the different experimental conditions, indicating that none of them has a significant impact on the overall accuracy of the responses. This suggests that stimulation, regardless of its type, does not affect the subjects' ability to respond correctly.

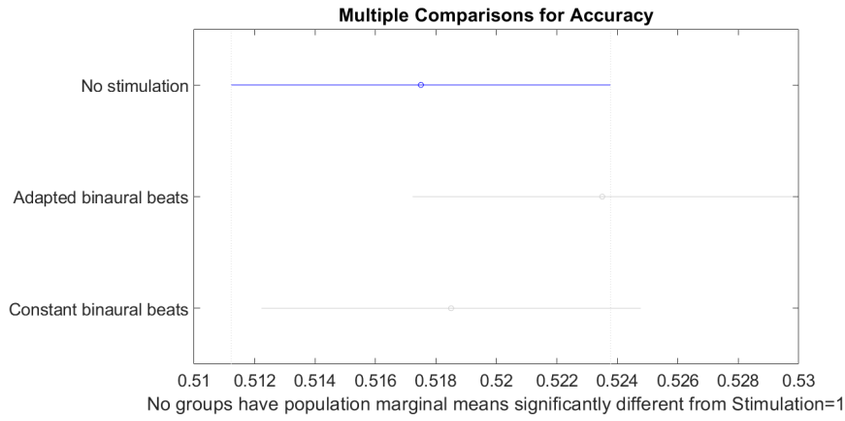

Figure 5.10: Multcompare analysis: Accuracy

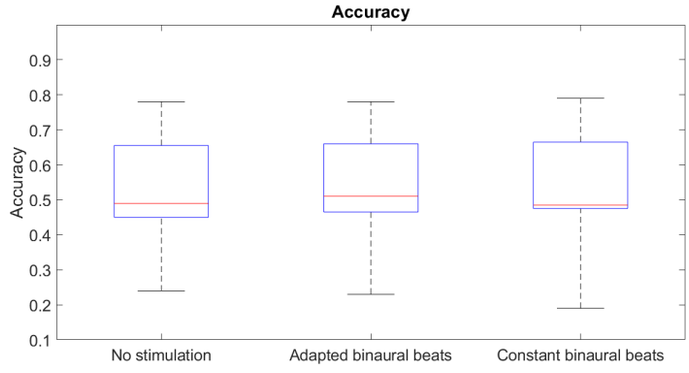

Figure 5.11: Accuracy distribution across the three experimental conditions in the total task

- **Reaction time analysis**

  Reaction time is an essential parameter to understand the speed with which participants process information and respond to stimuli. The ANOVA conducted on this parameter highlighted significant differences between the stimulation conditions as reported in Table 5.3. This result suggests that, regardless of the individual characteristics of the subjects, the type of stimulation substantially affects reaction times.

Source	Sum Sq.	d.f.	Mean Sq.	F	Prob > F
Subject	0.17969	19	0.00946	1.04	0.0539
Stimulation	0.36382	2	0.18191	35.41	0
Error	0.19521	38	0.00514		
Total	0.73872	59			

Table 5.3: Analysis of Variance (ANOVA) results.

Confirmation of the results was obtained through the post-hoc analysis (multcompare)

in Figure 5.12 and the observation of the boxplots in Figure 5.13, highlighting significant differences between the stimulation conditions. In particular, the use of adapted binaural beats led to faster reaction times than both constant binaural beats and no stimulation. The boxplot highlights that reaction times are shorter for the adapted stimulation than for the other two conditions. Between the absence of stimulation and stimulation with constant binaural beats there is a statistically significant difference, although smaller than that with adapted beats.

These results are in line with the studies analyzed and also indicate that stimulation with adapted binaural beats also has a positive effect on reaction time, accelerating the participants' response. This effect could be due to the ability of adapted stimulation to maintain a high level of attention and alertness of subjects, reducing the time needed to process and respond to stimuli. Constant stimulation and no stimulation instead seem to have a less pronounced impact. This result suggests that the adaptation of stimulation is a critical factor in optimizing response speed.

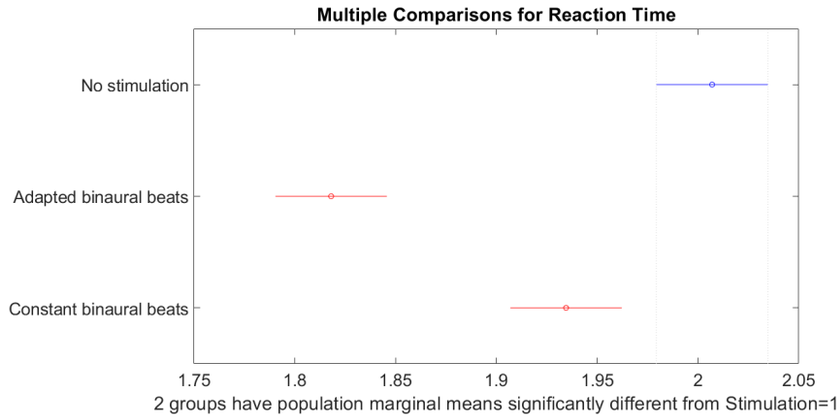

Figure 5.12: Multcompare analysis: Reaction Time

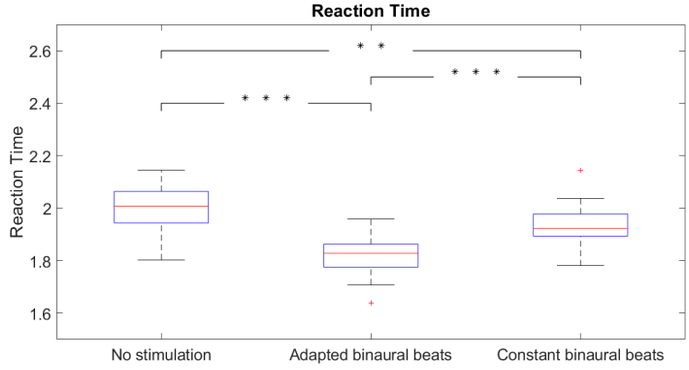

Figure 5.13: Reaction time distribution across the three experimental conditions in the total task ** $\Rightarrow p < 0.01$, *** $\Rightarrow p < 0.001$

- **Inverse Efficiency Index (IES) Analysis**

  The inverse efficiency score (IES), which combines reaction times with accuracy, was analyzed using the Friedman test given the non-parametric distribution of the data. The result of this test reported in Table 5.4 showed a highly significant difference between the stimulation conditions.

Source	SS	df	MS	Chi-sq	Prob > Chi-sq
Columns	25.9000	2	12.9500	25.9000	2.3762e-06
Error	14.1000	38	0.3711		
Total	40.0000	59			

Table 5.4: Results of the Friedman test.

The post-hoc analysis with the Wilcoxon test highlighted that the adapted stimulation condition is the one that differs the most from the others, suggesting that this stimulation has a distinctive effect on the overall efficiency of the performance. This can be seen both thanks to the multcompare in Figure 5.14 and in the boxplots of the IES data in Figure 5.15.

It is observed that the stimulation conditions with constant and adapted binaural beats present slightly lower IES values than the condition without stimulation, which indicates an improvement in efficiency under stimulation although it is slightly less significant for constant binaural beats. As for stimulation with adapted binaural beats, this shows lower IES values than both constant stimulation and no stimulation, indicating greater efficiency under this condition.

These results show the importance of stimulation as a whole and in particular suggest that stimulation, whether constant or adapted, not only accelerates reaction times, but does so without compromising accuracy, thus improving the overall efficiency of performance. These results are partly in line with those of the reference literature in which, in most cases, an improvement in accuracy was also noted. However, the results obtained in this study are particularly promising since they indicate that the increase in response speed is not due to random responses by participants. Indeed, accuracy remained high even with shorter reaction times, suggesting that stimulation improved attention and speed without compromising performance. This is particularly interesting in contexts where operational efficiency is crucial and where it is necessary to obtain maximum performance with minimum error.

The set of data collected from the statistical analyses conducted in this research provide a complete picture of the effects of the different stimulation conditions on the participants' performance. First of all, the fact that there are no significant differences in the accuracy of the responses between the various conditions suggests that stimulation does not affect

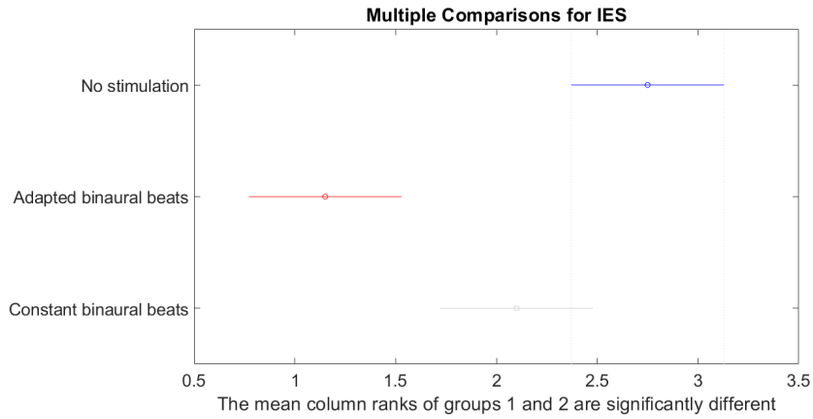

Figure 5.14: Multcompare analysis: Inverse Efficiency Score

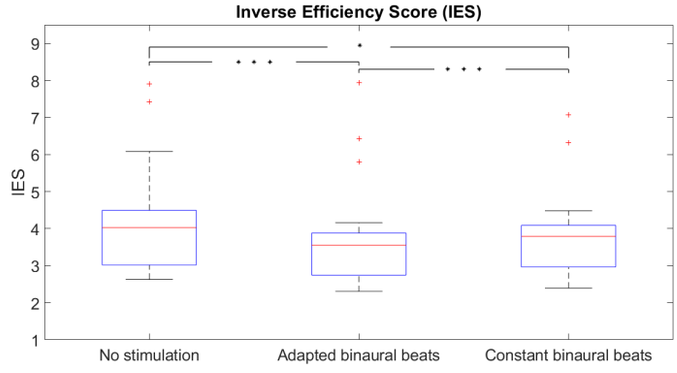

Figure 5.15: Distribution of IES across the three experimental conditions in the total task * $\Rightarrow p < 0.05$, *** $\Rightarrow p < 0.001$

the participants' ability to respond correctly. This result is comforting because it suggests that the stimulations do not cause discomfort to the subject.

At the same time, the reaction time and the Efficiency Index (IES) show that adapted stimulation has a significant and positive impact. Subjects subjected to this condition have demonstrated to respond more quickly and with greater efficiency than when they are exposed to constant stimulation or to no stimulation. These results are particularly relevant for the practical application of stimulations in contexts where it is important to reduce reaction times without sacrificing accuracy.

Adapted stimulation therefore seems to be the most advantageous condition, as it optimizes overall performance without compromising the accuracy of responses. It therefore seems that adapted stimulation, by modulating the intensity or frequency of stimuli based on the subject's response, could maintain the level of cognitive activation at an optimal level, avoiding cognitive overload.

5.2.2 Hard Task vs Easy Task

Since the effectiveness of constant binaural beats compared to no stimulation has already been demonstrated in several studies ([83], [84], [20], [21]), in this thesis we focused on comparing the two types of stimulation: constant binaural beats and adapted binaural beats.
To further deepen the understanding of the influence of stimulation conditions on cognitive performance, detailed statistical analyses were conducted focusing on the stimulation conditions with constant and adapted binaural beats by differentiating the level of difficulty of the task, separating the periods of more difficult questions (first 3 minutes) from those of easier questions (subsequent 2 minutes). The results are graphically shown in Figure 5.16.

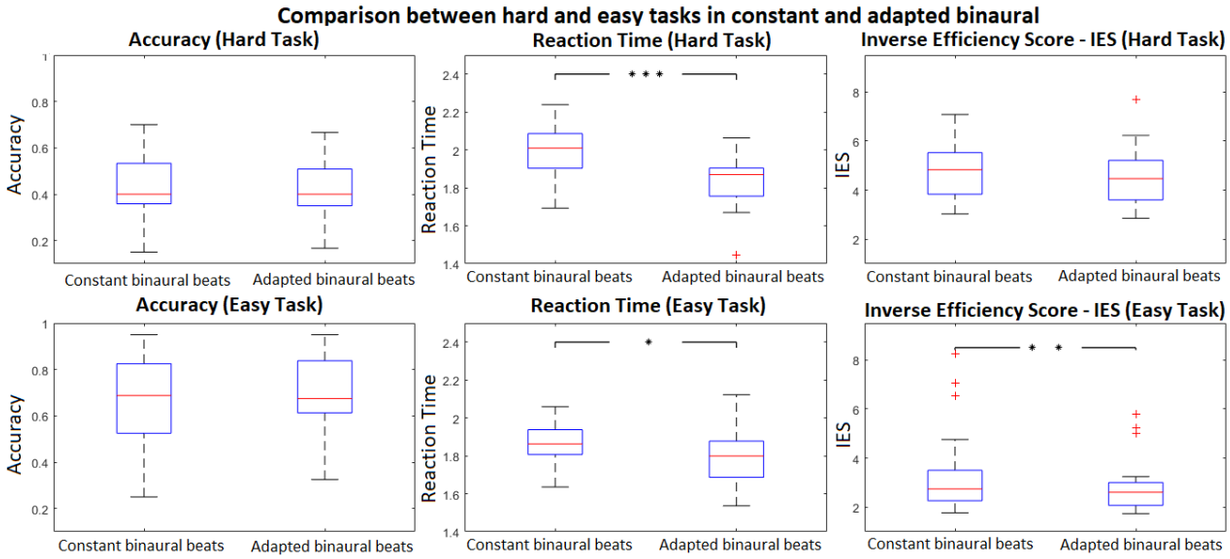

Figure 5.16: Boxplot distributions of accuracy, reaction time and inverse efficiency score: hard task vs easy task. * $\Rightarrow p < 0.05$, ** $\Rightarrow p < 0.01$, *** $\Rightarrow p < 0.001$

- **Accuracy**

  Regarding accuracy, statistical analyses conducted by ANOVA and t-test did not reveal significant differences, neither for the difficult nor for the easy part of the task. This result confirms previous observations, where no significant difference in the accuracy of responses had emerged between the different stimulation conditions. Again, it seems that the nature of the stimulation, whether constant or adapted, does not significantly influence the accuracy of participants' responses, regardless of the difficulty level of the task.

- **Reaction Time (RT)**

  Reaction time showed a more interesting picture. For the difficult part of the task, ANOVA and t-test revealed a significant difference between the two stimulation conditions, with reaction times during the adapted stimulation being significantly lower than

during the constant stimulation. This pattern was also observed for the easy part of the task, although with a slightly lower significance since for the difficult task the p-value is equal to 5.7939*10^-4 while for the easy one it is 1.8451*10^-2. Also in this case, the adapted stimulation led to faster reaction times compared to the constant stimulation.

These results are consistent with the previous ones, where the adapted stimulation was more effective in reducing reaction times compared to the constant stimulation. This confirms the idea that the adapted stimulation, by dynamically modulating the frequency of the stimuli, keeps the participants in a higher alert and reactive state, especially in conditions of variable difficulty. Interestingly, the effect of the adapted stimulation is evident both in the more difficult and in the easier tasks, suggesting that the adaptation of the stimulation is beneficial regardless of the difficulty level.

- **Inverse efficiency score (IES)**

  The analysis of the Efficiency Index (IES) revealed interesting results and partially in line with the previous ones. For the difficult part of the task, Friedman and Wilcoxon tests did not reveal statistically significant differences between stimulation conditions, although the IES during adapted stimulation was slightly lower than during constant stimulation. This suggests that, although not reaching statistical significance, adapted stimulation could still provide a slight advantage in terms of operational efficiency in the more difficult tasks.

  For the easy part of the task, however, a significant difference was found between conditions, with the IES during adapted stimulation being lower than during constant stimulation (p-value = 0.0045). Furthermore, the boxplot associated with the adapted condition indicates a lower variability in the participants' performance. This suggests that adapted stimulation not only improves the average efficiency, but does so more consistently across participants, reducing the dispersion of the results.

The results of these in-depth analyses are largely consistent with the observations made in the previous sub-chapter. Once again, it appears that adapted stimulation has a positive effect on reaction times, making them significantly shorter than constant stimulation, both in difficult and easy tasks. This confirms the effectiveness of adapted stimulation in maintaining subjects in a state of greater alertness and reactivity.

Regarding accuracy, the lack of significant divergences between the two stimulation conditions, regardless of the complexity of the task, suggests that stimulation did not affect the accuracy of responses. This result indicates that, although stimulation did not increase accuracy as documented in previous studies, it did not deteriorate performance either. Accuracy remained stable, demonstrating that stimulation did not cause discomfort or negatively impact participants' thinking while performing the tasks.

The IES analysis offers new nuances compared to the previous chapter: although there is no significant difference in IES for difficult tasks, adapted stimulation still shows a slight superiority. For easy tasks, a significant difference emerges in favor of adapted stimulation, with greater efficiency and less variability between participants. This could indicate that adapted

stimulation is particularly effective in improving performance in less demanding tasks, where participants can benefit more from stimulus modulation to optimize their responses.

It is interesting to note that the IES appears to have a statistical difference only in the easy task despite the fact that accuracy is not significant in either task and reaction time has a more pronounced statistical significance in the difficult task. In the latter, the fact that the IES does not have a statistical difference even if the reaction time is significantly different may seem counterintuitive, but it can be explained by the fact that the IES is based on a ratio. In the hard task, the differences in reaction time are marked, but since accuracy is very low and little variable, the resulting ratio (IES) does not present a statistically significant difference. In the easy task scenario, accuracy is not significantly different between groups. However, the differences in reaction time, even if less marked than in the difficult task, have a more evident impact on the IES when accuracy is high and more variable. A change in reaction time, in the presence of high and inconstant accuracy, is more evident in the IES. Thus, in the easy task, moderate differences in reaction time, combined with a medium high and variable accuracy, result in significant differences in IES. In the hard task, however, marked differences in reaction time are not significantly reflected in the IES because the relatively low and less variable accuracy in both stimulations reduces the effect of differences in reaction time by stabilizing the value of the ratio, making the Wilcoxon test less capable of detecting significant differences despite the evident differences in reaction time.

In conclusion, the results obtained largely confirm those already analyzed in the previous chapter, reinforcing the idea that adapted stimulation is particularly effective in improving reactivity and performance efficiency, without compromising accuracy. Furthermore, the differentiated analysis between difficult and easy tasks suggests that the effectiveness of stimulation on reaction time is independent of the difficulty level.

5.2.3 Constant Binaural Beats vs Adapted Binaural Beats

To further investigate cognitive performance under constant and adapted binaural beat stimulation, the data were broken down for each minute of the task, aiming to capture any dynamic variations in accuracy (Figure 5.17), reaction time (RT) (Figure 5.18) and Inverse efficiency score (IES) (Figure 5.19) during the task execution. It is important to remember that the first three minutes of the task were characterized by difficult questions, while the last two minutes featured easier questions.

- **Accuracy**

  The analysis of accuracy for each minute showed variable results:

  - 1st minute: A significant difference is observed with the highest accuracy under adapted stimulation. This suggests that, at the beginning of the task, participants under adapted stimulation were more accurate in their responses than those under constant stimulation. This could be attributed to the initial effect of the adapted stimulation, which probably kept participants in a higher state of alertness from the beginning.

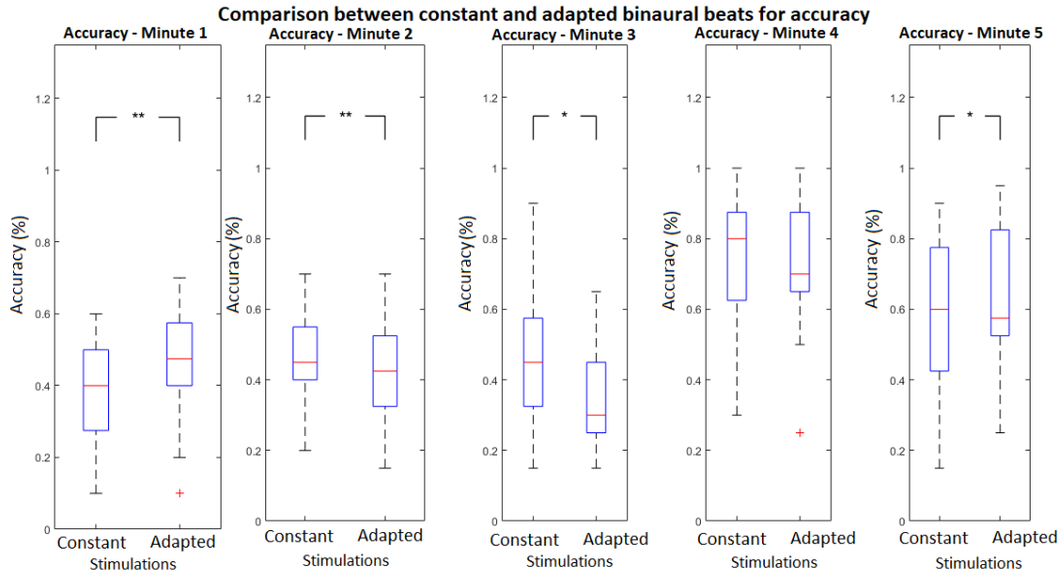

Figure 5.17: Accuracy distribution for each minute of the task. * $\Rightarrow p < 0.05$, ** $\Rightarrow p < 0.01$

- 2nd and 3rd minute: In the following minutes, accuracy reversed, showing a significant difference in favor of constant stimulation. This could indicate that, as the task became more demanding, constant stimulation helped participants maintain a more stable level of performance.
- 4th minute: As the task became easier, no significant difference was detected between the two stimulation conditions, suggesting that binaural beats did not have a significant impact on accuracy when moving to the less difficult condition.
- 5th minute: In the last minute of the task, the adapted stimulation again showed an advantage in terms of accuracy. This leads to the inference that participants under adapted stimulation recovered their accuracy perhaps thanks to a greater ability to adapt to the less demanding conditions.

- **Reaction Time (RT)**

  Analysis of reaction time for each minute revealed the following patterns:

  - Minute 1 and 2: In the first two minutes, reaction times were significantly faster under adapted stimulation. This suggests that, at the beginning of the difficult task, adapted stimulation facilitated a quicker response from participants. Adapted stimulation therefore appears to have maintained participants in a state of greater alertness and reactivity than constant stimulation.
  - Minute 3: At minute 3, no significant difference in reaction times emerged between the two conditions, indicating a possible convergence of performance or a point at which both types of stimulation had exhausted their distinctive effects.

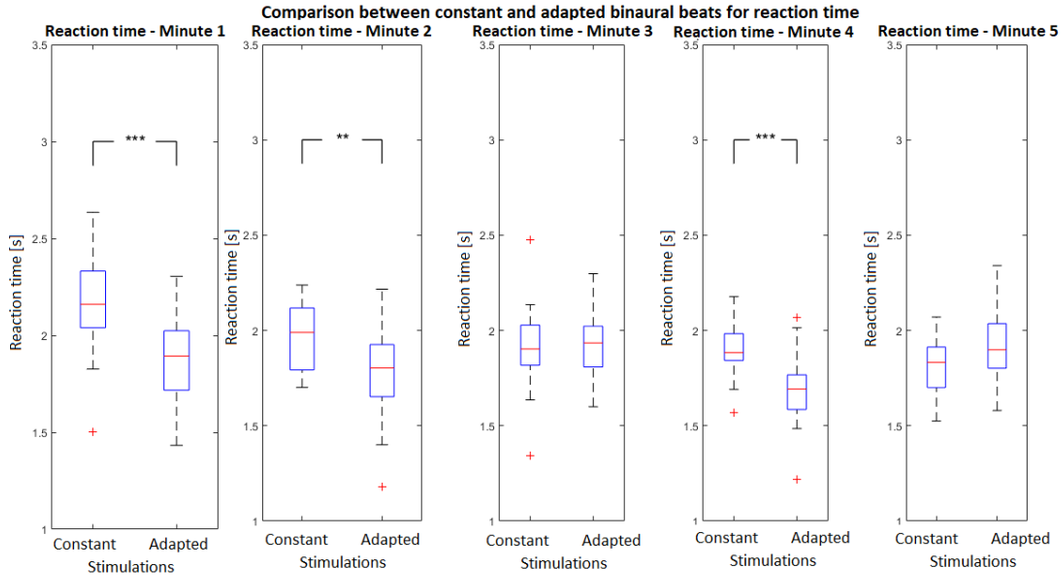

Figure 5.18: Reaction time distribution for each minute of the task. ** $\Rightarrow p < 0.01$,*** $\Rightarrow p < 0.001$

- 4th minute: As the task became easier, the adapted stimulation again showed an advantage in terms of faster reaction times, suggesting that this stimulation has an immediate effect following the transition to the easier task condition at least with regard to reaction time.
- 5th minute: In the last minute, no significant difference was observed, which may indicate that the effect of the stimulation leveled off towards the end of the task, perhaps due to adaptation or cognitive fatigue.

- **Efficiency Index (IES)**
  The analysis of the IES provided further insights into the dynamics of performance:
  - 1st minute: In the first minutes of the task, the IES was significantly better under adapted stimulation, suggesting that, at the beginning, adapted stimulation facilitated greater efficiency, with faster reaction times and higher accuracy.
  - 2nd and 3rd minutes: During the second and third minutes, no significant difference in the IES was detected, indicating a stabilization of performance or a possible exhaustion of the initial effect of stimulation.
  - 4th minute: As the task progressed to the easy portion, IES again improved under adapted stimulation, confirming that adapted stimulation maintained its effectiveness in promoting greater efficiency even under less demanding conditions.
  - 5th minute: In the final minute, IES did not show significant differences, suggesting further convergence of performance between the two stimulation conditions toward the end of the task.

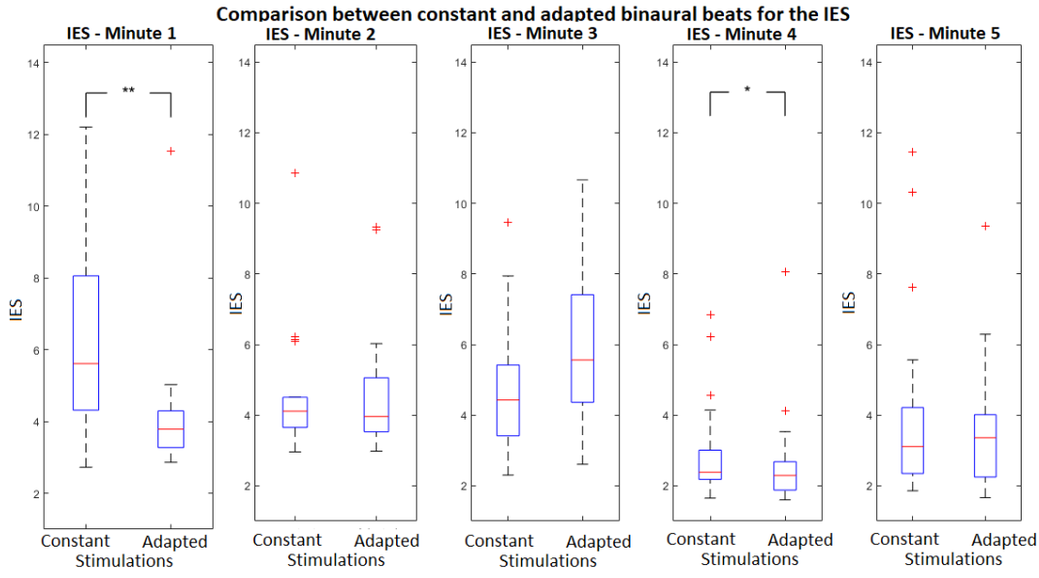

Figure 5.19: Inverse efficiency score distribution for each minute of the task.* $\Rightarrow p < 0.05$,** $\Rightarrow p < 0.01$

These results confirm that adapted stimulation is generally more effective in reducing reaction times, especially in the initial moments. Adapted stimulation seems to be particularly beneficial in maintaining participants in a state of greater alertness and reactivity, contributing to faster reaction times and, in the initial phases of the two tasks, to a better overall efficiency as indicated by the IES.

This interpretation highlights how adapted stimulation not only helps to maintain high accuracy, as also occurs with constant stimulation, but also favors a quicker and, therefore, more efficient response, especially in critical moments of the task. These results reinforce the idea that adapted stimulation could be particularly useful in contexts where high reactivity is required

These results provide a complex and dynamic picture of the impact of the two stimulation conditions on cognitive performance. In the first minutes of the difficult task, adapted stimulation favored faster reaction times and a better IES, which could indicate that stimulation with adapted binaural beats helps participants to maintain a high level of alertness and operational efficiency. This observation is further strengthened by the fact that reaction times significantly improved in the transition from the difficult to the easy task phase. As regards accuracy, the adapted stimulation showed an initial advantage, suggesting that a dynamic modulation of the stimuli can improve the precision of the responses at the beginning of the task. Continuing with the task, the constant stimulation seems to be better even if the difference in accuracy between the two stimulations is not excessive unlike that which occurs in the first minute in favor of the adapted binaural beats.

In the fifth minute and therefore at the end of the task, the adapted stimulation recovers in terms of accuracy but loses statistical difference in terms of reaction time, reflected in a non-significant IES for the last minute of the task. This could indicate that, when the task is less demanding and the subjects have had enough time to adapt to the change in difficulty, overall performance does not show important differences between the two types of stimulation.

These results are partly aligned with those previously analyzed. Adapted stimulation tends to favor faster reaction times and greater efficiency at the beginning of the two task phases. Additional information on accuracy has been obtained with respect to those of the previous chapters, as the general trend is observed for which adapted stimulation offers advantages in terms of accuracy at the initial and final moments of the task.

This minute-by-minute analysis highlights the complexity of the interaction between the type of stimulation and the dynamics of the task, suggesting that the effectiveness of stimulation can vary over time and according to the difficulty of the task, with important implications for the design of targeted and personalized cognitive interventions.

5.2.4 A Closer Look at Adapted Binaural Beats

The analysis of the stimulation condition with adapted binaural beats has been further deepened by observing the trend of the stimulation frequencies and the distributions of reaction time and accuracy over time, obtaining a complex but extremely informative view on the effectiveness and the need for a modulated and adaptive stimulation approach.

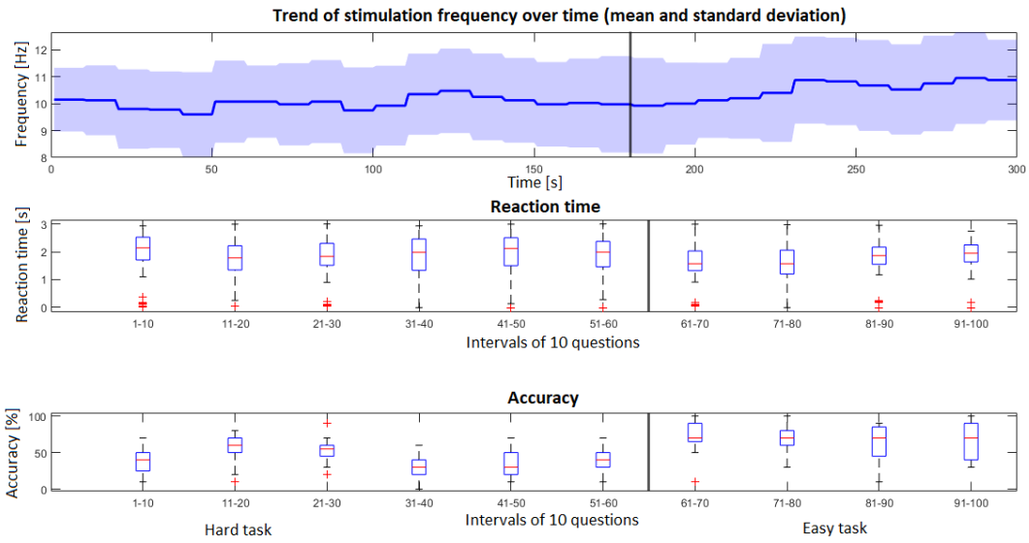

Figure 5.20: Trend stimulation frequency over time, accuracy and reaction time for 10 question intervals

In Figure 5.20 the first graph shows the average trend of the adapted stimulation frequencies. The blue line represents the average frequency of stimulation over time that remained stable around 10-11 Hz which are on average the individual alpha frequency values measured during the relaxation phase, while the shaded area around the line indicates the standard deviation, providing a measure of the variability in the applied frequencies. Regarding this, it is clearly noted that the standard deviation is lower at the beginning of the task and tends to increase as the experiment proceeds. This increase in the standard deviation suggests that there is no single optimal stimulation frequency that can be universally applied to all subjects and kept constant over time, in fact, the increase in variability indicates that each subject, as they tackle the task, may require a different modulation of the stimulation to maintain or improve their performance.

This trend underlines the importance of a modulated and adaptive approach, in which the stimulation frequency dynamically adapts to the specific needs of each subject over time.

The growth of the standard deviation can be interpreted as a signal that the stimulation system was effective in recognizing the different cognitive and physiological needs that emerge during the task. The adaptation must not be static but fluid, responding to the variations of each individual to maximize the effectiveness of the intervention.

Analyzing the reaction times and accuracy for segments of 10 questions lasting 30 seconds, it is observed that the reaction times remain stable during the task with medians that vary little between the various intervals, indicating that the participants maintain a good level of attention and readiness, despite the duration and difficulty of the task.

As for accuracy, this tends to show a constant trend over the entire task, except for a slight drop in the final part of the difficult task that is immediately recovered in the less complex tasks in which a constant trend can be observed again. The accuracy boxplots show a consistency in the precision of the responses on average, with medians remaining stable and distributions not indicating a significant dispersion upwards or downwards suggesting that the subjects, not only responded quickly, but also accurately throughout the task.

This suggests that the increase in the standard deviation in the stimulation and therefore a more personalized adaptation helped to maintain or even stabilize the subjects' performance on average, resulting not in a reflection of random variations, but in an indicator of the effectiveness of an adaptive approach that responds to the different needs of the subjects essential to maintain a stable and sustained cognitive performance, as demonstrated by the data on reaction times and accuracy.

These results are particularly interesting because they support the idea that stimulation with adapted binaural beats can be an effective method to modulate stress and improve cognitive performance. The ability to maintain a high and constant performance suggests that this type of stimulation could have practical applications in contexts in which it is necessary to sustain a high level of attention and accuracy over time, such as in the workplace or study.

5.2.5 Analysis of the Missing Responses

The analyses continue by examining the number of unanswered questions in the three experimental conditions, breaking down the data minute by minute. These results allow us to further deepen our understanding of the effects of stimulation on participants' cognitive performance.

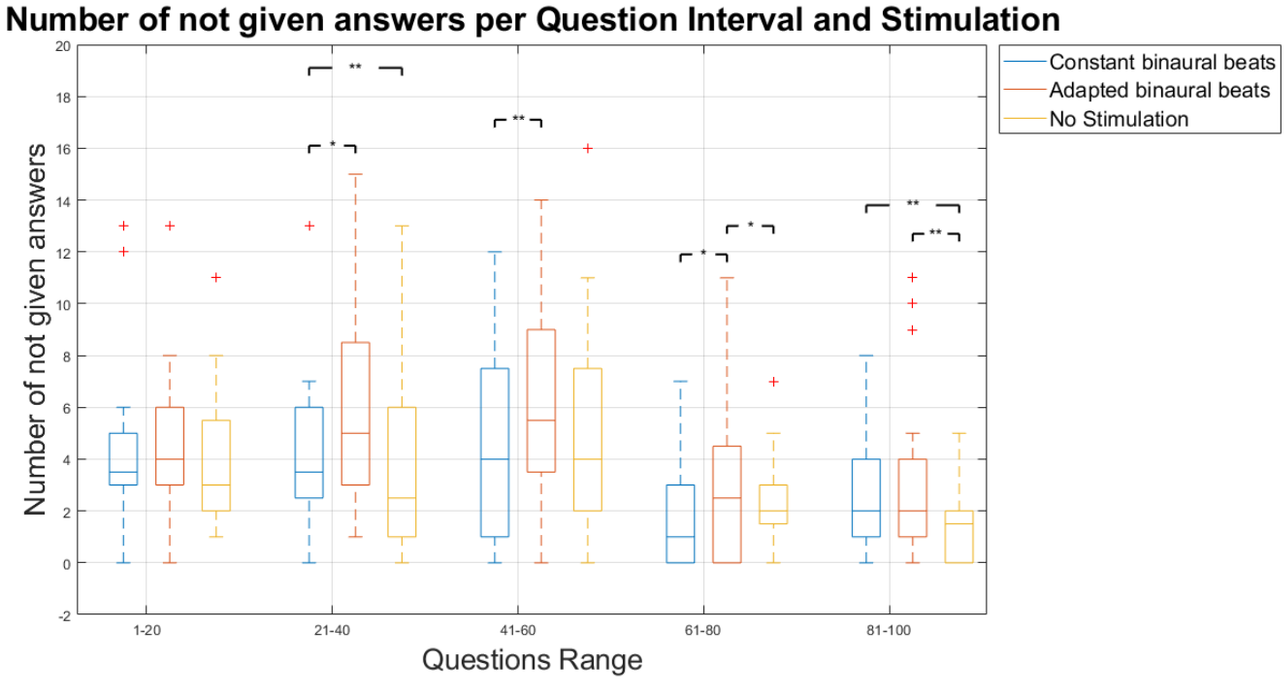

Figure 5.21: Distributions in the three experimental conditions of non-responses for each minute.* $\Rightarrow p < 0.05$, ** $\Rightarrow p < 0.01$

As can be seen in Figure 5.21, in the first minute no significant differences emerged, this finding suggests that, at the beginning, the stimulations do not affect the accuracy of the task.

During the second, the third and the fourth minutes, a significant difference was found between the constant and adapted binaural beats stimulation conditions, with a slightly higher number of non-responses in the adapted condition. This can be interpreted as a moments in which the adapted stimulation led participants to be more thoughtful and cautious in their responses, at the expense of a higher number of non-responses. The same occurs also when comparing the constant stimulation with the no stimulation condition in the second minute and the adapted stimulation and the no stimulation in the fourth minute.

In the last minute, no significant difference was observed between the constant and adapted binaural beats conditions, which is positive since both conditions seem to have supported participants' performance in a similar way towards the end of the task. However, in comparison with the condition without stimulation, both the conditions with adapted and constant binaural beats showed a higher number of unanswered questions. This could indicate that, at the end of the task, when fatigue begins to appear, stimulation leads to maintaining a high

level of attention, being cautious in responding, but with the risk of increasing the number of unanswered questions due to lack of time.

Stimulation with adapted binaural beats, showing in some cases a slightly higher number of unanswered questions compared to other conditions, may suggest a more reflective and less impulsive attitude in participants, who may have preferred not to respond rather than providing incorrect answers. This aspect highlights another nuance of the results obtained from this study: both types of stimulation and especially the one with adapted binaural beats seem to make subjects more reflective without significantly affecting the overall accuracy of the task, which, as seen from previous analyses, remains approximately the same regardless of the presence or absence of stimulation.

Furthermore, the lack of significant differences in the number of non-responses across some minutes of the task indicates that adapted stimulation was effective in keeping individuals engaged and focused, without affecting their ability to complete the task. This is a significant achievement, especially considering that cognitive performance usually declines over time.

Overall, the analysis of the number of non-responses still shows that stimulation with adapted binaural beats is an effective method to support cognitive performance, because it appears to ensure a balance between accuracy and reactivity. Although it may have led to slightly more non-responses at some points, this can be seen as a sign of greater reflection and attention on the part of participants, rather than an indicator of poorer performance. Adapted stimulation thus emerges as a promising strategy to improve the quality of responses and sustain performance over time, especially in complex and cognitively demanding tasks.

5.2.6 Response Trends after the "Wrong Answer" Feedback

A further aim of the investigation was to explore how negative feedback affects the cognitive performance of subjects in different stimulation conditions. To this end, an artificial stress element was introduced by displaying the message "Wrong Answer!" following responses provided by the subjects, regardless of the actual correctness of the answer. Subsequently, the subjects' performance in the three questions following the feedback was analyzed, as represented in the graphs in Figure 5.22.

In the condition of stimulation with constant binaural beats, the feedback was mainly shown consistently with the subjects' performance, that is, it was shown in questions to which on average the subjects actually answered incorrectly. In the easy part of the test, however, the message was shown even when on average the subjects answered correctly, and analyzing the subsequent answers, it seems that the constant stimulation helped the subject in managing stress, resulting in positive performances following the stressful feedback, even if this could also be associated with the lower difficulty level of the task.

In the condition with adapted stimulation, the results seem promising in managing the induced stress. Even in the presence of incorrect negative feedback, the subjects maintained a high level of correct responses, as indicated by the numerous positive indicators and the limited presence of negative indicators. This suggests that stimulation with adapted binaural beats provided a favorable environment for concentration and cognitive resilience, allowing the

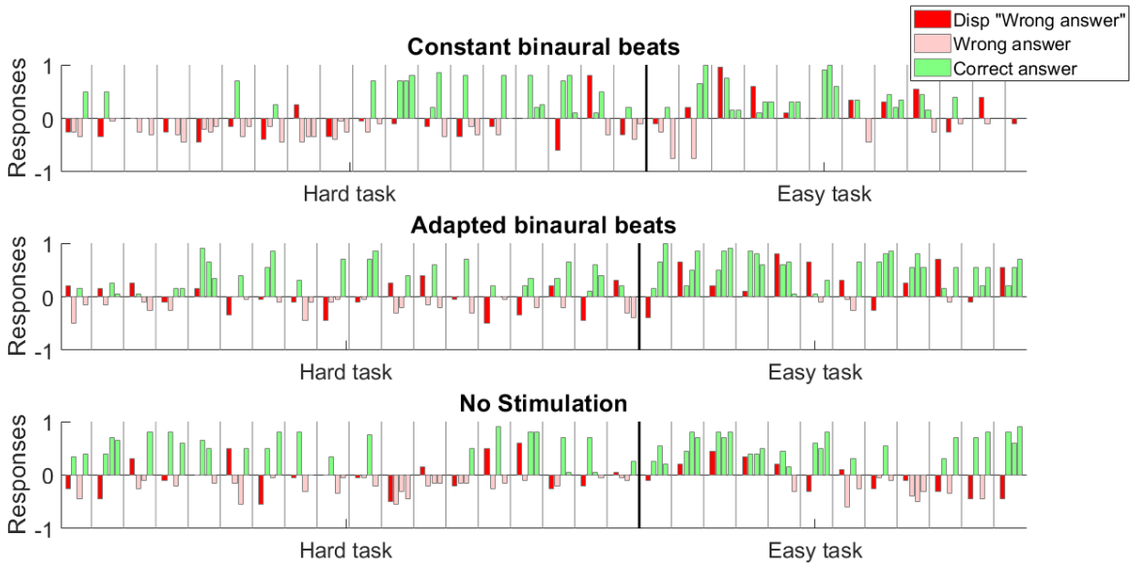

Figure 5.22: Response to stress-inducing negative feedback

subjects to better manage the additional difficulties imposed by the experimental protocol, contributing positively to stress management and improving the subjects' ability to maintain performance even in pressure situations.

Finally, in the no-stimulation condition, a significant number of correct answers were highlighted, even after the message "Wrong Answer!" was displayed. However, it is important to underline that, as it happened in the constant stimulation, in the difficult part of the test, negative feedback was often truthful, reflecting real errors in the answers provided by the subjects, which indicates that the stressful stimulus was not actually an additional factor in those cases. Also here in the easy part of the test, negative feedback was shown even when the answer was correct. This did not seem to have significantly influenced the stress and the performance of the subjects, confirming that it could be linked to the lower level of difficulty of the task.

In summary, while the no-stimulation condition allowed the subjects to maintain a baseline performance without significant improvements in stress management, constant stimulation seems to have introduced a greater variability in cognitive performance under pressure, stimulation with adapted binaural beats demonstrated a positive effect in supporting the subjects' resilience in the face of induced stress, facilitating a more stable performance and less susceptible to the effects of negative feedback. The trends reported in Figure 5.22 do not, however, present a clear distinction between the three conditions. This is due to the fact that all participants, at the end of the protocol, admitted to having noticed the presence of incorrect feedback sent on several answers in which they were sure they had answered correctly. Although at the beginning they might have had doubts about the actual correctness of their answers, towards the end of the protocol they realized that in reality their answers were correct and that the incorrect feedback only served to mislead them to increase stress.

5.2.7 Heart Rate and RMSSD: Baseline vs Task

One of the fundamental objectives of this thesis is to determine whether the stimulation used is able to reduce the subjects' stress level, while improving their cognitive performance. To obtain valid and relevant results, it is crucial that the experimental protocol is actually stressogenic, that is, capable of inducing a significant increase in the level of stress in participants during the task phase compared to the baseline phase. An effective method to measure stress levels is through heart rate monitoring (BPM - beats per minute), a physiological indicator commonly associated with stress. This can also be supported by the Root Mean Square of the Successive Differences (RMSSD) which is an additional ECG metric used to detect stress as reported in several studies: [88], [91], [52].

The variation in heart rate HRV is a phenomenon that reflects the balance between the sympathetic nervous system (SNS) and the parasympathetic nervous system (PNS) [89]. Following a stressful condition, the sympathetic system prevails leading to an increase in heart rate [90]. Therefore, if the heart rate (BPM) increases, both the RR intervals decrease and HRV decrease leading to lower values of SDNN and RMSSD. This trend was indeed also obtained in the following studies [88], [91], where stress was detected via ECG signals: during the stress condition, BPM increased, while temporal domain features, such as RMSSD, decreased compared to the resting condition, indicating sympathetic activation.

To verify the robustness of the protocol, BPM and RMSSD recorded during the baseline and task phases were compared for each of the three experimental conditions (Figure 5.23 and Figure 5.26): constant binaural beat stimulation, adapted binaural beat stimulation and no stimulation. The statistical analyses, conducted using the Wilcoxon test due to the non-parametric nature of the distributions, performed highlighted significant differences between the two phases in all conditions, with a p-value lower than 0.001 for both metrics, indicating a clear distinction between the subjects' stress levels in the two phases of the protocol.

In all three conditions, the Shapiro Wilk test revealed a non-Gaussian trend for both BPM and RMSSD, therefore the Wilcoxon test was used to analyze statistical differences. BPM was always significantly higher during the task phase compared to the baseline phase, while RMSSD was lower (p-values are all less than 0.001). These trends confirm that the protocol was able to induce a physiological response associated with stress in participants, as expected. The increase in BPM and the decrease in RMSSD is a clear signal that subjects perceived the task as demanding and stressful, thus validating the effectiveness of the protocol in creating a state of stress.

It is important to note that, despite the presence of significant statistical differences between baseline and task in terms of BPM, the median of BPM remained unchanged between the two phases in all three conditions. Thus, although the task did indeed cause an increase in stress in the subjects, this increase was uniform and consistent, without extreme peaks that could have indicated excessive variability or anomalous reactions among participants.

The fact that the median remained constant between baseline and task indicates that the

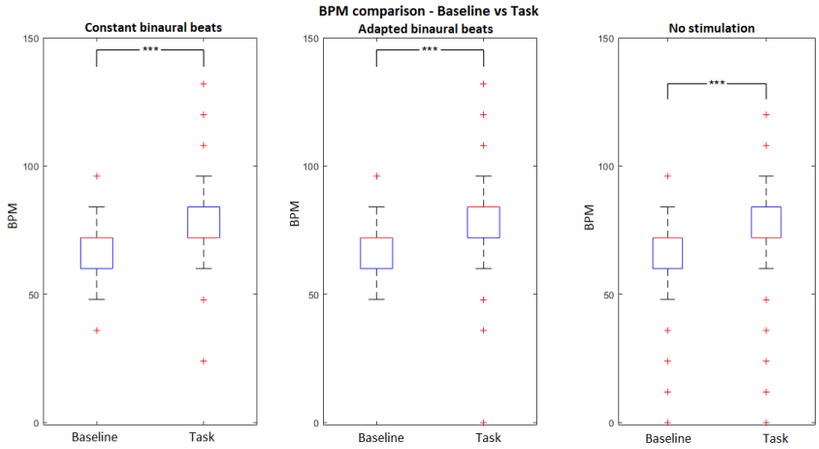

Figure 5.23: BPM distribution in the three experimental conditions: baseline vs task. *** $\Rightarrow p < 0.001$

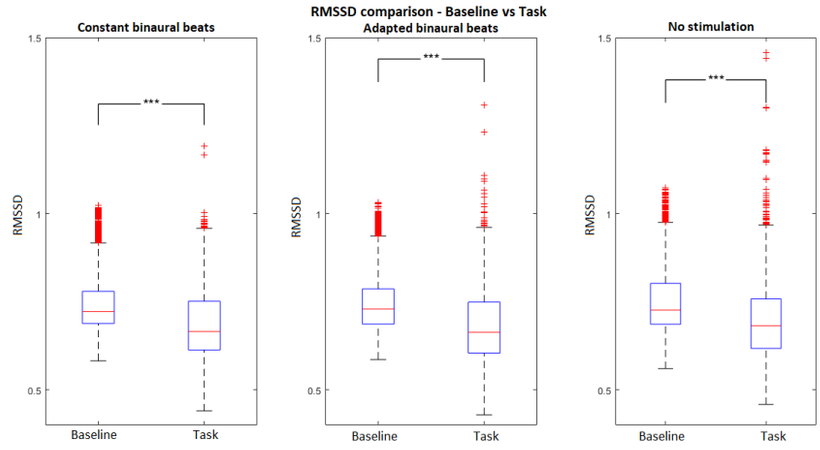

Figure 5.24: RMSSD distribution in the three experimental conditions: baseline vs task.*** $\Rightarrow p < 0.001$

increase in stress level was perceived in a similar way by participants in the three conditions, reinforcing the reliability and repeatability of the experimental protocol. In other words, the protocol induced a controlled and predictable stress response, without excessive differences between the different stimulation modalities or between individual subjects. This result is particularly important, since it allows us to attribute any differences in cognitive performance or residual stress levels directly to the effect of the stimulation, rather than to intrinsic variations in the protocol.

These results confirm that the experimental protocol used is sufficiently stressful to evaluate the effectiveness of the stimulation in reducing stress. Since the task leads to a clear increase in heart rate and a reduction in RMSSD compared to the relaxation phase, it can be deduced that the protocol used was adequate to test the main hypothesis of the research.

5.2.8 Stress Analysis

Before submitting the subjects to the protocol, they were asked to fill out the PSS questionnaire, which provides an indicative result of the level of stress perceived by the subjects in relation to the events of the previous days. As explained in chapter 4, the PSS score starting from which a subject is considered to be in a condition of high perceived stress is 27 [49].

For the purposes of this study, the test was useful to verify that the level of stress perceived by the participants was not influenced by external events, independent of the protocol. Following what was done in [103], the PSS scores were evaluated for each participant (reported in Figure 5.25) and the mean and standard deviation were calculated (present in table 5.5).

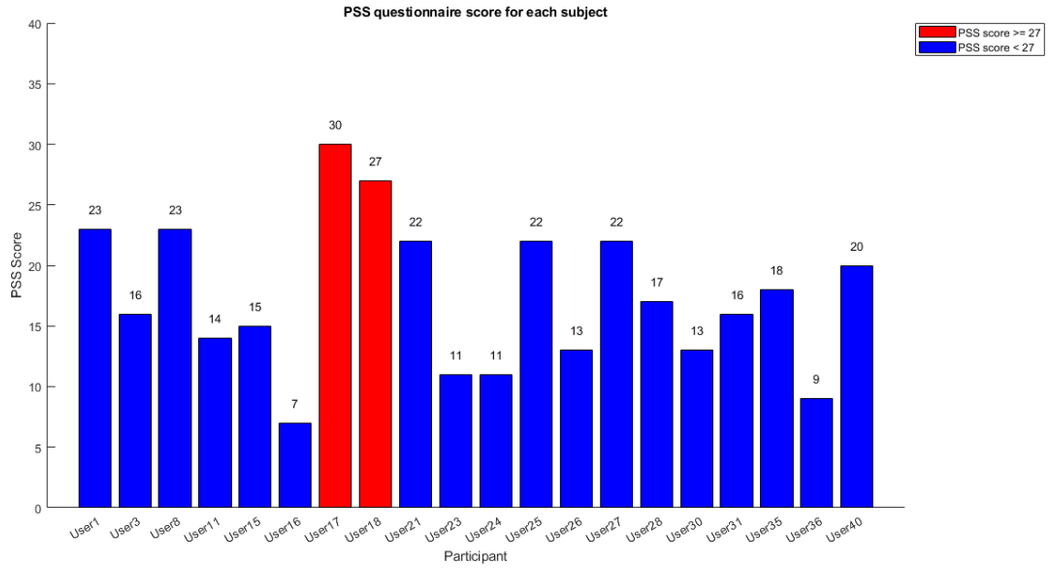

Figure 5.25: PSS questionnaire score for each participant

.

Mean	Standard deviation
17.45	6.0912

Table 5.5: Mean and standard deviation of PSS questionnaire scores

In Figure 5.25 is possible to see two subjects with PSS score values equal to or higher than 27. Considering all the participants, it can be concluded that, on average, they were in a similar starting stress condition, that is, medium-low stress. This is also confirmed by the mean and standard deviation values. The presence of some subjects with higher scores does not affect the general finding that the group was not in a state of acute stress.

In all four recordings, the participants evaluated the perceived stress at the end of the two phases of the protocol (baseline and mathematical test) through the visual analogue scale (VAS). The stress levels normalized according to the baseline were calculated for each of the four experimental conditions: calibration, stimulation with constant binaural beats, stimulation with adapted binaural beats, and without stimulation. The mean and standard deviation of the stress for each condition are reported in Table 5.6.

Condition	**Mean**	**Standard deviation**
Calibration	3.15	1.73
Constant	2.45	1.96
Adapted	2.65	1.69
No stimulation	2.65	2.13

Table 5.6: Mean and standard deviation of self-reported stress values in different experimental conditions

The results show that the calibration condition had the mean increase in stress from baseline to the highest task condition (M = 3.15), followed by the no stimulation and adapted binaural beat stimulation (M = 2.65), and constant binaural beat stimulation (M = 2.45) conditions. The adapted stimulation condition, although having the mean identical to that of the condition without stimulation, however has a much lower standard deviation. The standard deviations, in general, are all quite similar, indicating considerable variation in stress levels among users within each condition.

To determine whether the differences in stress levels between the four conditions were statistically significant, a repeated measures ANOVA was performed. The results of the ANOVA are reported in Table 5.7.

Source	**SS**	**df**	**MS**	**F**	**p-value**
Columns	5.3500	3	1.7833	0.5009	0.6828
Error	270.6000	76	3.5605		
Total	275.9500	79			

Table 5.7: ANOVA results. SS = Sum of Squares, df = Degrees of Freedom, MS = Mean Squares, F = F-statistic value, p-value = p-value.

The ANOVA revealed no statistically significant differences between the experimental conditions ($F(3, 76) = 0.5009$, $p = 0.6828$). This result suggests that the normalized stress levels do not differ significantly between the experimental conditions, and subsequently performing the Student's t test between the possible pairs of conditions confirmed that there is no significant difference between the conditions, as shown in Figure 5.26

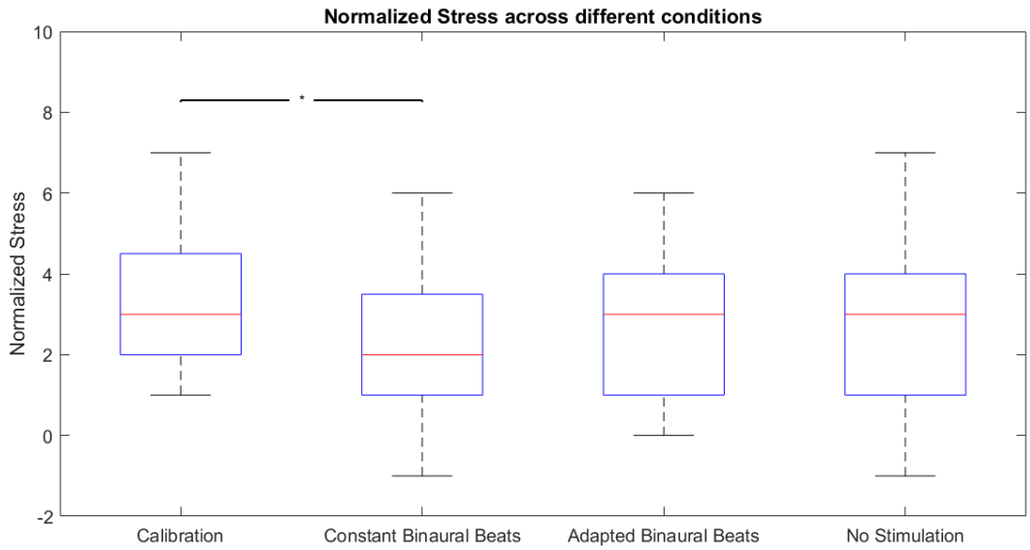

Figure 5.26: Self-reported stress distributions in the four experimental conditions

In summary, these analyses show that the study participants all started from a similar stress condition, as indicated by the mean and standard deviation of the PSS questionnaire scores. Furthermore, participants tend to maintain a certain consistency in the answers provided in the VAS. At the same time, the differences in the levels of self-reported stress through the VAS were not statistically significant between the conditions. The only statistical difference occurs between the calibration and the constant BBs but with a p-value equal to 0.04926 and therefore slightly lower than the threshold (p-value = 0.05).

Chapter 6

Conclusion and future developments

This chapter provides an overview of the results obtained in this thesis, highlighting the observations deduced and possible future developments.
The conclusions reported are related to the use of a protocol that has been shown to be effectively stress-inducing. For completeness, each participant answered a questionnaire commonly used to measure psychological stress, in order to determine their level of stress before the start of the experiment. Through the PSS it was assessed that on average the subjects started from a medium-low stress condition.

6.1 Conclusions

In this thesis 40 subjects were subjected to an experimental protocol that included an initial relaxation phase of 3 minutes, followed by 5 minutes of mathematical test, broken down into 3 minutes of difficult task and 2 minutes of easy task. All this was repeated 4 times in order to compare different stimulation conditions. The four conditions were:

1. Calibration: always performed as the first recording;
2. Stimulation with constant binaural beats;
3. Stimulation with binaural beats adapted to the subject;
4. Absence of stimulation;

For each subject, the order of the last three conditions was randomized so as to make the results independent of learning effects. Following the exclusion criteria adopted, half of the dataset was discarded. For the remaining 20 subjects, the data analysis was carried out with the aim of evaluating the efficiency or otherwise of the stimulation and in particular the comparison between the stimulation with binaural beats adapted to the subject and the stimulation with constant binaural beats was studied in depth.

First, the method used to adapt the beats to the subject in real time was evaluated. To do this, the output of the regressor of each participant was analyzed with the relative pattern of

the stimuli sent to the subject. This evaluation suggested that real-time adaptation of binaural beats can have a significant impact on stress management as it actually led to a decrease in stress during the mathematical task for some subjects, but at the same time it highlighted that each subject has a different behavior, highlighting the importance of adapting stimulation and treatment to the individual specificities of the subjects themselves. However, the dynamic interaction between stress levels and adaptive stimuli was evident, highlighting the potential use of finely tuned binaural beats to manage stress in real time. A similar result was also obtained by comparing the variation of frequency in subjects with the accuracy and reaction time values for each minute of the task. It was indeed found that there is no frequency that is optimal for each subject and therefore it is advisable to modulate the stimulus sent according to the conditions of the subject himself in order to maintain or improve his performance. The results of this thesis suggest the importance of an adapted approach, in which the stimulation frequency dynamically adapts to the specific needs of each subject in real time to modulate and potentially improve cognitive performance under controlled stress conditions.

Before focusing the study on the evaluation of the efficiency of the adapted binaural beats on the participants' performance during the mathematical test, we wanted to explore which were the features and channels of the EEG that, according to the feature selection method used, were the best to distinguish relaxation and stress. In general, all the channels were quite important, except for Fz which is the one with the least occurrence. Among the features, the standard deviation was the most selected by the Fisher Ratio, contrasting with the alpha asymmetry calculated between F3 and F4 and the Fuzzy Entropy which were never chosen for the regressor training. In line with the occurrences of features and channels seen separately, the channel-feature pair that was found to be most relevant for the assessment of stress was the left parietal channel P3 together with the standard deviation. Overall, the parietal channels were found to be the two most relevant in the analysis of stress, suggesting a bilateral distribution of the relevance of the parietal regions and underlining the critical role of parietal areas in the context of stress analysis. Next in line were the Fp2 and Fp1 channels, located in the right and left frontoparietal region. The relevance of the Fp1 and Fp2 channels highlights the involvement of the frontal regions in this study, but it is worth noting that there is variability in the specific frontal localizations implicated in stress detection. In line with the results of other studies, also in this thesis in the parietal area the left hemisphere was found to be more relevant, while comparing the channels of the frontal area, the right hemisphere prevailed over the left.
With regard to the ECG features, it emerged that the RMSSD emerges as the only feature with a weight comparable to the main EEG features, which therefore, overall, appears to be more relevant for the assessment of stress.
The importance of an accurate selection of features for specific applications and the use of robust techniques for their evaluation is evident, furthermore, including the EEG signal in a study context such as this seems to be fundamental for an accurate detection and analysis of stress. It is important to point out that, in this study, as regards the acquisition of the ECG, it was carried out using the same equipment used for the EEG, limiting the use of a single electrode. Furthermore, only four features were extracted from the signal. The results obtained are certainly dependent on these limitations, and therefore, future research with 12-

lead electrocardiographs could lead to the extraction of more information from the ECG signal, such as the temporal duration of different waveforms. This could result in different conclusions, potentially revealing a greater importance of ECG features in the study of stress.

The evaluation of the use of a stimulation on the performance of the participants, evaluated in terms of accuracy, reaction time and IES, produced comforting results for the purposes of this thesis, highlighting the actual efficiency of the binaural beats, whether they were sent to the subject in a constant or adapted way. Specifically, significant differences were found in the reaction time and in the IES, highlighting the importance of the stimulation as a whole. The stimulation accelerated the reaction times, in line with what was observed in other studies, but had no effect on the accuracy. This somewhat anomalous result compared to the reference literature suggests that the increase in response speed was not due to random responses by the participants. The increase in reaction time without compromising accuracy is still a promising result as it led to an overall improvement in performance efficiency. This is particularly interesting in contexts where operational efficiency is crucial and where it is necessary to obtain maximum performance with minimum error. This conclusion is also supported by the observation obtained by evaluating the self-reported stress responses that the subjects evaluated using the Visual Analogue Scale at the end of the two phases of the protocol. The results showed that the two types of stimulation recorded lower increases in stress levels between baseline and the mathematical task, indicating that, in addition to improving performance, they also help to reduce perceived stress during a stressful context.
Continuing with specific analyses to compare the two types of stimulation, variable results were obtained that alternately favored one or the other, especially in the in-depth analysis investigating specifically each minute of the mathematical task. Overall, the data highlighted the adapted stimulation as the best. In fact, it has been shown to have a positive effect especially on the reaction time, accelerating the participants' response. This effect could be due to the ability of the adapted stimulation to maintain a high level of attention and readiness of the subjects, reducing the time needed to process and respond to the stimuli. From the minute-by-minute analysis, in fact, it was noted that the adaptation of the frequency speeded up the responses especially at the beginning of the mathematical test and after the variation in difficulty of the task.
The results of the statistical analyses provide a clear understanding of the effect of the different stimulation conditions on the participants' performance. Overall, both the reaction time and the Efficiency Index (IES) indicate that the stimulations positively and significantly influence the performance. In particular, the adapted stimulation emerges as the most advantageous condition, optimizing the overall performance without compromising the accuracy of the responses. Participants subjected to this condition respond faster and more efficiently than when they are exposed to constant stimulation or no stimulation, thus improving the overall efficiency as shown by the IES. At the same time, they also appear to have at times a less impulsive and more reflective behavior, as seen in the study of the no-response cases, but this does not affect the overall performance since the reaction time and the IES are still generally better than the other conditions. The adapted stimulation not only maintains a high level of accuracy, as also

observed with the constant stimulation, but also favors faster and more reactive responses. These results are particularly relevant for the practical application of stimulations in contexts where it is essential to reduce reaction times without sacrificing accuracy.

6.2 Future developments

The results obtained underline the contribution given by stimulation to the subject, especially that with adapted binaural beats. Specifically, the reaction time and the Efficiency Index (IES) clearly indicate that adapted stimulation can significantly improve cognitive performance, making it a potential area of interest for further research and applications.

During this study, the use of limited instrumentation allowed us to collect significant data, but it also imposed restrictions on the collection of the electrocardiographic signal, from which we were only able to analyze the tachogram. Further investigations are needed to better understand the importance of ECG in stress detection and, consequently, its potential use for adapting stimulation and modulating perceived stress. It would be desirable to conduct more comprehensive studies, using, for example, the standard 12-lead ECG system, in order to obtain a more detailed view of cardiac activity, allowing to extract more information from the signal and thus assess its relationship with stress more thoroughly.
Another area of interest could be the integration of other features, such as those that correlate ECG and EEG signals. This combination could reveal more complex patterns of physiological and neurological activity, thus improving the understanding of the dynamics underlying stress phenomena.

To increase the validity and reliability of the results, it would be appropriate to perform analyses using a ground truth. In the context of stress, cortisol is commonly used as a biomarker and its inclusion as a reference would make the analyses more robust and interpretable. The absence of a ground truth that could have been used to assess the actual state of stress of the subjects during the protocol represents an important limitation of this study.

Another factor that could influence the results is the quality of sleep of the participants the night before data acquisition. The protocol in fact consists of a mathematical test and the evaluations carried out were mainly based on the performance of the participants, which however could be influenced by tiredness in the case in which the subject examined did not sleep enough. Taking into account the hours of sleep could therefore provide further useful information to better understand the individual variations in the signals collected and better interpret the results obtained, helping to eliminate potential bias.

In terms of data analysis, algorithms that adapt the frequency to the subject in a different way than what was done in this study could also be tested. By comparing different algorithmic approaches, it could be possible to reveal which method is more effective for adapting the stim-

ulation and therefore which method allows for better stress reduction and higher performance. It could also be useful to further explore the mechanism through which adapted stimulation affects cognitive performance, and also consider integrating other physiological and psychological measures to better understand the effect that stimulation has on performance and stress mediation. Such studies could lead to a more complete view of the benefits obtained from adapted stimulation and also further optimize it for specific applications.

In our study, the artificial stressor was recognized by all participants, thus nullifying its use. Therefore, in future studies, it could be considered to reduce the number of questions in which the incorrect feedback is presented or to think about a protocol in which a different artificial stressor is introduced. This would allow us to more effectively evaluate how negative feedback affects the cognitive performance of subjects in different stimulation conditions.

Finally, a clear limitation of this study is the limited number of participants. Future research should therefore try to involve a larger sample of subjects in order to be able to generalize the results more and obtain more robust verification of the hypotheses.

This area of research can have practical implications in several fields, including the optimization of work and school performance by working on improving reactivity and efficiency without compromising the accuracy of performance and even the treatment of clinical conditions such as chronic stress and attention deficit/hyperactivity disorder (ADHD) which, with an approach finely studied for the needs of the subject, can help reduce the state of stress and therefore improve the overall condition of the subject also helping him to increase concentration on specific tasks thanks to lower levels of perceived stress. In conclusion, while acknowledging the limitations of our research, future development prospects offer numerous possibilities to deepen and improve the understanding of the relationships between ECG, EEG and stress signals and their use to adapt stimulation to the subject. These developments could significantly contribute to the creation of treatments increasingly targeted to the needs of the patient.

Appendix A

Real-Time Regression Results

This appendix presents the results of the real-time regression analysis and the related variation of the stimuli sent for all the users who participated in the study.

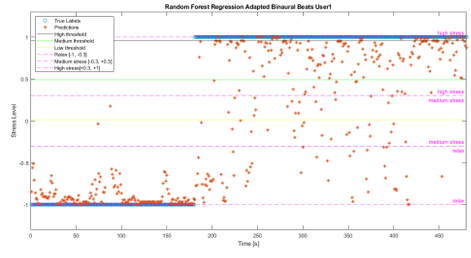

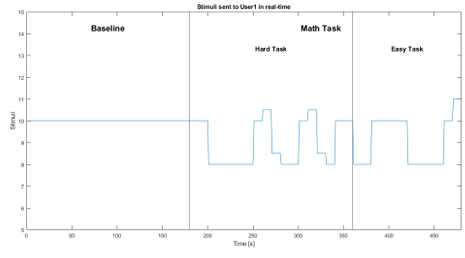

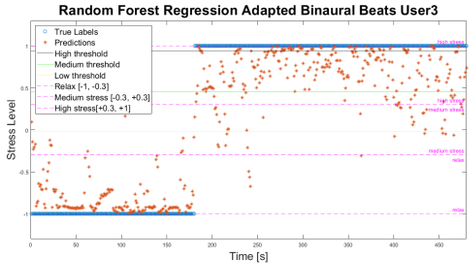

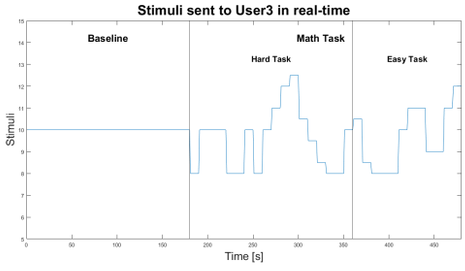

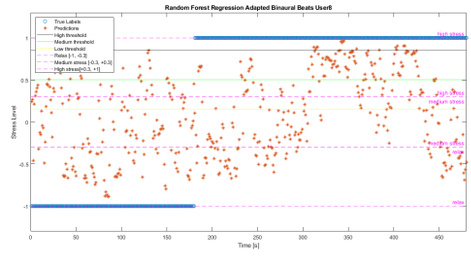

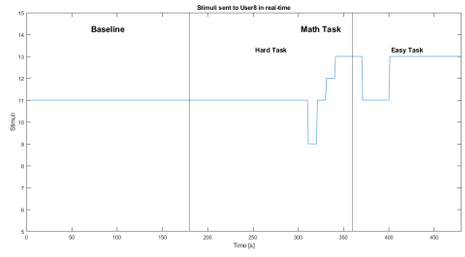

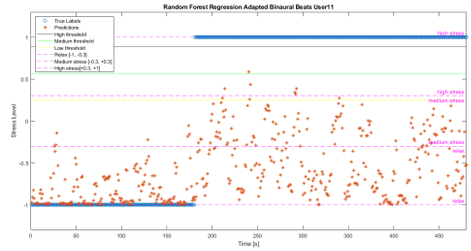
Random Forest Regression Adapted Binaural Beats User11
True Labels
Predictions
High threshold
Medium threshold
Low threshold
Relax [-1, -0.3]
Medium stress [-0.3, +0.3]
High stress[+0.3, +1]
high stress
high stress
medium stress
medium stress
relax
relax
Stress Level
Time [s]

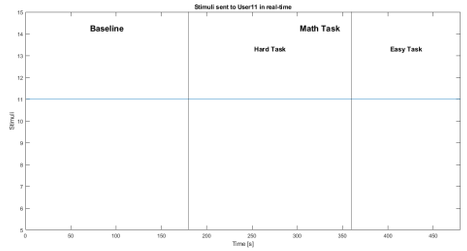
Stimuli sent to User11 in real-time
Baseline
Math Task
Hard Task
Easy Task
Stimuli
Time [s]

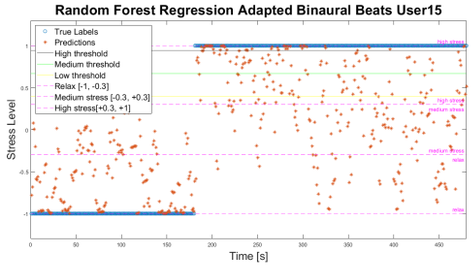
Random Forest Regression Adapted Binaural Beats User15
True Labels
Predictions
High threshold
Medium threshold
Low threshold
Relax [-1, -0.3]
Medium stress [-0.3, +0.3]
High stress[+0.3, +1]
high stress
high stress
medium stress
medium stress
relax
relax
Stress Level
Time [s]

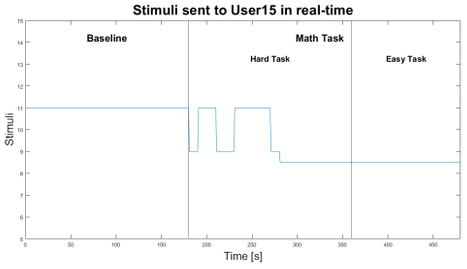
Stimuli sent to User15 in real-time
Baseline
Math Task
Hard Task
Easy Task
Stimuli
Time [s]

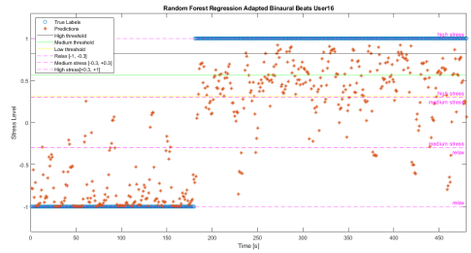
Random Forest Regression Adapted Binaural Beats User16
True Labels
Predictions
High threshold
Medium threshold
Low threshold
Relax [-1, -0.3]
Medium stress [-0.3, +0.3]
High stress[+0.3, +1]
high stress
high stress
medium stress
medium stress
relax
relax
Stress Level
Time [s]

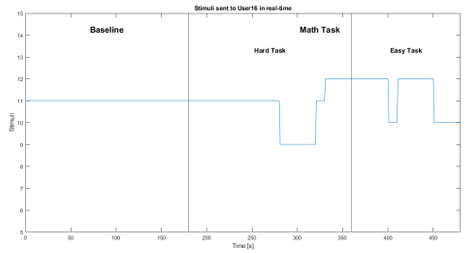
Stimuli sent to User16 in real-time
Baseline
Math Task
Hard Task
Easy Task
Stimuli
Time [s]

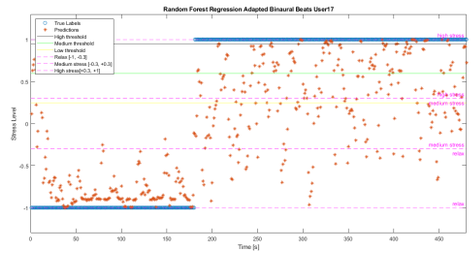
Random Forest Regression Adapted Binaural Beats User17
True Labels
Predictions
High threshold
Medium threshold
Low threshold
Relax [-1, -0.3]
Medium stress [-0.3, +0.3]
High stress[+0.3, +1]
high stress
high stress
medium stress
medium stress
relax
relax
Stress Level
Time [s]

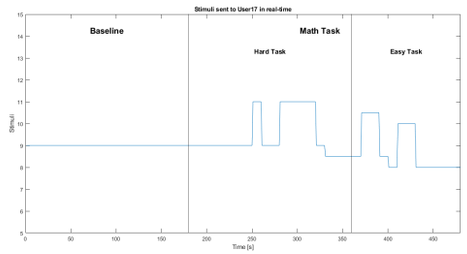
Stimuli sent to User17 in real-time
Baseline
Math Task
Hard Task
Easy Task
Stimuli
Time [s]

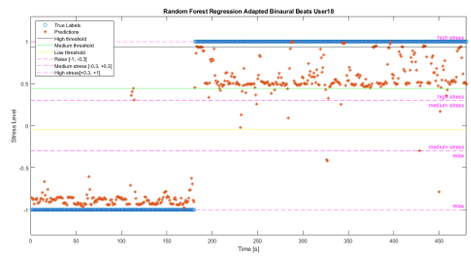
Random Forest Regression Adapted Binaural Beats User18
True Labels
Predictions
High threshold
Medium threshold
Low threshold
Relax [-1, -0.3]
Medium stress [-0.3, +0.3]
High stress[+0.3, +1]
high stress
high stress
medium stress
medium stress
relax
relax
Stress Level
Time [s]

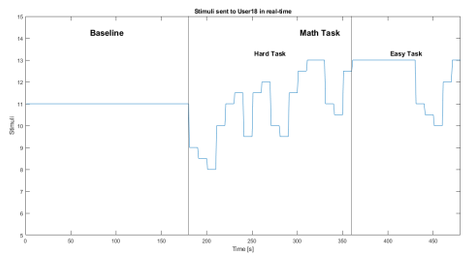
Stimuli sent to User18 in real-time
Baseline
Math Task
Hard Task
Easy Task
Stimuli
Time [s]

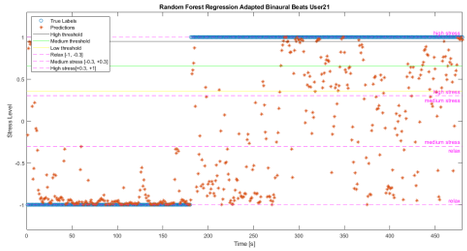
Random Forest Regression Adapted Binaural Beats User21
True Labels
Predictions
High threshold
Medium threshold
Low threshold
Relax [-1, -0.3]
Medium stress [-0.3, +0.3]
High stress[0.3, +1]
high stress
medium stress
relax
Stress Level
Time [s]

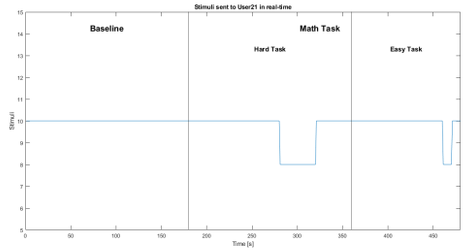
Stimuli sent to User21 in real-time
Baseline
Math Task
Hard Task
Easy Task
Stimuli
Time [s]

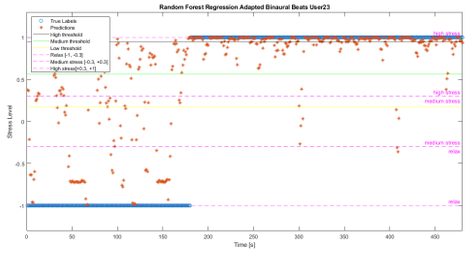
Random Forest Regression Adapted Binaural Beats User23
True Labels
Predictions
High threshold
Medium threshold
Low threshold
Relax [-1, -0.3]
Medium stress [-0.3, +0.3]
High stress[0.3, +1]
high stress
medium stress
relax
Stress Level
Time [s]

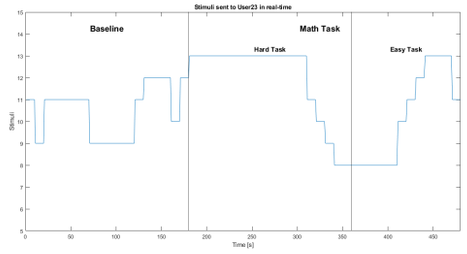
Stimuli sent to User23 in real-time
Baseline
Math Task
Hard Task
Easy Task
Stimuli
Time [s]

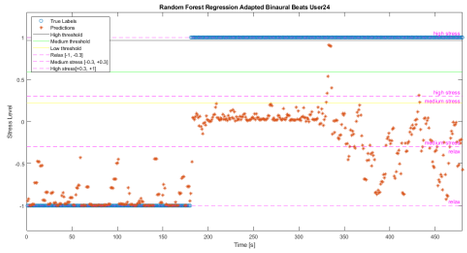
Random Forest Regression Adapted Binaural Beats User24
True Labels
Predictions
High threshold
Medium threshold
Low threshold
Relax [-1, -0.3]
Medium stress [-0.3, +0.3]
High stress[0.3, +1]
high stress
medium stress
relax
Stress Level
Time [s]

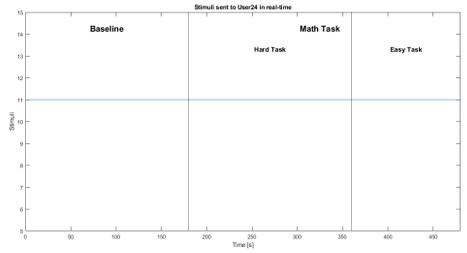
Stimuli sent to User24 in real-time
Baseline
Math Task
Hard Task
Easy Task
Stimuli
Time [s]

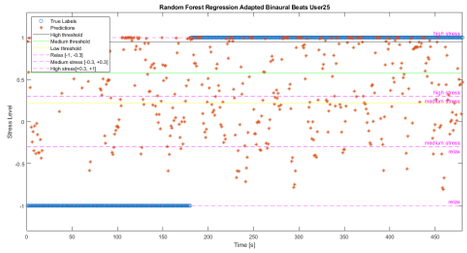
Random Forest Regression Adapted Binaural Beats User25
True Labels
Predictions
High threshold
Medium threshold
Low threshold
Relax [-1, -0.3]
Medium stress [-0.3, +0.3]
High stress[0.3, +1]
high stress
medium stress
relax
Stress Level
Time [s]

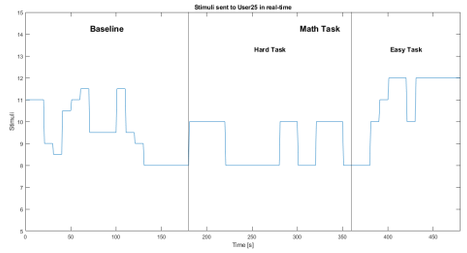
Stimuli sent to User25 in real-time
Baseline
Math Task
Hard Task
Easy Task
Stimuli
Time [s]

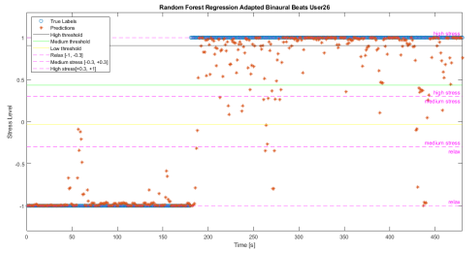
Random Forest Regression Adapted Binaural Beats User26
True Labels
Predictions
High threshold
Medium threshold
Low threshold
Relax [-1, -0.3]
Medium stress [-0.3, +0.3]
High stress[0.3, +1]
high stress
medium stress
relax
Stress Level
Time [s]

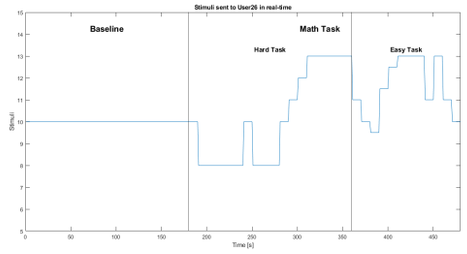
Stimuli sent to User26 in real-time
Baseline
Math Task
Hard Task
Easy Task
Stimuli
Time [s]

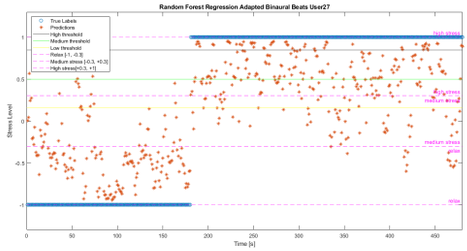
Random Forest Regression Adapted Binaural Beats User27
True Labels
Predictions
High threshold
Medium threshold
Low threshold
Relax [-1, -0.3]
Medium stress [-0.3, +0.3]
High stress[0.3, +1]
high stress
medium stress
relax
Stress Level
Time [s]

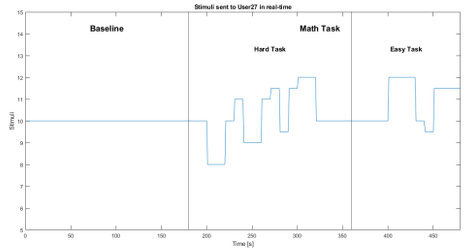
Stimuli sent to User27 in real-time
Baseline
Math Task
Hard Task
Easy Task
Stimuli
Time [s]

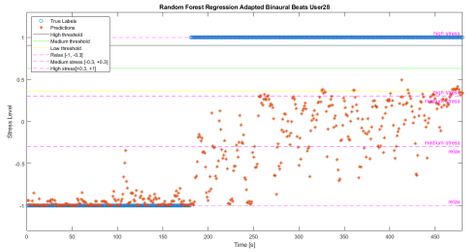
Random Forest Regression Adapted Binaural Beats User28
True Labels
Predictions
High threshold
Medium threshold
Low threshold
Relax [-1, -0.3]
Medium stress [-0.3, +0.3]
High stress[0.3, +1]
high stress
medium stress
relax
Stress Level
Time [s]

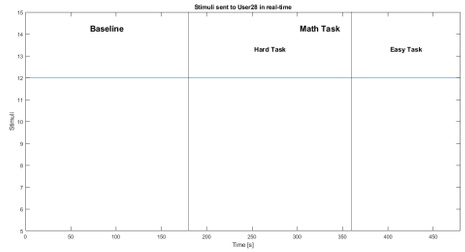
Stimuli sent to User28 in real-time
Baseline
Math Task
Hard Task
Easy Task
Stimuli
Time [s]

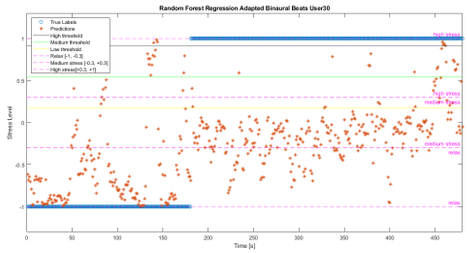
Random Forest Regression Adapted Binaural Beats User30
True Labels
Predictions
High threshold
Medium threshold
Low threshold
Relax [-1, -0.3]
Medium stress [-0.3, +0.3]
High stress[0.3, +1]
high stress
medium stress
relax
Stress Level
Time [s]

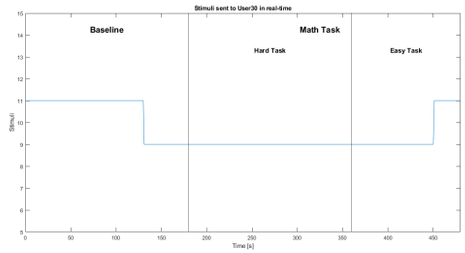
Stimuli sent to User30 in real-time
Baseline
Math Task
Hard Task
Easy Task
Stimuli
Time [s]

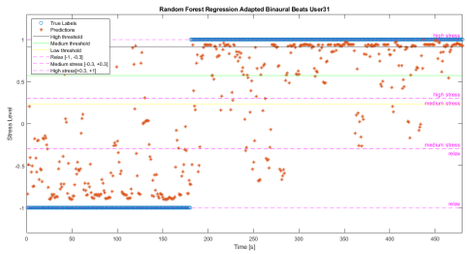
Random Forest Regression Adapted Binaural Beats User31
True Labels
Predictions
High threshold
Medium threshold
Low threshold
Relax [-1, -0.3]
Medium stress [-0.3, +0.3]
High stress[0.3, +1]
high stress
medium stress
relax
Stress Level
Time [s]

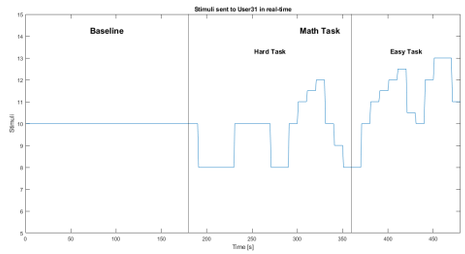
Stimuli sent to User31 in real-time
Baseline
Math Task
Hard Task
Easy Task
Stimuli
Time [s]

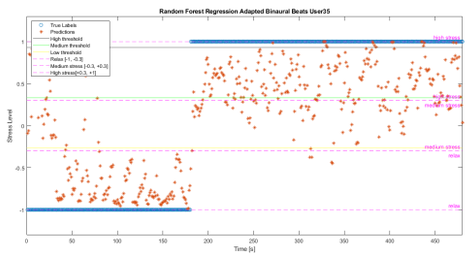
Random Forest Regression Adapted Binaural Beats User35
True Labels
Predictions
High threshold
Medium threshold
Low threshold
Relax [-1, -0.3]
Medium stress [-0.3, +0.3]
High stress[0.3, +1]
high stress
medium stress
relax
Stress Level
Time [s]

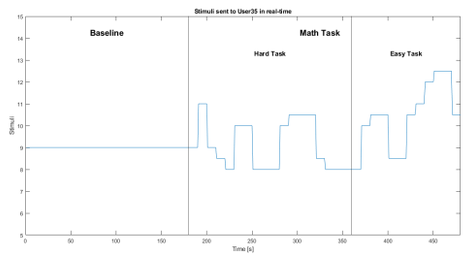
Stimuli sent to User35 in real-time
Baseline
Math Task
Hard Task
Easy Task
Stimuli
Time [s]

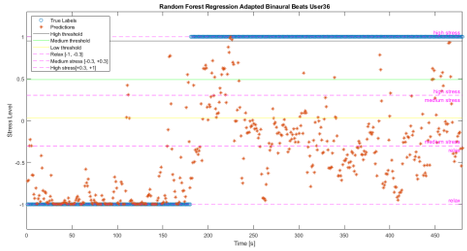

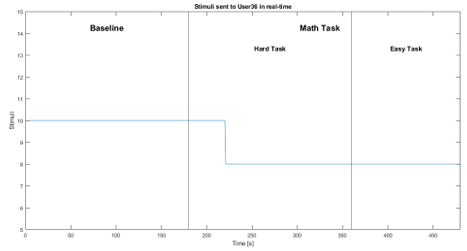

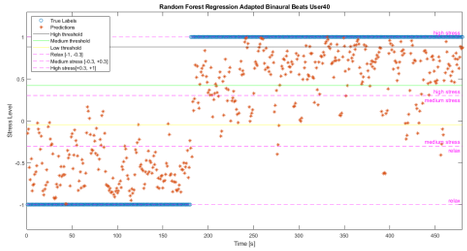

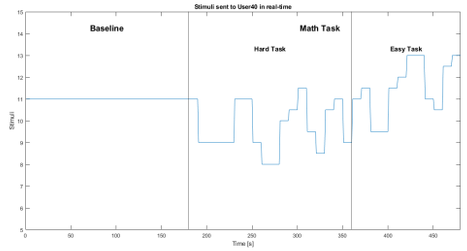

Figure A.1: Random Forest Regression Adapted Binaural Beats

Figure A.2: Stimuli Sent to Users in Real-Time

Appendix B

Perceived Stress Scale questions

1. Over the past month, how often have you felt out of sorts because something unexpected happened?	**0 1 2 3 4**
2. Over the past month, how often have you felt like you were out of control over important things in your life?	**0 1 2 3 4**
3. Over the past month, how often have you felt nervous or "stressed"?	**0 1 2 3 4**
4. Over the past month, how often have you felt confident in your ability to handle your personal problems?	**0 1 2 3 4**
5. Over the past month, how often have you felt that things were going your way?	**0 1 2 3 4**
6. Over the past month, how often have you felt like you couldn't keep up with all the things you needed to do?	**0 1 2 3 4**

7. Over the past month, how often have you felt like you could control the things that irritate you in your life?	**0 1 2 3 4**
8. Over the past month, how often have you felt like you were in control of the situation?	**0 1 2 3 4**
9. Over the past month, how often have you felt angry about things that were out of your control?	**0 1 2 3 4**
10. Over the past month, how often have you felt like difficulties were piling up to the point where you couldn't get past them?	**0 1 2 3 4**

Appendix C

Questionnaires

Participant n°: _____ Age: _____ Gender: _____ Date: _____

Preliminary Questionnaire

Before Participation In the last 24 hours, have you...

1. ... exercised?
   ❒ No ❒ Yes, at what time: _____
2. ... drank alcohol?
   ❒ No ❒ Yes, what time: _____
3. ... drank caffeinated beverages (e.g. coffee, energy drinks)?
   ❒ No ❒ Yes, what time: _____
4. ... used tobacco (e.g. cigarettes, pipes, chewing tobacco)?
   ❒ No ❒ Yes, what time: _____ Which type: _____
5. ... used recreational drugs (e.g. marijuana, cocaine)?
   ❒ No ❒ Yes, what time: _____ Which type: _____
6. ... eaten?
   ❒ No ❒ Yes, what time: _____
7. ... brushed or flossed your teeth?
   ❒ No ❒ Yes, what time: _____
8. What is your weight and height? _____ cm _____ kg
   Note: We will use this data to determine your Body Mass Index (BMI)

9. Do you have any of the following medical conditions?
   ❒ Arthritis ❒ Asthma ❒ Cardiovascular Disease ❒ Cancer Previous ❒ Type 2 Diabetes ❒ High Cholesterol ❒ High Blood Pressure
   ❒ Obesity ❒ Other: _____

10. Are you a night worker?
    ❒ No ❒ Yes, since when (year): _____

11. How often do you drink coffee per week?
    ❒ Less than once per week
    ❒ 1–2 times per week
    ❒ 3–4 times per week
    ❒ 5–6 times per week
    ❒ Daily

12. How much coffee do you drink per day?
    ❒ I don't drink coffee regularly
    ❒ 1–2 cups
    ❒ 3–4 cups
    ❒ 5–6 cups
    ❒ More than 7 cups

13. Do you currently smoke or have you ever smoked tobacco products such as cigarettes, cigars, or pipes?
    ❒ No, I have never smoked cigarettes
    ❒ Yes, I smoke cigarettes I smoke _____ cigarette(s) per day
    ❒ I smoke _____ pack(s) per week I have smoked for _____ year(s)
    ❒ Yes, I have smoked cigarettes I have smoked _____ cigarette(s) per day
    ❒ I have smoked _____ pack(s) per week I have smoked for _____ year(s)
    ❒ I have quit for _____ year(s)

14. How often do you drink alcohol per week?
    ❒ Less than once a week
    ❒ 1–2 times a week
    ❒ 3–4 times a week
    ❒ 5–6 times a week
    ❒ Daily

15. When you drink alcohol, how much do you usually drink?
    ❒ I don't drink alcohol regularly
    ❒ 1–2 drinks
    ❒ 3–4 drinks
    ❒ 5–6 drinks
    ❒ More than 7 drinks

16. Have you ever been diagnosed with an alcohol use disorder?
    ❒ No ❒ Yes

17. Do you use recreational drugs (e.g., marijuana, cocaine)?
    ❒ No ❒ Yes
    Which type: _____

18. Have you ever been diagnosed with a substance use disorder?
    ❒ No ❒ Yes

19. In the past year, have you received a mental health diagnosis (e.g., depression, anxiety) or been treated for a mental health disorder?
    ❒ No ❒ Yes

20. Please provide the name and dosage of any medications you have taken in the past 24 hours:
    _____
    _____
    _____
    _____
    _____
    _____
    _____

Thank you for answering these questions.

Female participants only

Please answer the following questions:

1. Do you have a regular menstrual cycle?
    ❒ No ❒ Yes
    If you have a regular menstrual cycle, the last day of your period was _____ days ago.

2. Do you use hormonal contraception?
    ❒ No ❒ Oral contraceptive pill ❒ Contraceptive patch
    ❒ Vaginal ring ❒ Intrauterine contraception (IUC) ❒ Injectable contraception
    If you marked an answer, indicate since when (year): _____

3. Are you pregnant or have you ever been pregnant?
   - ❒ No
   - ❒ Yes, I am pregnant: How many weeks pregnant? _____
   - ❒ Yes, I have been pregnant: When was your last birth, abortion or miscarriage (year)? _____

4. Are you in menopause?
   - ❒ No ❒ Yes, since when (month/year)? _____

5. Are you in menopause?
   - ❒ No
   - ❒ Yes, I am in the menopause transition period
   - ❒ Yes, I have been through menopause Since when (year)? _____

6. If you are in menopause, are you taking hormone replacement therapy?
   - ❒ No ❒ Yes, since when (year)? _____

Bibliography

[1] Saladin, Kenneth S. 2011. *Human Anatomy.* 6th ed. Piccin.

[2] G.L.Cerone, M. Gazzoni, M. Knaflitz, 2023 *Strumentazione Biomedica*

[3] Oriano Mecarelli, 2009 *Manuale teorico pratico di elettroencefalografia*, Wolters Kluwer Health

[4] National Library of Medicine,2022, *Physiology, Cardiovascular* https://www.ncbi.nlm.nih.gov/books/NBK493197/#:~:text=The%20cardiovascular%20system%20provides%20blood,arteries%2C%20veins%2C%20and%20capillaries.

[5] IRCCS, Humanitas, research hospital https://www.humanitas.it/enciclopedia/anatomia/apparato-cardiocircolatorio/cuore/

[6] Università di Torino *LE ONDE DELL'ELETTROCARDIOGRAMMA* https://medtriennalisl.campusnet.unito.it/html/Studiare/Tirocinio/materiali_tirocinio/07.ECGMIO_-_ONDE_DELLECG.pdf

[7] International Cardiovascular Forum Journal 6, S. Sammito, I. Böckelmann, 2016 *Factors Influencing Heart Rate Variability* https://pdfs.semanticscholar.org/0f22/02a8c36713dd6161c4cb58ea9ffe924bcead.pdf

[8] Hye-Geum Kim, Eun-Jin Cheon, Dai-Seg Bai, Young Hwan Lee, and Bon Hoon Koo.2018 *Stress and Heart Rate Variability: A Meta-Analysis and Review of the Literature* https://pubmed.ncbi.nlm.nih.gov/29486547/

[9] 2012 International Conference and Exposition on Electrical and Power Engineering, R. Costin; C. Rotariu; A. Pasarica, 2012 *Mental stress detection using heart rate variability and morphologic variability of EeG signals* https://ieeexplore.ieee.org/abstract/document/6463870

[10] Edizioni il punto di incontro, Guy Lacroix, 26 Sep 2022 *Il cuore ti parla. Parla al tuo cuore*

[11] A. Fedotchev, S. Parin, S. Polevaya, A. Zemlianaia, 20 Maggio, 2021, *Human Body Rhythms in the Development of Non-Invasive Methods of Closed-Loop Adaptive Neurostimulation*, https://www.mdpi.com/2075-4426/11/5/437

[12] National Library of Medicine, 2019, *Closed-Loop Neuromodulation in Physiological and Translational Research*, https://www.ncbi.nlm.nih.gov/pmc/articles/PMC6824403/

[13] A.I. Fedotchev e A.T. Bondar, Human Physiology, 2022 *Adaptive Neurostimulation, Modulated by Subject's Own Rhythmic Processes, in the Correction of Functional Disorders*

[14] Pubmed.Ruth Maria Ingendoh, Ella S. Posny, Angela Heine. *Binaural beats to entrain the brain? A systematic review of the effects of binaural beat stimulation on brain oscillatory activity, and the implications for psychological research and intervention* https://www.ncbi.nlm.nih.gov/pmc/articles/PMC10198548/

[15] Licklider JCR, Webster JC, Hedlun JM. On the frequency limits of binaural beats. *The journal of the acoustical society of america*

[16] Goodin P, Ciorciari J, Baker K, Carey A-M, Carrey A-M, Harper M, et al. *A high-density EEG investigation into steady state binaural beat stimulation.*

[17] Perrott DR, Nelson MA. *Limits for the detection of binaural beats. The journal of the acoustical society of America.*

[18] Kuwada S, Yin TC, Wickesberg RE. *Response of cat inferior colliculus neurons to binaural beat stimuli: possible mechanisms for sound localization.*

[19] Youtube https://www.youtube.com/watch?v=nnJGKHZ5yUw

[20] Badr Y, Al-Shargie F, Tariq U, Babiloni F, Al-Mughairbi F, Al-Nashash H. *Mental Stress Detection and Mitigation using Machine Learning and Binaural Beat Stimulation.* Annu Int Conf IEEE Eng Med Biol Soc. 2023 Jul; https://pubmed.ncbi.nlm.nih.gov/38083737/

[21] Fares Al-Shargie, Yara Badr, Usman Tariq, Fabio Babiloni, Fadwa Al-Mughairbi, Hasan Al-Nashash *Classification of Mental Stress Levels using EEG Connectivity and Convolutional Neural Networks* https://pubmed.ncbi.nlm.nih.gov/38083224/

[22] Rateb Katmah, Fares Al-Shargie, Usman Tariq, Fabio Babiloni, Fadwa Al-Mughairbi, Hasan Al-Nashash *Mental Stress Management Using fNIRS Directed Connectivity and Audio Stimulation* https://pubmed.ncbi.nlm.nih.gov/37022071/

[23] MeLisa A Gantt 1, Stephanie Dadds 2, Debra S Burns 3, Dale Glaser 4, Angelo D Moore 5. *The Effect of Binaural Beat Technology on the Cardiovascular Stress Response in Military Service Members With Postdeployment Stress.* https://pubmed.ncbi.nlm.nih.gov/28544507/

[24] Katherine Kelton, Terri L Weaver, Lisa Willoughby, David Kaufman, Anna Santowski. *The Efficacy of Binaural Beats as a Stress-buffering Technique.* https://pubmed.ncbi.nlm.nih.gov/32619206/

[25] Elizabeth Krasnoffcorresponding author 1 , and Gaétan Chevalier 2 *Case report: binaural beats music assessment experiment.* https://www.ncbi.nlm.nih.gov/pmc/articles/PMC10196448/

[26] International Journal of Science and Research (IJSR). Batta Mahesh, 2018, *Machine Learning Algorithms - A Review* https://www.researchgate.net/profile/Batta-Mahesh/publication/344717762_Machine_Learning_Algorithms_-A_Review/links/5f8b2365299bf1b53e2d243a/Machine-Learning-Algorithms-A-Review.pdf?eid=5082902844932096

[27] Corinna Cortes and Vladimir Vapnik. (Sept. 1995) *Support-Vector Networks* https://link.springer.com/article/10.1007/BF00994018

[28] Neuroelectrics. *Enobio 8 - Neuroelectrics.* https://www.neuroelectrics.com/solutions/enobio/8.

[29] Neuroelectrics. *Neuroelectrics Wiki - NIC 2.0.* https://www.neuroelectrics.com/wiki/index.php/NIC2.0.

[30] Neuroelectrics. *Neuroelectrics Wiki - MatNIC Matlab Toolkit..* https://www.neuroelectrics.com/wiki/index.php/MatNIC_Matlab_Toolkit.

[31] Transmission Control Protocol https://it.wikipedia.org/wiki/Transmission_Control_Protocol.

[32] LabStreamingLayer. *LabStreamingLayer Documentation.* https://labstreaminglayer.readthedocs.io/info/intro.html.

[33] MDPI - Bioengineering *Closed-Loop Transcranial Electrical Neurostimulation for Sustained Attention Enhancement: A Pilot Study towards Personalized Intervention Strategies* https://www.mdpi.com/2306-5354/11/5/467

[34] Google Machine Learning Education *Valutazione out-of-bag* https://developers.google.com/machine-learning/decision-forests/out-of-bag?hl=it

[35] MathWorks *oobPermutedPredictorImportance* https://it.mathworks.com/help/stats/classreg.learning.classif.classificationbaggedensemble.oobpermutedpredictorimportance.html

[36] P. Bobade and M. Vani, *Stress Detection with Machine Learning and Deep Learning using Multimodal Physiological Data*, 2020 Second International Conference on Inventive Research in Computing Applications (ICIRCA), Coimbatore, India, 2020, pp. 51-57, https://ieeexplore.ieee.org/document/9183244

[37] Ravinder Ahuja e Alisha Banga, *Rilevamento dello stress mentale negli studenti universitari mediante algoritmi di apprendimento automatico*,2019, https://www.sciencedirect.com/science/article/pii/S1877050919306581?via%3Dihub

[38] Md Junayed Hasan e Jong-Myon Kim, *Un algoritmo ibrido di rilevamento dello stato di stress emotivo basato su un pool di funzionalità mediante segnali EEG*, Brain sciences, 2019, https://www.mdpi.com/2076-3425/9/12/376.

[39] Corso di Laurea in Scienze e Tecniche Psicologiche, *Elementi di Fisiologia Umana, stress*, 2017/2018, https://www.disputer.unich.it/sites/st13/files/stress.pdf.

[40] P. Subathra and S. Malarvizhi, *A Comparative Analysis of Regression Algorithms for Prediction of Emotional States using Peripheral Physiological Signals*, 2023, International Conference on Recent Advances in Electrical, Electronics, Ubiquitous Communication, and Computational Intelligence (RAEEUCCI), https://ieeexplore.ieee.org/document/10134253.

[41] F. Gioia et al., *Potential physiological stress biomarkers in human sweat*, 2022 IEEE International Symposium on Medical Measurements and Applications (MeMeA), Messina, Italy, 2022, https://ieeexplore.ieee.org/document/9856534.

[42] Y. Antonacci, L. Astolfi, A. Busacca, R. Pernice, G. Nollo and L. Faes, *Model-Based Transfer Entropy Analysis of Brain-Body Interactions with Penalized regression techniques*, 2020 11th Conference of the European Study Group on Cardiovascular Oscillations (ESGCO), Pisa, Italy, https://ieeexplore.ieee.org/document/9158165.

[43] M. Pontil, R. Tifkin e T. Evgeniou, *From Regression to Classification in Support Vector Machines*, Technical Repast AI Memo n. 1649, Artificial Intelligence Laboratory, MIT, Cambridge, 1998, https://dspace.mit.edu/handle/1721.1/7258.

[44] A Parmar, R Katariya, and V Patel. *Lecture Notes on Data Engineering and Communications Technologies*, Vol. 26. Springer Science and Business Media Deutschland GmbH, 2019, pp. 758–763 (cit. on pp. 16, 17).

[45] N. Adnan, Z. Islam, *Improving the Random Forest Algorithm by Randomly Varying the Size of the Bootstrap Samples for Low Dimensional Data Sets*, January 2015, Conference: ESANNAt: Bruges, Belgium, https://www.researchgate.net/publication/308802773_Improving_the_Random_Forest_Algorithm_by_Randomly_Varying_the_Size_of_the_Bootstrap_Samples_for_Low_Dimensional_Data_Sets.

[46] Giovanna U.Frisch, Jan A. Hausser, Andreas Mojzisch *The Trier Social Stress Test as a paradigm to study how people respond to threat in social interactions*, February 2015, https://www.frontiersin.org/journals/psychology/articles/10.3389/fpsyg.2015.00014/full.

[47] Andrew P. Allen, Paul J. Kennedy, Samantha Dockray, c John F. Cryan, Timothy G. Dinan and Gerard Clarkea,*The Trier Social Stress Test: Principles and practice*, February 2017, https://www.ncbi.nlm.nih.gov/pmc/articles/PMC5314443/.

[48] Wang, Z., e Shah, P.*The effect of pressure on high- and low-working-memory students: an elaboration of the choking under pressure hypothesis*, 2014, https://scholar.google.com/scholar_lookup?author=Z.+Wang&author=P.+Shah+&publication_year=2014&title=The+effect+of+pressure+on+high-+and+low-working-memory+students%3A+an+elaboration+of+the+choking+under+pressure+hypothesis&journal=Brit.+J.+Educ.+Psychol.&volume=84&pages=226-238.

[49] State of New Hampshire Employee Assistance Program*Perceived Stress Scale*, https://www.das.nh.gov/wellness/docs/percieved%20stress%20scale.pdf.

[50] MathWorks*lasso*, https://it.mathworks.com/help/stats/lasso.html.

[51] Elizabeth Krasnoff and Gaétan Chevalier *Case report: binaural beats music assessment experiment*, https://www.ncbi.nlm.nih.gov/pmc/articles/PMC10196448/.

[52] Apit Hemakom, et al. *ECG and EEG based detection and multilevel classification of stress using machine learning for specified genders: A preliminary study.* Thippa Reddy Gadekallu, Editor September 2023; https://pubmed.ncbi.nlm.nih.gov/22356966/

[53] Fares Al-Shargie, Yara Badr, Usman Tariq, Fabio Babiloni, Fadwa Al-Mughairbi, Hasan Al-Nashash *Classification of Mental Stress Levels using EEG Connectivity and Convolutional Neural Networks*, https://pubmed.ncbi.nlm.nih.gov/38083224/.

[54] : Eyad Talal Attar, Advisor: Mehmet Kaya, Ph. D. *Stress Analysis Based on ECG and EEG*, https://repository.fit.edu/cgi/viewcontent.cgi?article=1610&context=etd.

[55] L. Gonzalez-Carabarin, E.A. Castellanos-Alvarado, P. Castro-Garcia , M.A. Garcia-Ramirez *Machine Learning for personalised stress detection: Inter-individual variability of EEG-ECG markers for acute-stress response*, https://www.sciencedirect.com/science/article/pii/S0169260721003886.

[56] G. Giannakakis, M. Pediaditis, D. Manousos, E. Kazantzaki, et al. *Stress and anxiety detection using facial cues from videos*

[57] Eduardo Perez-Valero,1,2 Miguel A. Vaquero-Blasco,2,3 Miguel A. Lopez-Gordo,2,3,* and Christian Morillas *Quantitative Assessment of Stress Through EEG During a Virtual Reality Stress-Relax Session*, https://www.ncbi.nlm.nih.gov/pmc/articles/PMC8317646/.

[58] F. Pedregosa et al.*Scikit-learn: Machine Learning in Python. In: Journal of Machine Learning Research 12 (2011).*

[59] Qi M, Gao H, Guan L, Liu G, Yang J. *Subjective Stress, Salivary Cortisol, and Electrophysiological Responses to Psychological Stress.* Front Psychol. 2016 Feb 18, https://www.ncbi.nlm.nih.gov/pmc/articles/PMC4757705/

[60] V. Mueller et al. *The Stroop Competition: A Social-Evaluative Stroop Test for Acute Stress Induction*. 2022 IEEE-EMBS International Conference on Biomedical and Health Informatics (BHI), Ioannina, Greece, 2022, pp. 1-4, doi: 10.1109/BHI56158.2022.9926835. https://www.ncbi.nlm.nih.gov/pmc/articles/PMC5314443/.

[61] FARES AL-SHARGIE, MASASHI KIGUCHI, NASREEN BADRUDDIN, SARAT C. DASS, AHMAD FADZIL MOHAMMAD HANI, AND TONG BOON TANG *Mental stress assessment using simultaneous measurement of EEG and fNIRS* . October 2016

[62] MARKO JELICIC ELKE GERAERTS HARALD MERCKELBACH RAMONA GUERRIERI *ACUTE STRESS ENHANCES MEMORY FOR EMOTIONAL WORDS, BUT IMPAIRS MEMORY FOR NEUTRAL WORDS* . Jannuary 2004

[63] Katarina Dedovic, Robert Renwick, Najmeh Khalili Mahani, Veronika Engert, Sonia J. Lupien, and Jens C. Pruessner *The Montreal Imaging Stress Task: using functional imaging to investigate the effects of perceiving and processing psychosocial stress in the human brain* . September 2005

[64] Dr. Mary Ellen Wewers, Nancy K. Lowe *A critical review of visual analogue scales in the measurement of clinical phenomena* . August 1990

[65] Omneya Attallah *An Effective Mental Stress State Detection and Evaluation System Using Minimum Number of Frontal Brain Electrodes* .Diagnostics (Basel). 2020 May 9;10(5):292. doi: 10.3390/diagnostics10050292. PMID: 32397517; PMCID: PMC7278014.

[66] Yoorim Choi, Minjung Kim, Chungyoon Chun *Measurement of occupants' stress based on electroencephalograms (EEG) in twelve combined environments* .

[67] Michal Teplan, Anna Krakovská *EEG features of psycho-physiological relaxation* . https://ieeexplore.ieee.org/stamp/stamp.jsp?tp=&arnumber=5373654

[68] MathWorks Italia. *Find outliers in data - MATLAB isoutlier.* . https://it.mathworks.com/help/matlab/ref/isoutlier.html.

[69] S. S. Shapiro and M. B. Wilk *An Analysis of Variance Test for Normality (Complete Samples)* . In: Biometrika 52.3/4 (1965), http://www.jstor.org/stable/2333709

[70] BITTNER & ASSOCIATES *Analysis-of-Variance (ANOVA) Assumptions Review:Normality, Variance Equality, and Independence* . September 15-16, 2022, https://www.researchgate.net/publication/365406539_Analysis-of-variance_ANOVA_Assumptions_Review_Normality_Variance_Equality_and_Independence

[71] Tae Kyun Kim *T test as a parametric statistic* . September 15-16, 2022, https://www.ncbi.nlm.nih.gov/pmc/articles/PMC4667138/

[72] M R Sheldon, M J Fillyaw, W D Thompson *The use and interpretation of the Friedman test in the analysis of ordinal-scale data in repeated measures designs* . Physiother Res Int. 1996; https://pubmed.ncbi.nlm.nih.gov/9238739/

[73] Frank Wilcoxon *Individual Comparisons by Ranking Methods* . In: Biometrics Bulletin 1.6 (1945)

[74] N.F. Narvaez Linares, V. Charron, A.J. Ouimet, P.R. Labelle, H. Plamondon. *A systematic review of the Trier Social Stress Test methodology: Issues in promoting study comparison and replicable research* . June 2020

[75] Raymond BRUYER and Marc BRYSBAERT *COMBINING SPEED AND ACCURACY IN COGNITIVE PSYCHOLOGY: IS THE INVERSE EFFICIENCY SCORE* . 2011

[76] *Theory Behind BrainWave Generator* . 2020 https://www.bwgen.com/theory.html

[77] N. Ali, J. P. Nitschke, C. Cooperman, M. W. Baldwin and J. C. Pruessner, *Systematic manipulations of the biological stress systems result in sex-specific compensatory stress responses and negative mood outcomes*, Neuropsychopharmacology, vol. 45, no. 10, pp. 1672-1680, 2020, https://www.nature.com/articles/s41386-020-0726-8

[78] A. F. Arnsten, *Stress weakens prefrontal networks: molecular insults to higher cognition*, Nature neuroscience, vol. 18, no. 10, pp. 1376, 2015, https://www.nature.com/articles/nn.4087

[79] H. Norhazman et al., *Behaviour of EEG Alpha Asymmetry when stress is induced and binaural beat is applied*, 2012 International Symposium on Computer Applications and Industrial Electronics (ISCAIE), Kota Kinabalu, Malaysia, 2012, pp. 297-301, https://ieeexplore.ieee.org/abstract/document/6482116

[80] L. Shekar, C.A. Suryavanshi, K.R., Nayak, *Effect of alpha and gamma binaural beats on reaction time and short-term memory*, 2018, https://njppp.com/fulltext/28-1512287434.pdf

[81] C. Braboszcz, A. Delorme, *Lost in thoughts: neural markers of low alertness during mind wandering*, https://pubmed.ncbi.nlm.nih.gov/20946963/

[82] C.R. Clark, M.D. Veltmeyer, R.J. Hamilton, E. Simms, R. Paul, D. Hermens, E. Gordon, *Spontaneous alpha peak frequency predicts working memory performance across the age span*, https://pubmed.ncbi.nlm.nih.gov/15172130/

[83] V.D. Cruceanu, V.S. Rotarescu, *Alpha brainwave entrainment as a cognitive performance activator*, ResearchGate, 2013, https://www.researchgate.net/publication/289030858_Alpha_brainwave_entrainment_as_a_cognitive_performance_activator

[84] McMurray J. C., *Binaural beats enhance alpha wave activity, memory and attention in healthy aging seniors* (Dissertation thesis). Available at ProQuest Dissertations & Theses data-base (UMI No. 3226624), 2006.

[85] J. Kraus, M. Porubanova, *The effect of binaural beats on working memory capacity*, 2015, https://www.researchgate.net/publication/275655551_The_effect_of_binaural_beats_on_working_memory_capacity

[86] Al-Shargie F, Katmah R, Tariq U, Babiloni F, Al-Mughairbi F, Al-Nashash H., *Stress management using fNIRS and binaural beats stimulation*, Biomed Opt Express. 2022 May 24, https://www.ncbi.nlm.nih.gov/pmc/articles/PMC9208616/

[87] Diersing, Christina L., *The Effect of Binaural Tones on EEG Waveforms and Human Computational Performance*, (2021). Graduate Theses and Dissertations. 6975. https://ecommons.udayton.edu/graduate_theses/6975

[88] Attar ET, Balasubramanian V, Subasi E, Kaya M. *Stress Analysis Based on Simultaneous Heart Rate Variability and EEG Monitoring*, IEEE J Transl Eng Health Med. 2021, https://www.ncbi.nlm.nih.gov/pmc/articles/PMC8407658/

[89] R. Costin, C. Rotariu and A. Pasarica, *Mental stress detection using heart rate variability and morphologic variability of EeG signals*, 2012 International Conference and Exposition on Electrical and Power Engineering, Iasi, Romania, 2012, pp. 591-596, https://ieeexplore.ieee.org/document/6463870

[90] T N Guidelines and Guidelines American. *Guidelines Heart rate variability*. In: European Heart Journal 17 (1996), pp. 354–381 (cit. on pp. 6, 7, 9).

[91] Moridani MK, Mahabadi Z, Javadi N. *Heart rate variability features for different stress classification*. Bratisl Lek Listy. 2020, https://pubmed.ncbi.nlm.nih.gov/32990009/

[92] Qi M, Gao H, Liu G. *The effect of mild acute psychological stress on attention processing: an ERP study*. Exp Brain Res. 2018 Jul, https://pubmed.ncbi.nlm.nih.gov/29748696/

[93] Wheeler RE, Davidson RJ, Tomarken AJ. *Frontal brain asymmetry and emotional reactivity: a biological substrate of affective style*. Psychophysiology. 1993 Jan; https://pubmed.ncbi.nlm.nih.gov/8416065/

[94] Cipresso P, Gaggioli A, Serino S, Pallavicini F, Raspelli S, Grassi A, Sellitti L, Riva G. *EEG alpha asymmetry in virtual environments for the assessment of stress-related disorders*. Stud Health Technol Inform. 2012; https://pubmed.ncbi.nlm.nih.gov/22356966/

[95] U. Shirole, M. Joshi, P. K. Bagul, *Linear and Nonlinear Analysis of Cardiac and Diabetic Subjects: Third International Conference on Intelligent Information Technologies, ICIIT 2018, Chennai, India, December 11–14, 2018, Proceedings*. December 2018. https://www.researchgate.net/publication/329277767_Linear_and_Nonlinear_

Analysis_of_Cardiac_and_Diabetic_Subjects_Third_International_Conference_on_Intelligent_Information_Technologies_ICIIT_2018_Chennai_India_December_11-14_2018_Proceedings

[96] Attar ET, Balasubramanian V, Subasi E, Kaya M. *Stress Analysis Based on Simultaneous Heart Rate Variability and EEG Monitoring*. IEEE J Transl Eng Health Med. 2021 Aug 23; https://www.ncbi.nlm.nih.gov/pmc/articles/PMC8407658/#ref17

[97] Tucker, DM *Lateral brain function, emotion, and conceptualization.*. Psychol. Bull. 1981 , 89 , 19. https://psycnet.apa.org/record/1981-04957-001

[98] Seo, S.; Gil, Y.; Lee, J. *The Relation between Affective Style of Stressor on EEG Asymmetry and Stress Scale during Multimodal Task.*. In Proceedings of the 2008 Third International Conference on Convergence and Hybrid Information Technology, Busan, Corea, 11-13 novembre 2008; pp. 461-466. https://ieeexplore.ieee.org/abstract/document/4682070

[99] N. H. A. Hamid, N. Sulaiman, Z. H. Murat, and M. N. Taib,*"Brainwaves stress pattern based on perceived stress scale test*; in Proceedings - 2015 6th IEEE Control and System Graduate Research Colloquium, ICSGRC 2015 https://ieeexplore.ieee.org/abstract/document/4682070

[100] Emad Alya, Naufal M. Saad,Nidal Kamel ,Mohd Zuki Yusoff ,Mohd Azman Zakariya ,Mohammad Abdul Rahman ,Christophe Guillet and Frederic Merienne *Frontal Electroencephalogram Alpha Asymmetry during Mental Stress Related to Workplace Noise*. 11 March 2021https://www.mdpi.com/1424-8220/21/6/1968

[101] R. Gupta, M. A. Alam, and P. Agarwal *"Modified Support Vector Machine for Detecting Stress Level Using EEG Signals.*

[102] A. Hag, D. Handayani, T. Pillai, T. Mantoro, M. H. Kit, and F. Al-Shargie *Eeg mental stress assessment using hybrid multi-domain feature sets of functional connectivity network and time-frequency features*. Sensors, vol. 21, no. 18, Sep. 2021 https://www.mdpi.com/1424-8220/21/18/6300

[103] S.M.U. SAEED,S.M. ANWAR, M. MAJID, *Quantification of Human Stress Using Commercially Available Single Channel EEG Headset*, 2017.

[104] Giuseppe Guglielmo Leggiero, *Osservazioni sull'utilizzo di binaural-beats in ambito psicopatologico*, 13 Feb. 2020.

[105] Beatriz García-Martínez, Antonio Fernández-Caballero, Raúl Alcaraz, Arturo Martínez-Rodrigo, *Assessment of dispersion patterns for negative stress detection from electroencephalographic signals*, Pattern Recognition, Volume 119, 2021, 108094, ISSN 0031-3203, https://www.sciencedirect.com/science/article/pii/S0031320321002818

[106] R.J. Davidson, *Affect, cognition, and hemispheric specialization*, Emotion, Cognition, and Behavior, Cambridge University Press, New York (1988), pp. 320-365, https://scholar.google.com/scholar_lookup?title=Affect%2C%20cognition%2C%20and%20hemispheric%20specialization&publication_year=1988&author=R.J.%20Davidson

[107] Draper, N.R. and Smith, H. (1998). *EEG alpha and theta oscillations reflect cognitive and memory performance: a review and analysis.*

[108] Wolfgang Klimesch. *Applied Regression Analysis. Wiley-Interscience.* In: Brain Research Reviews 29.2 (1999) https://www.sciencedirect.com/science/article/pii/S0165017398000563

[109] Lu Shen et al *Successful alpha neurofeedback training enhances working memory updating and event-related potential activity.* In: Neurobiology of Learning and Memory 205 (2023) https://www.sciencedirect.com/science/article/pii/S1074742723001156

[110] MathWorks *Spectral entropy of signal - MATLAB pentropy.* https://www.mathworks.com/help/signal/ref/pentropy.html.

[111] Akira Ishikawa, Hiroshi Mieno *The fuzzy entropy concept and its application.* Volume 2, Issue 2, 1979,https://www.sciencedirect.com/science/article/abs/pii/0165011479900204

[112] LARIS—Laboratoire Angevin de Recherche en Ingénierie des Systèmes, University of Angers *Multiscale Entropy Approaches and Their Applications.* Entropy (Basel). 2020 Jun, https://www.ncbi.nlm.nih.gov/pmc/articles/PMC7517182/

[113] T. Higuchi*Approach to an irregular time series on the basis of the fractal theory..* In: Physica D: Nonlinear Phenomena 31.2 (June 1988)http://dx.doi.org/10.1016/0167-2789(88)90081-4.

[114] Michael J. Katz.*Fractals and the analysis of waveforms». In: Computers in Biology and Medicine.* Jan. 1988http://dx.doi.org/10.1016/0010-4825(88)90041-8.

[115] Mulligan Daniel J. , Palopoli Ava C. , van den Heuvel Marion I. , Thomason Moriah E. , Trentacosta Christopher J. *Frontal Alpha Asymmetry in Response to Stressor Moderates the Relation Between Parenting Hassles and Child Externalizing Problems.* 2022 https://www.frontiersin.org/journals/neuroscience/articles/10.3389/fnins.2022.917300/full

[116] Y. Tran, R. A. Thuraisingham, N. Wijesuriya, H. T. Nguyen and A. Craig*Detecting neural changes during stress and fatigue effectively: a comparison of spectral analysis and sample entropy.* 2007 3rd International IEEE/EMBS Conference on Neural Engineering, Kohala Coast, HI, USA, 2007 https://ieeexplore.ieee.org/document/4227287

[117] Marzieh Barzegar, Gila Pirzad Jahromi, Gholam Hossein Meftahi, and Boshra Hatef2 *The Complexity of Electroencephalographic Signal Decreases during the Social Stress*. 2023 Jan-Mar;https://www.ncbi.nlm.nih.gov/pmc/articles/PMC10246589/

[118] Qiang Wang; Olga Sourina*Real-Time Mental Arithmetic Task Recognition From EEG Signals*. in IEEE Transactions on Neural Systems and Rehabilitation Engineering, vol. 21, no. 2,https://ieeexplore.ieee.org/abstract/document/6408308

[119] Luca Mesin *Estimation of Complexity of Sampled Biomedical Continuous Time Signals Using Approximate Entropy*. In: Frontiers in Physiology 9 (2018). issn: 1664-042X.https://www.frontiersin.org/articles/10.3389/fphys.2018.00710

[120] O. Thorsten Unke, D. Koner, S. Patra et al, *High-dimensional potential energy surfaces for molecular simulations: from empiricism to machine learning*. February 2020. https://www.researchgate.net/publication/339489944_High-dimensional_potential_energy_surfaces_for_molecular_simulations_from_empiricism_to_machine_learning

[121] Sara Frezzotti, Laura Burattini, Ilaria Marcantoni *Analysis of the heart-rate variability for the monitoring of the nervous system in stress conditions*. Tesi di laurea anno accademico 2020/2021, UNIVERSITÀ POLITECNICA DELLE MARCHE FACOLTÀ DI INGEGNERIA https://tesi.univpm.it/retrieve/50c1256f-02d2-4235-953d-24c95a857456/Analisi%20della%20variabilit%C3%A0%20del%20ritmo%20cardiaco%20per%20il%20monitoraggio%20del%20sistema%20nervoso%20in%20condizioni%20di%20stress.pdf

[122] Gärtner Matti, Grimm Simone, Bajbouj Malek, *Frontal midline theta oscillations during mental arithmetic: effects of stress*, Frontiers in Behavioral Neuroscience, volume 9, 2015, https://www.frontiersin.org/journals/behavioral-neuroscience/articles/10.3389/fnbeh.2015.00096/full

[123] Juebin Huang, MD, PhD, *Panoramica sulla funzione cerebrale*, Frontiers in Behavioral Department of Neurology, University of Mississippi Medical Center, Manuale MSD, 2023 https://www.msdmanuals.com/it-it/professionale/malattie-neurologiche/funzione-e-disfunzione-dei-lobi-cerebrali/panoramica-sulla-funzione-cerebrale

[124] Sedghamiz. H, *Matlab Implementation of Pan Tompkins ECG QRS detector.*, March 2014, https://www.researchgate.net/publication/313673153_Matlab_Implementation_of_Pan_Tompkins_ECG_QRS_detector

[125] J. Pan and W. J. Tompkins, *A Real-Time QRS Detection Algorithm*, in IEEE Transactions on Biomedical Engineering, vol. BME-32, no. 3, pp. 230-236, March 1985, https://ieeexplore.ieee.org/document/4122029

[126] Hooman Sedghamiz (2024). *Complete Pan Tompkins Implementation ECG QRS detector* https://www.mathworks.com/matlabcentral/fileexchange/45840-complete-pan-tompkins-implementation-ecg-qrs-detector, MATLAB Central File Exchange. Recuperato settembre 9, 2024.

[127] T N Guidelines and Guidelines American. *Guidelines Heart rate variability*. In: European Heart Journal 17 (1996), pp. 354–381 (cit. on pp. 6, 7, 9).

[128] Kim HG, Cheon EJ, Bai DS, Lee YH, Koo BH. *Stress and Heart Rate Variability: A Meta-Analysis and Review of the Literature*. Psychiatry Investig. 2018 Mar, https://www.ncbi.nlm.nih.gov/pmc/articles/PMC5900369/

[129] F.P. Branca, *Fondamenti di Ingegneria Clinica*, Springer-Verlag, volume 1, 2000

[130] McCraty R., Atkinson M., Tomasino D., Bradley R.T. (2009). *The coherente heart: Heart-Brain interactions, psychophysiological coherence and the emergence of system-wide order*.

[131] Gantt MA, Dadds S, Burns DS, Glaser D, Moore AD. *The Effect of Binaural Beat Technology on the Cardiovascular Stress Response in Military Service Members With Postdeployment Stress*. J Nurs Scholarsh. 2017 Jul;

[132] Benichou T, Pereira B, Mermillod M, Tauveron I, Pfabigan D, Maqdasy S, Dutheil F. *Heart rate variability in type 2 diabetes mellitus: A systematic review and meta-analysis*. PLoS One. 2018 Apr 2. https://pubmed.ncbi.nlm.nih.gov/29608603/

[133] A. Scarito *La cognizione della lingua. Psicolinguistica ed embodied cognition a supporto della didattica dell'italiano nelle scuole secondarie di primo grado*. November 2017. https://www.researchgate.net/publication/361467779_Alessio_Scarito_La_cognizione_della_lingua_Psicolinguistica_ed_embodied_cognition_a_supporto_della_didattica_dell%27italiano_nelle_scuole_secondarie_di_primo_grado/figures?lo=1

[134] D. Costarelli, M. Seracini, A.Travaglini, G. Vinti *Alzheimer biomarkers esteem by sampling Kantorovich algorithm*. April 2023. https://www.researchgate.net/publication/370264992_Alzheimer_biomarkers_esteem_by_sampling_Kantorovich_algorithm

[135] Katarzyna Szramowiat-Sala *Artificial Intelligence in Environmental Monitoring: Application of Artificial Neural Networks and Machine Learning for Pollution Prevention and Toxicity Measurements*. July 2023. https://www.researchgate.net/publication/372525032_Artificial_Intelligence_in_Environmental_Monitoring_Application_of_Artificial_Neural_Networks_and_Machine_Learning_for_Pollution_Prevention_and_Toxicity_Measurements

[136] Xiaoqing Gu, Yiqing Fan, Jie Zhou, Jiaqun Zhu, *Optimized Projection and Fisher Discriminative Dictionary Learning for EEG Emotion Recognition*.

https://www.frontiersin.org/journals/psychology/articles/10.3389/fpsyg.2021.705528/full#B31

[137] Ş. Bayrak, B, Karlik, D. Fatma, *Comparison Feature Extraction and Neural Net- works Algorithms for Epileptic Seizure Detection*. June 2010. https://www.researchgate.net/publication/337293252_Comparison_Feature_Extraction_and_Neural_Net-_works_Algorithms_for_Epileptic_Seizure_Detection

[138] J. Ahmed, *Brain Machine Interface using EEG Sci-fi to Reality Neural Interface Engineering Brain Machine Interface using EEG 1 BRAIN MACHINE INTERFACE USING EEG*. December 2016. https://www.researchgate.net/publication/312332212_Brain_Machine_Interface_using_EEG_Sci-fi_to_Reality_Neural_Interface_Engineering_Brain_Machine_Interface_using_EEG_1_BRAIN_MACHINE_INTERFACE_USING_EEG

[139] A. O. Aseeri, *Uncertainty-Aware Deep Learning-Based Cardiac Arrhythmias Classification Model of Electrocardiogram Signals*. June 2021. https://www.researchgate.net/publication/352496313_Uncertainty-Aware_Deep_Learning-Based_Cardiac_Arrhythmias_Classification_Model_of_Electrocardiogram_Signals